

DIGITAL ACCESS TO SCHOLARSHIP AT HARVARD
DASH.HARVARD.EDU

HARVARD LIBRARY


Control of human telomerase activity by nucleotide metabolism

Citation

Mannherz, William. 2024. Control of human telomerase activity by nucleotide metabolism. Doctoral dissertation, Harvard University Graduate School of Arts and Sciences.

Link

https://nrs.harvard.edu/URN-3:HUL.INSTREPOS:37378760

Terms of use

This article was downloaded from Harvard University's DASH repository, and is made available under the terms and conditions applicable to Other Posted Material (LAA), as set forth at

https://harvardwiki.atlassian.net/wiki/external/NGY5NDE4ZjgzNTc5NDQzMGIzZWZhMGFlOWI2M2EwYTg

Accessibility

https://accessibility.huit.harvard.edu/digital-accessibility-policy

Share Your Story

The Harvard community has made this article openly available.
Please share how this access benefits you. Submit a story

HARVARD
Kenneth C. Griffin

GRADUATE SCHOOL
OF ARTS AND SCIENCES

DISSERTATION ACCEPTANCE CERTIFICATE

The undersigned, appointed by the

Division of Medical Sciences

in the subject of Biological and Biomedical Sciences

have examined a dissertation entitled

Control of human telomerase activity by nucleotide metabolism

presented by William Peter Mannherz

candidate for the degree of Doctor of Philosophy and hereby certify that it is worthy of acceptance.

Signature: Benjamin Ebert
Benjamin Ebert (Feb 9, 2024 16:51 EST)

Typed Name: Dr. Benjamin Ebert

Signature: Grant Rowe
Grant Rowe (Feb 9, 2024 13:35 EST)

Typed Name: Dr. Robert Rowe

Signature: Titia de Lange
Titia de Lange (Feb 9, 2024 13:31 EST)

Typed Name: Dr. Titia de Lange

Signature: Patricia Opresko
Patricia Opresko (Feb 11, 2024 09:35 EST)

Typed Name: Dr. Patricia Opresko

Date: February 09, 2024

Control of human telomerase activity by nucleotide metabolism

A dissertation presented

by

William Peter Mannherz

to

The Division of Medical Sciences

in partial fulfillment of the requirements

for the degree of

Doctor of Philosophy

in the subject of

Biological and Biomedical Sciences

Harvard University

Cambridge, Massachusetts

February 2024

© William Peter Mannherz

All rights reserved

Control of human telomerase activity by nucleotide metabolism

Abstract

Telomeres are nucleoprotein structures which flank linear chromosomes and promote genome integrity. Telomere synthesis by the telomerase reverse transcriptase must be tightly controlled to promote cellular function and human health, yet our understanding of the processes which enable telomere length homeostasis is incomplete. Here, I performed the first genome-wide CRISPR-Cas9 screen for telomere length regulating genes in human cells and identified dNTP metabolism as a pathway critical for human telomere length control. Using targeted genetic screening, I found that loss of thymidine nucleotide synthesis or salvage genes led to telomere attrition, whereas loss of the dNTP degrading gene SAMHD1 drove telomere lengthening. Remarkably, I found that supplementation of thymidine nucleoside drove robust telomere lengthening across multiple cell lines, including at doses which had no detectable effects on cell growth, and in a manner which required the presence of telomerase. To further characterize the intersection between dNTP metabolism and telomerase activity control, I developed a method for Telomerase Rapid Assessment in the Cellular Environment, or TRACE. Using TRACE, I identified that guanine nucleotide salvage occupies a critical juncture in telomerase activity control: salvage to form guanosine ribonucleotides drives telomerase inhibition, while salvage to form dGTP stimulates telomerase activation. I propose that dNTP metabolism alters telomere length via the substrate level control of telomerase, adding a new

layer to current models of telomerase regulation. Inherited defects in the telomerase components and related genes cause premature telomere shortening and drive a spectrum of fatal disorders called telomere biology disorders (TBDs), manifesting as bone marrow failure, liver and lung fibrosis, and other degenerative diseases throughout the body. There are currently no effective systemic therapies to lengthen telomeres to treat the TBDs, and accordingly the patients diagnosed with these disorders face daunting prognoses. Here, I identify multiple strategies to promote telomere lengthening in TBD patient derived cells by upregulating dNTP metabolism, including supplementation with thymidine, inhibition of the dNTPase SAMHD1, supplementation with deoxyguanosine combined with the PNP inhibitor ulodesine, and expression of an efficient deoxynucleoside kinase from *Drosophila melanogaster*. Collectively, my work has expanded our understanding of human telomere length control by revealing that telomerase is highly sensitive to manipulations of its dNTP substrates. My findings offer an explanation for emerging human genetic data linking genetic variation in dNTP metabolism genes with telomere length and telomere disease. I propose that the targeted manipulation of dNTP metabolism could provide an avenue to control telomerase activity within a therapeutic window to treat the TBDs. Nucleotide metabolism offers a new lens with which to examine the origins and evolution of telomerase and telomeres.

Table of Contents

Title Page ..... **i**

Copyright ..... **ii**

Abstract ..... **iii**

Table of Contents ..... **v**

Chapter 1: Introduction **1**

The hypothesis and discovery of telomeres and telomerase 2

Pathways governing human telomere length homeostasis 4

Telomerase enzymology 11

dNTP metabolism 16

dNTP metabolism and telomerase: knowns and unknowns 18

Telomere length and human disease 19

Chapter 2: Thymidine nucleotide metabolism controls human telomere length **29**

Attributions 30

Abstract 31

Introduction 31

Results 32

Discussion 65

Materials and Methods 69

Chapter 3: Metabolic constraint of human telomere length by nucleotide salvage efficiency **85**

Attributions 86

Abstract....87

Introduction....87

Discussion....111

Materials and Methods....117

Chapter 4: Discussion....126

Rapid and high throughput methods for studying telomere length within the cellular environment....127

Nucleotide metabolism controls human telomere length....130

The telomerase substrate-level control model to explain the link between dNTP metabolism and telomere length....134

Consideration of alternative mechanisms by which dNTP metabolism could influence telomere length homeostasis....140

Why thymidine?....144

Why telomeres?....146

Telomeres, nucleotides, and human disease....147

dNTP metabolism in patients with telomere biology disorders....149

Therapeutic prospects to promote telomerase activity via dNTP metabolism to treat the TBDs....151

An evolutionary perspective on the relationship between telomeres, telomerase, and dNTP metabolism....158

Concluding Statement....163

References....164

Appendix....194

Supplementary Figures....195

Acknowledgements

I am extremely grateful for the many people who helped make this dissertation possible. First, I am incredibly thankful to have had the opportunity to work with my thesis advisor, Suneet Agarwal. Suneet is a one-of-a-kind person, who combines intellect and curiosity with a deep ability to connect with and care for the people in his life. Suneet dedicated countless hours to my development as a scientist. Talking about project ideas or experiments with him was a highlight of my week, every week, and always left me feeling energized. Suneet, you are an exemplary mentor, scientist, and leader, as well as a role model for what makes a career as a physician scientist worthwhile. Thank you for making my PhD truly fun, and shaping me into the scientist who I am today. I couldn't have asked for more from my PhD experience.

Next, I need to thank my parents, Kathy and Dave, for the unending love and support they have given me over my life. Growing up, you helped me believe that I could do whatever I set my mind to. I still look back fondly that fateful lunch at the Cheesecake Factory during my freshman year of college when I told you that I wanted to switch majors and study biology. You were supportive of my career change then and your support hasn't wavered for the last ten years. Together with my younger brothers, Jack, Trevor, and Kyle, you have always made me feel loved and secure with who I am. I am grateful to have such a wonderful and caring family.

I also need to give many thanks to the people who supported my scientific growth over the years. First, thank you to Len Zon, who took a chance and hired me as a research technician with little bench science experience. Len welcomed me into his lab, and has been a supportive mentor to me both throughout my time in his lab and in graduate school. I was fortunate to spend my time in the Zon lab working with Serine Avagyan and Jonathan Henninger. Serine, your

passion for both science and people inspired me to pursue a career as a physician scientist. I am so grateful to have had you rigorously teach me the ropes in lab, and to stay a close mentor in the years since. You have shaped my career for the better, and I am happy to have you as a friend. Jon, you certainly set a high bar for what a successful graduate student looks like! I am so appreciative of your commitment to teaching me, and look to you as a role model of someone who can powerfully combine molecular biology with computational methods. A big thank you as well to my dissertation advisory committee members, Mark Fleming, Naama Kanarek, and Benjamin Ebert, who offered me support and guidance throughout my PhD training.

My time working in the Agarwal lab would not have been the same without my lab mates, including Zach, Noah, Pattra, Liang, Sonia, Roman, and Neha. Thank you all for making lab a pleasure to be in, and in particular thanks to Zach for countless conversations about science and life (as well as for the reminders to eat lunch!), and thanks to Noah for your dedication to our work and for being such a positive force in the lab. Thanks also to my amazing friends for countless hang-outs, dinners, trips, chicken wings, pizza, and movie nights, including Quique, Alaina, Leonard, Leah, Niko, Travis, Jelly, Blake, Audrey, Nate, Matt, Jason, Sam, and many others.

Finally, Jaya, my life partner, thank you for all of your tireless support these past four years. You have been there for me every day since the start of my PhD, and have ridden both the highs and the lows with me over the years. Thank you for filling these four years with adventure.

This thesis is dedicated to my parents,
Kathleen and David Mannherz

Chapter 1: Introduction

The hypothesis and discovery of telomeres and telomerase

Telomeres are repetitive DNA-protein structures which cap the termini of linear chromosomes and promote genome integrity. Telomeres were initially conceptualized in the 1930's based on the observed stability of natural chromosome ends compared with the instability of ends produced by DNA damaging agents[1,2]. Interpreting these results in 1938, Hermann Muller hypothesized that "the terminal gene must have a special function, that of sealing the end of the chromosome… This gene may accordingly be distinguished by a special term, the telomere."[2] Later, based on the discovery by Arthur Kornberg and colleagues that DNA replication requires initiation with an RNA-primer[3–5], it was recognized by Alexey Olovnikov[6] and James Watson[7] that a terminal portion of linear chromosomes would be lost during cell division, termed the 'end replication problem'. The central roles of telomeres were thus identified as: 1) "sealing" the ends of chromosomes to prevent fusions with other DNA ends and 2) preventing the loss of genetic information during genome replication.

The first molecular characterization of telomere ends was driven by Elizabeth Blackburn who led a series of discoveries about the molecular nature of telomeres by taking advantage of the unique genomic architecture of *Tetrahymena,* which harbor abundant linear minichromosomes. Sequencing the ends of these minichromosomes revealed they terminated in tandem 5'-TTGGGG-3' repeats[8]. Evidence from *Tetrahymena*[9] and later in yeast[10,11] suggested telomere repeats were actively synthesized by an enzyme. Carol Greider, working in the Blackburn lab, became the first to identify a telomere repeat synthesizing enzymatic activity by incubating (5'-TTGGGG-3') x 4 oligonucleotides and dNTPs with *Tetrahymena* extracts[12]. Greider and Blackburn went on to show this enzyme complex harbors an RNA component with a template encoding the telomere

repeat[13,14], offering reverse transcription as an explanation for how telomeres are synthesized and how the end replication problem is solved. The telomeric repeat sequence, TTAGGG[15], and telomerase catalytic protein (TERT)[16] and RNA (TERC)[17,18] components would later be identified in humans.

While the maintenance of telomere length appeared to be explained by telomerase, the means by which telomeres protect the ends of chromosome from DNA damage response was not clear. Work led by Titia de Lange identified and characterized the telomere-specific DNA binding proteins she collectively termed shelterin, as a complex that 'seals' the DNA termini[19]. This critical protein complex fulfills numerous roles to promote telomeres, including by limiting the activation of DNA damage response signaling pathways, preventing telomere resection and fusion, and regulating telomerase activity[20,21]. More recently, an appreciation for the importance of the CST complex in C strand maintenance of the telomere has also come into light[22].

Together, the *de novo* synthesis of telomeric repeats by telomerase, along with the maintenance of the C-strand by CST, generates a scaffold to bind the shelterin complex, thereby allowing telomeres both to seal the linear chromosome ends and prevent the loss of genomic information during cell division. These fundamental features of telomeres as repetitive arrays of TTAGGG-like repeats synthesized via reverse transcription and coated with specialized protein factors are observed across diverse eukaryotic kingdoms of life, and likely originated in the early stages of the development of linear chromosomes[18,23–25]. In the ensuing eons since their origination, telomere architecture has diversified, becoming tailored to the unique cellular and organismal requirements for the maintenance of genome integrity[25,26]. Remarkably, the dysregulation of telomere maintenance has been identified as the common cause of a range of severe inherited and acquired human diseases. Continued progress towards a complete

understanding of telomere homeostasis may prove to be therapeutically useful for patients with disorders caused by telomere dysfunction.

Pathways governing human telomere length homeostasis

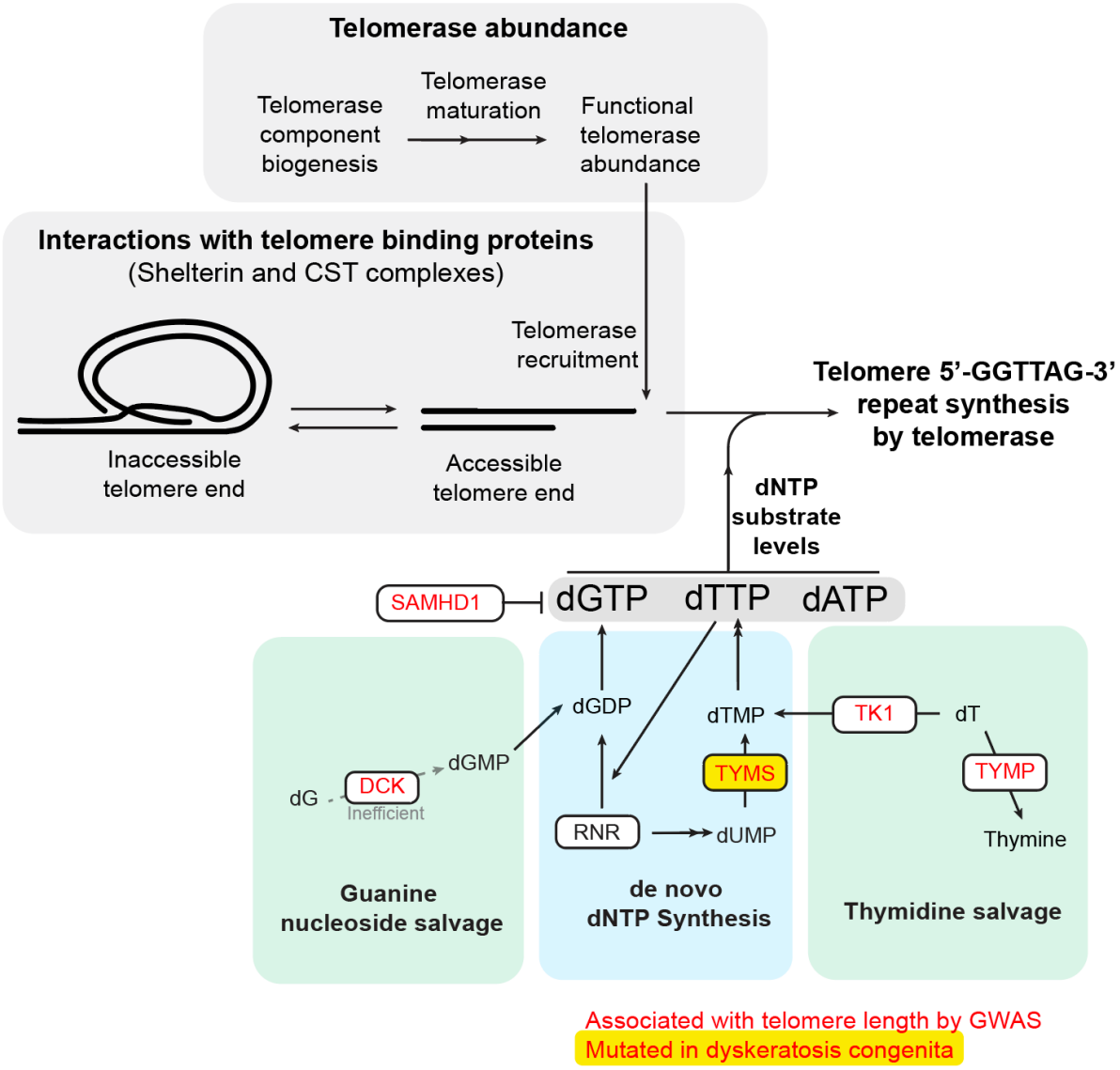
Telomeres shorten with cell division due to the end replication problem, and when critically short, drive cells to exit from the cell cycle and become senescent[27–29]. This shortening is counteracted by the addition of telomeric repeats by the telomerase reverse transcriptase, a process which is tightly regulated. The balance between telomere synthesis and erosion is understood to enable controlled cellular replication while limiting the excessive cell growth which occurs in cancer. The rate of telomere synthesis by telomerase is considered to be governed by: 1) the abundance of the telomerase holoenzyme, and 2) the interactions between telomerase and the telomere binding proteins[21]. In this thesis, I propose dNTP metabolism as third factor critical for the control of human telomerase activity and required for telomere length homeostasis, offering an explanation for the recent association of dNTP metabolism genes with telomere length and telomere related disease (**Figure 1-1**). Here, I discuss the canonical pathways governing telomere length homeostasis.

In cultured somatic cells which do not express telomerase, ~50-100 bp of telomere repeat which is lost from chromosome ends with each division[27,30]. This rate of attrition can be exacerbated by disruption of the machinery responsible for the maintenance of telomere ends which includes the shelterin complex, the CST complex, and telomere accessory factors such as RTEL1[20]. Together, these factors promote the replication of telomeres, and regeneration of the characteristic 3’ overhang and T-loop through controlled binding, resection and fill-in reactions[20].

Impairments in these factors can lead to telomere shortening telomere ends by cleavage, resection, and impaired fill-in of the C-strand[20,31].

Figure 1-1. An updated model of human telomere length regulation. Human telomere length homeostasis is generally understood to be governed by (1) the abundance of telomerase, and (2) the interactions between telomerase and the telomere binding proteins. Based on my findings as well as emerging human genetic evidence, I propose an updated model including a third critical factor regulating human telomere length: the availability of dNTP substrates for telomere 5'-GGTTAG-3' repeat synthesis by telomerase. dNTP substrate accumulation is limited by deoxnucleoside salvage efficiency including deoxyguanosine (dG) metabolism by DCK, and thymidine (dT) conversion to dTTP via TK1**.** dTTP can increase dGTP production by allosteric binding to ribonucleotide reductase (RNR). Enhancing cellular deoxnucleoside salvage through dG or dT supplementation or by augmenting deoxynucleoside kinase activity robustly increases telomerase activity and telomere length. Mutations that impair dTTP *de novo* synthesis lead to reduced telomerase substrate levels and impaired telomerase activity, as observed in patients with TYMS locus mutations who develop the telomere biology disorder dyskeratosis congenita[32]. The dNTPase SAMHD1 prevents the accumulation of dNTPs and negatively regulates telomerase activity and telomere length. My model provides a mechanistic framework for the recent association between genetic variation in dNTP metabolism genes and telomere length in states of health and disease[32–34].

Figure 1-1. (Continued)



Telomere shortening is counteracted by the telomerase holoenzyme complex, consisting of TERT, the catalytic protein component, TERC, the RNA which encodes the template for telomere repeat synthesis, as well as the H/ACA domain components dyskerin, NAF1, NHP2 and GAR1, and the Cajal body associated protein TCAB1[35]. Of note, the histone proteins H2A and H2B have been recently reported as telomerase complex members, however the significance of this association remains undefined[35]. In contrast to telomere shortening which occurs in all dividing cells due to the end replication problem, telomere lengthening by telomerase is highly constrained by the cell-type specific expression of TERT. Expression of TERT is largely restricted to the germline, fetal tissues, self-replicating stem cells, lymphocytes, and cancer cells, and is absent from most other somatic cells[36–38]. Engineered ectopic expression of TERT in somatic cells increases telomere length and extends replicative capacity[39]. Mutations in the promoter of TERT which impair its transcriptional silencing can increase telomere length and have been commonly identified in many tumor types[40,41]. In addition to regulation at the RNA expression level, TERT production is also regulated by alternative splicing[42]. TERT expression can be considered as an on-off switch for telomerase activity within cells.

In cells which express TERT, the level of TERC has been shown to determine the accumulation of telomerase holoenzymes and can be limiting for telomere lengthening capacity[43]. Additionally, while the abundance of the H/ACA components is not considered limiting for telomerase biogenesis, inherited mutations in the members of this complex including dyskerin, NAF1, NOP10, and NHP2 can impair TERC accumulation and reduce telomere length[31]. Upon being transcribed, TERC is bound by H/ACA complex members, and its 3’ end undergoes processing including oligoadenylation by PAPD5 followed by trimming to its mature length by PARN. Loss of PARN leads to degradation of TERC in the RNA exosome, inhibiting TERC

accumulation and shortening telomere length[44] in a manner which can be rescued by PAPD5 inhibition[45]. Following TERC assembly with the H/ACA factors and 3' end processing, TERC and TERT become complexed in a process promoted by TCAB1[46,47]. A clear demonstration of the importance of TERC and TERT levels on telomere length control is observed in the rapid telomere lengthening seen in when both factors are overexpressed[48].

In addition to regulation at the level of telomerase abundance, telomere synthesis is also regulated by the shelterin and CST complexes which coordinate the recruitment of telomerase to the telomere and govern the accessibility of the telomere 3' end. The six-member shelterin protein complex, which includes POT1, TERF1, TERF2, TERF2IP (RAP1), TINF2, and TPP1, plays roles both as a positive and negative regulator of telomerase activity[21]. The shelterin component TPP1 recruits telomerase to the telomere end by directly binding TERT at the TEL patch[49–51]. Disruption of the TEL patch or loss of TPP1 impairs telomerase localization and reduces telomere length[50]. Both TPP1 as well as POT1, the ssDNA binding component of the shelterin complex, have additionally been shown to bind to telomerase and promote its enzymatic activity, discussed below. In addition to this stimulatory role, shelterin also plays an inhibitory role in the control of telomerase activity. The abundance of the three DNA binding members of the shelterin complex, TRF1[52], TINF2[53], and POT1[54], negatively regulates telomere length in a telomerase dependent manner. Shorter telomeres are preferentially lengthened by telomerase[55,56], and the higher abundance of shelterin complexes on longer telomeres has been proposed to explain this phenomena[21,55,56]. While the relationship between shelterin abundance, telomerase activity, and telomere length is clear, the precise mechanisms by which this occurs remains undefined, and alternative hypotheses have been proposed, such as a model where telomerase is delivered to the

telomere end via the replication fork in a manner sensitive to telomere length and shelterin abundance[57].

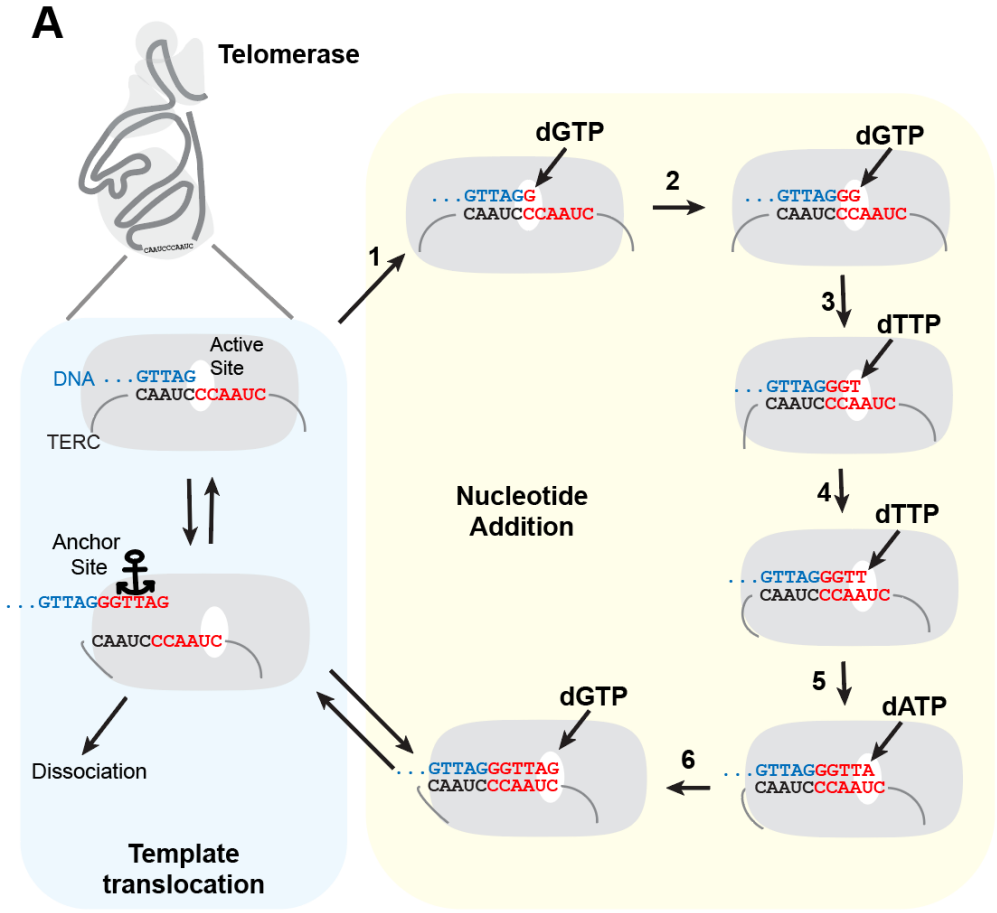
The CST complex, comprised of CTC1, STN1 and TEN1, is critical for the maintenance of the telomere C-strand strand and also has a role in restricting telomere synthesis by telomerase. Depletion of the CST complex members CTC1 and STN1 has been shown to increase telomerase activity in cells[58,59]. Studies using purified telomerase and CST supports a model where CST binds to the telomeric ssDNA and sequesters it away from telomerase, preventing multiple rounds of binding and telomere synthesis by telomerase[58,60]. CST may also interfere with recruitment of telomerase to the telomere end by TPP1[61,62]. While the importance of CST for telomere length homeostasis is well understood, the timing and molecular details underlying how CST restricts telomerase activity are areas of active investigation[61,62].

In sum, the rate telomere synthesis is commonly considered to be governed by the control of telomerase accumulation and the interactions between telomerase and the telomere binding proteins. This model has provided considerable insight into how telomere length homeostasis is maintained, and has offered explanations for how mutations in telomere-associated genes lead to telomere length dysregulation and cause disease. In generating this model, both cell-based studies and enzymatic evaluations of purified telomeric proteins have provided essential and complimentary details. While developing my revised model for telomere length control which incorporates telomerase regulation by dNTP metabolism, a detailed understanding of telomerase enzymology has similarly proven valuable.

Telomerase enzymology

Once assembled, recruited, and bound to the telomere end, telomerase uses its integral RNA template to synthesize 5'-GGTTAG-3' repeats in a ratcheting mechanism (**Figure 1-2a**)[63]. Following the synthesis of one repeat, the telomerase RNA template must dissociate from the telomeric overhang and then realign at the newly generated 3' end to enable another round of repeat synthesis. This transition is a vulnerable portion of the catalytic cycle when telomerase is at greater risk of dissociating from the telomere end. The addition of the first nucleotide in the repeat is thus relatively inefficient, with lower processivity (repeat addition processivity) compared with the processivity of addition of the subsequent nucleotides (nucleotide addition processivity)[63]. The propensity for telomerase dissociation during this phase of realignment is evidenced by the relatively high signal intensity observed at every sixth nucleotide position when extension products are resolved on a polyacrylamide gel[64]. Human telomerase is moderately processive, and has been shown to synthesize tens of repeats within one binding event before dissociating[65]. To facilitate multiple repeat synthesis rounds in a single event of telomerase binding, TERT utilizes a domain away from the catalytic site termed the anchor site, which binds to the telomere overhang and limits telomerase dissociation from the DNA substrate during template realignment[66,67]. The binding between telomerase and its telomere substrate at the anchor site is enhanced by the presence of TPP1 and POT1, and accordingly the presence of these factors increases telomerase processivity[65,66]. In human cells, telomerase has been found to add on average ~60 nucleotides or ten telomere repeats in a single binding event[68,69]. The limited processivity of telomerase likely plays a major role in telomere length control, as demonstrated by the diverse variants in TERT which impair telomerase processivity and also lead to reduced telomere length in human cells[70].

Figure 1-2.



B

Position	dNTP	Km
1	dGTP	120 +/- 8
2	dGTP	ND
3	dTTP	4 +/- 0.4
4	dTTP	ND
5	dATP	31+/- 0.8
6	dGTP	5 +/- 0.1

Figure 1.2 Telomerase enzymology. A. Schematic of the telomerase catalytic cycle, adapted from Bagshaw et al (2021)[63]. B. Km of different positions throughout the telomerase catalytic cycle, measured by Chen et al. (2018) using a modified 'template-free' telomerase system[71].

The activity of purified human telomerase is highly sensitive to changes in the levels of its dNTP substrates[72–74]. The concentration dependence of nucleotide addition efficiency at different positions in the catalytic cycle was studied in detail by Julien Chen's group, who found that the Km for the first nucleotide position in the repeat (5'-**G**GTTAG-3') was much higher (120 μM), compared with the other positions evaluated (4-30 μM) (**Figure 1-2b**)[71]. The relatively high value for the first nucleotide in the repeat is consistent with the low efficiency of repeat addition processivity compared with nucleotide addition processivity. These Km values are also relatively high compared with the corresponding values for the cellular replicative DNA polymerases which range from 0.2-10 μM[75], and are near or above cellular dNTP levels (**Figure 1-3a**)[76], suggesting that changes in dNTP levels within the physiologic range could influence telomerase activity within cells. Of note, this evaluation was performed using a modified 'template-free' enzyme system where the telomerase RNA template was removed from the telomerase complex, and instead pre-hybridized to DNA oligonucleotide substrates, an experimental change which likely alters enzyme kinetics. Nonetheless, in measurements of intact telomerase isolated from human cells, repeat synthesis is also highly sensitive to changes in dNTP levels within the physiologic range, with dGTP levels being relatively more important than dTTP and dATP levles[64,71,77]. Further exemplifying the importance of dNTP levels on telomerase activity, elevation of dGTP has been shown to promote telomerase activity even in TERT mutants with impaired processivity[70]. Despite the clear importance of dNTP concentrations on telomerase enzymatic activity, little work has been done to evaluate the relevance of dNTP metabolism on telomerase activity and telomere length in human cells.

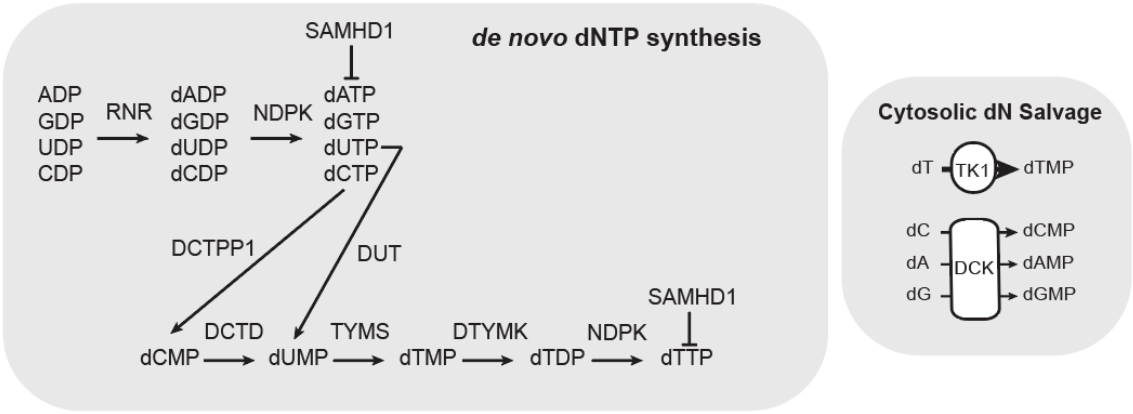
Figure 1-3. Overview of dNTP homeostasis. A. Concentrations of average cellular NTPs and dNTPs. Data from Traut (1994)[76]. B. Schematic of *de novo* and salvage dNTP synthesis pathways. The SAMHD1 dNTPase, a major factor in dNTP homeostasis, is also depicted. C. Schematic of human RNR allosteric regulation. Schematic adapted from Matsuda et al. (2018)[78]. dTTP binding to the specificity site promotes reduction of GDP to form dGDP and inhibit the reduction of the pyrimidines CDP and UDP. dGTP binding the specificity site promotes ADP reduction. ATP binding to the activity site promotes overall enzyme activity, while dATP binding to the specificity site inhibits overall enzyme activity. D. Relative catalytic efficiency of TK1 and DCK for their deoxynucleoside substrates. Data for DCK from Bohman and Eriksson (1988)[79], data for TK1 from Munch-Petersen et al. (1991)[80], comparison originally made by Knect et al. (2002)[81].

Figure 1-3. (Continued)

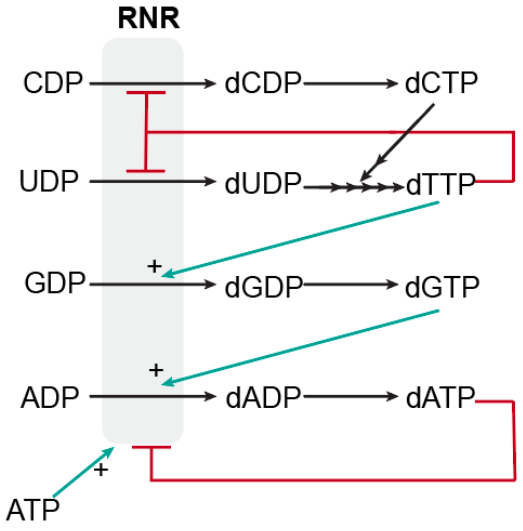
A

NTPs		dNTPs	
Nucleotide	**Concentration (μM)**	**Nucleotide**	**Concentration (μM)**
ATP	3152	dATP	24
GTP	468	dGTP	5
CTP	278	dCTP	29
UTP	567	dUTP	0.2
		dTTP	37

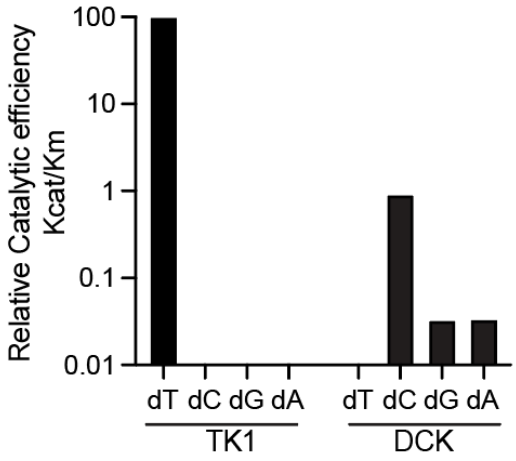
B



C



D



dNTP metabolism

dNTPs are common precursors for cellular processes including nuclear genome replication, mitochondrial genome replication, DNA repair, and telomere synthesis by telomerase. dNTPs can be either *de novo* synthesized from ribonucleotides or salvaged (**Figure 1-3b,c**), and both of these processes are highly allosterically and temporally regulated. However, despite the clear relationship between changes in dNTP levels and the enzymatic activity of purified telomerase discussed above, dNTP metabolism has not been well studied as a node of telomerase regulation within human cells.

dNTP *de novo* synthesis from ribonucleotides occurs at the diphosphate level by ribonucleotide reductase (RNR). Ribonucleotides are approximately 10-100 times more abundant than deoxyribonucleotides (**Figure 1-3a**)[76], with ATP being the most abundant. The conversion of ribonucleotide diphosphates to deoxyribonucleotide diphosphates by RNR is highly allosterically regulated by two sites called the activity site and the specificity site. The activity site can either bind ATP which stimulates RNR activity, or can bind dATP which inhibits RNR activity. The specificity site governs substrate preference and is bound by dNTPs (**Figure 1-3c**)[82,83]. In addition to allosteric regulation, expression of RNR is cell cycle regulated through both transcription and degradation[84]. Following their production by RNR, dNDPs can be phosphorylated by NDPK using a 'ping-pong' mechanism where a phosphate is transferred from ATP or another triphosphate. NDPK activity is not considered to play a role in influencing dNTP levels[85].

In contrast with the other dNTPs, thymidine has no ribonucleotide equivalent and requires several steps for its *de novo* synthesis following dNDP production by RNR. Thymidine *de novo* synthesis occurs via the addition of a methyl group to dUMP from a N^5,N^{10}-methylene tetrahydrofolate donor by the enzyme thymidylate synthase (TYMS), which is subsequently

phosphorylated by thymidine monophosphate specific kinase DTYMK and then by NDPK to form dTTP[86]. The dUMP substrate for TYMS can be derived via degradation of dUTP to form dUMP by DUT, or by following degradation of dCTP to dCMP by DCTPP1 then from dCMP to dUMP by DCTD[87], or via the salvage pathway. DCTD is allosterically activated by dCTP and allosterically inhibited by dTTP[88].

In addition to *de novo* synthesis from ribonucleotides, dNTPs can alternatively be salvaged from deoxynucleosides. In humans, nucleoside salvage occurs through different enzymes in the mitochondria and in the cytosol. In the mitochondria, TK2 can phosphorylate dT and dC, while DGUOK can phosphorylate dG and dA. Impairments in either of these genes leads to mitochondrial DNA depletion disorders[89]. In the cytosol, DCK can salvage dC and less efficiently dA, or dG[79] while TK1 can efficiently salvage dT and dU[81,90] (**Figure 1-3d**). Of note, TK1 is allosterically inhibited by dTTP, and is most active during S-phase[90], while DCK activity is similar throughout the cell cycle[91].

dNTP levels are also strongly influenced by rates of catabolism, a process predominantly controlled by the dNTPase SAMHD1[92]. SAMHD1 activity is lowest in S-phase of the cell cycle which is thought to contribute to the relatively higher dNTP pools during genome division[93]. The dNTPase activity of SAMHD1 is thought to contribute to its role in restricting lentiviral infections by inhibiting viral reverse transcription[94]. Other dNTP degrading enzymes include DUT and DCTPP1 which degrade dUTP and dCTP respectively[87,95].

Collectively, nucleotide metabolism is highly regulated both temporally and by feedback mechanisms to maintain dNTP pool homeostasis. Manipulation of dNTP metabolism is widely used to treat diseases ranging from inborn errors of metabolism to autoimmune diseases to cancer[96,97]. While the dysregulation of dNTP pools has been linked with disorders of mitochondrial

DNA depletion[89], and mutagenesis in cancer[85], a relationship between dNTP metabolism and human telomerase regulation has not been well described to date.

dNTP metabolism and telomerase: knowns and unknowns

Telomerase has been known to use dNTP substrates since its initial biochemical description in *Tetrahymena*[12], however investigations linking telomerase activity with dNTP metabolism have remained limited, particularly in humans. Early evaluations of telomere length across *S. cerevisiae* mutant strains identified that *cdc8* (encoding thymidylate kinase), and cdc21 (encoding thymidylate synthase) deficient strains had short telomere length, although no mechanistic studies were performed[98]. Further characterization of these strains confirmed their telomere length defects, and also showed that inhibiting thymidylate synthase using the thymidine analog FUdR altered telomere length in telomerase deficient cells, suggesting that a telomerase independent mechanism could be at play[99]. Later, another study demonstrated a correlation between dGTP levels and telomere length across a panel of *S. cerevisiae* strains with mutations in genes regulating dNTP metabolism. They also interestingly found changes in the base pair composition of telomeres in the mutants, which they attributed to alterations of the variable telomerase repeat of yeast[100]. Of note, while many aspects of yeast and human biology are conserved, both telomerase regulation and dNTP metabolism have diverged significantly between these species. For example the telomere repeat is variable in yeast, yeast telomerase has limited processivity compared with the human enzyme[101], and yeast lack deoxynucleoside salvage kinases. Presently, dNTP metabolism is not considered a major factor in the control of human telomerase activity.

While the relationship between dNTP metabolism and telomere length in human cells has gone largely unexplored, more investigation has been done exploring how human telomerase is

influenced by non-canonical nucleotides. Modified nucleotides are commonly used therapeutically to treat cancer and viral infections, notably via reverse transcriptase inhibition[102]. The identification of telomerase as a reverse transcriptase has spurred significant investigation into whether therapeutic reverse transcriptase inhibitors may inhibit telomerase, with mixed results demonstrative of the unique substrate preferences between telomerase and other reverse transcriptases[77,103–105]. The unique substrate preferences of telomerase are being actively explored in order to specifically target telomerase expressing cancer cells while sparing somatic cells which do not express telomerase[106]. Modified dNTPs also exist in native cellular nucleotide pools, for example 8-oxo-dGTP, a mutagenic nucleotide which is generated from oxidative stress that has been found to be a chain terminator of telomere extension by telomerase[107]. The incorporation of ribonucleotides by telomerase has also been hypothesized to play roles in telomere homeostasis[108]. In sum, the incorporation of non-canonical substrate nucleotides by telomerase as well as the resulting effects on telomere function are areas of active investigation.

Telomere length and human disease

Telomere length was originally hypothesized as a factor which could contribute to human disease in Olovnikov's seminal 1973 paper[6]. In addition to recognizing the end replication problem and hypothesizing that telomere shortening to a critical length could halt cell division, Olovnikov further speculated that telomere attrition could drive organismal aging, and that the enzyme which counteracts telomere shortening may be present in cancer to enable cell immortalization. In the subsequent decades, many of Olovnikov's hypotheses including the association of telomere length with diseases of aging and cancer would prove to be prescient.

Telomere length in the population

Telomere length in the human population declines with age in most tissues[109]. Telomere length in the blood has been most widely studied[110,111]. Average leukocyte telomere and has shown to range from ~11kb in newborns to ~4.5kb in the elderly. This telomere shortening is most rapid in the first year of life, then the rate of decline stabilizes to 50 bp per year in the blood during adulthood[111]. While most tissues display telomere shortening with age, some tissues have stable telomere lengths in adulthood, including tissues which undergo limited cell division such as muscle and neurons as well as germline tissues such as testis[109]. Telomere length is highly heritable[112], and the genetic determinants of telomere length include sex, paternal age, and race, as well as several common genetic variants associated with telomere length[33,112,113]. While variation exists, telomere lengths across populations are tightly bounded, with 80% of the population falling within a ~4kb range and 99% within a ~5kb range for a given age[110].

Telomere length in humans has been associated with lifespan and a variety of diseases[33]. While it can be challenging to use observational data to identify causal relationships between telomere length and longevity, in recent studies applying causal inference based methods such as mendelian randomization, telomere length remains associated with lifespan. For example, in one mendelian randomization study based on data from the UK Biobank, 40-year-old individuals with 1 standard deviation genetically instrumented longer telomeres had a life expectancy on average 2.5 years longer than individuals with 1 standard deviation genetically instrumented shorter telomeres[33]. While longer telomeres may be associated with longevity, both long and short telomeres can predispose to lethal diseases.

Long telomere length and human disease

Telomere shortening has been hypothesized to limit cellular replicative capacity and thereby prevent cancer progression. In line with this hypothesis, inherited common genetic variation leading to long telomeres has been associated with increased rate of several malignancies at the population level[33,114]. In addition to common genetic variation, inherited rare variants in genes which cause telomere lengthening have been identified in families with high rates of multiple tumors including melanoma. This includes inherited mutations in several shelterin components including POT1[115], TIN2[116], TERF2IP (RAP1), ACD (TPP1)[117], as well as activating mutations in the *TERT* promoter[40]. In addition to limiting telomere length, shelterin components such as POT1 also play roles in suppressing DNA damage signaling at telomere ends[118], and increased telomeric DNA damage has been offered as an alternative mechanism for tumor predisposition in these patients[119]. However, a recent study found that cancer associated *POT1* mutations are proficient in preventing DNA damage response, but cannot restrain telomere length, supporting the notion that long telomeres themselves underly the cancer predisposition in patients with germline *POT1* mutations [120]. Mutations in *POT1* have also been found to predispose to elevated rates of clonal hematopoeisis[121], a clonal expansion of blood cells which can transform into leukemia. As previously mentioned, telomerase activation is also commonly observed in cancer[122], and the widespread occurrence of *TERT* promoter mutations in varied tumor types[40,41] which have been shown to abrogate TERT silencing[123].

Short telomere length and human disease

Inherited mutations which impair telomere maintenance and cause short telomere length were initially associated with the disease dyskeratosis congenita (DC), a condition characterized by mucocutaneous abnormalities and predisposition to bone marrow failure[124]. Following the cloning

of the human telomerase RNA gene, *TERC*, Kathleen Collins and colleagues showed that that the 3' end of TERC has an architecture consistent with that of H/ACA snoRNAs[125]. Contemporaneously, mutations in the gene encoding dyskerin, *DKC1*, which showed homology to the yeast H/ACA snoRNA associated pseudouridine synthase protein Cbf5p, had been associated with DC. The Collins group showed that dyskerin co-purifies with the telomerase complex, and found that DC patient cells had low TERC levels, low telomerase activity, and short telomere lengths. These data suggested that impaired telomere synthesis was the underlying cause of DC[126]. The subsequent identification of germline mutations in *TERC* itself in families with autosomal dominant DC[127] provided further strong support for the notion that the common underlying molecular cause of DC was aberrantly short telomeres.

Presently, inherited mutations in the telomerase components and related genes have been identified as causing several diseases beyond DC, including familial idiopathic pulmonary fibrosis (IPF)[128,129], aplastic anemia[130], as well as the early childhood onset disorders Hoyeraal-Hreidarsson syndrome(HH)[131], Revesz syndrome (RS)[132], and Coats plus syndrome[133,134]. It is now understood that these disorders exist as a spectrum, and patients can present with overlapping features. These disorders are collectively referred to as the telomere biology disorders (TBDs)[31]. TBDs can present at ages ranging from infancy in HH and RS, to late adulthood, such as in patients who develop pulmonary fibrosis and myelodysplastic syndrome. The prevalence of TBDs varies, with the earlier onset conditions DC, RS, and HH being rare, on the order of 1 in a million, while later onset presentations such as IPF are observed more commonly[135].

Presently, there are 18 genes which have been identified as causing the TBDs[31,32]. These include several components of the telomerase holoenzyme complex (*TERT*, *TERC*, *DKC1*, *NOP10*, *NHP2*, *WRAP53* (TCAB1)), several components of the shelterin complex (*TINF2*, *ACD*

(TPP1), *POT1*), and several components of the CST complex (*CTC1*, *TEN1*), as well as telomerase biogenesis factors (*PARN*, *NAF1*, *ZCCHC8*), telomere replication associated genes (*RTEL1*, *DCLRE1B* (Apollo), *RPA1*)[31], and the newly associated gene *TYMS* which encodes thymidylate synthase[32]. Of note, there have been no reports of a telomerase-null patient, and this is likely incompatible with life. There is some association between genotype and phenotype which have been observed, such as mutations clustered in exon 6 of *TINF2* which lead to extremely short telomeres and early onset disease in most cases[136]. In another example, while short telomere length is considered a diagnostic criteria for TBD diagnosis, there are reported cases where that mutations in certain genes may cause diseases driven by telomere dysfunction in the absence of global telomere shortening, such as observed in the Apollo cases[137] and in some patients with POT1 mutations[138], however, in general short telomere length is widely observed and thought to drive disease.

Patients diagnosed with TBDs generally face poor prognoses. Treatment for these disorders centered on supportive care and organ transplant[139]. Bone marrow transplant has been successfully used to treat TBD related bone marrow failure. Recent advances in transplant conditioning regimens using less intensive conditioning protocols have improved outcomes[140], however even after successful bone marrow transplant patients are at high risk for developing other life-threatening TBD manifestations including hepatic and pulmonary fibrosis[141]. In addition to transplant and blood transfusions, treatment with androgens can improve blood production in patients with bone marrow failure including TBD patients. In one study, the androgen danazol was found to significantly reduce the rate of telomere shortening in DC patients[142] using qPCR to measure telomere length, however this finding was not replicated in a follow up study employing the more accurate Flow-FISH method for telomere length measurement[143]. While androgen

therapy can be effective to improve blood counts, its duration of effect is not permanent, it can have side effects including virilization and dyslipidemia that can cause many patients to halt therapy, and is not considered a curative treatment for bone marrow failure in the TBDs[141]. Lung transplant can be considered to treat TBD related IPF patients, however outcomes are poor[144,145]. Presently, there are no approved targeted therapies to treat the underlying cause of TBDs and lengthen telomeres.

In addition to inherited rare mutations in telomere related genes which cause TBDs, common genetic variation leading to short telomeres is associated with increased risk of coronary artery disease and IPF[114]. Inherited short telomere length is a particularly strong risk factor for IPF, with one meta-analysis of mendelian randomization studies calculating that a genetically instrumented 1SD shorter telomere length is associated with a 5.81 fold higher odds of IPF (95% CI 3·56–9·50; $p=2{\cdot}19 \times 10^{-12}$)[146]. Collectively, both rare and common genetic variants which cause short telomeres predispose to severe disorders with poor outcomes.

The therapeutic hypothesis for telomere elongation as a treatment for the TBDs

There is significant human genetic evidence supporting the hypothesis that a therapeutic approach to lengthen telomeres would be beneficial in the treatment of the TBDs. Here, I review the relevant human genetic data available in support of this hypothesis.

First, there is strong evidence that short telomeres cause the TBDs:

1. *Telomere shortening is a common molecular defect downstream of TBD-causing mutations.* As described above, telomere length control is a common function shared between the telomerase components and shelterin complex. Short telomere length is widely observed

in TBD patients, and telomere length testing aids in the diagnosis and management of patients presenting with TBD manifestations[110]. Of note, the subcategory of TBD patients who have Coats plus disease commonly have mutations in CST complex genes and can present without short telomeres[31]. Coats plus will be treated as a separate category from the other TBDs going forward in this dissertation.

2. *Telomere length predicts age of onset of disease.* Telomere length declines with age, and molecular defects which cause more severe telomere shortening lead to earlier onset of disease manifestations[110,147].
3. *Genetic anticipation observed in TBDs suggests that inheriting short telomeres along with the disease-causing variant increases disease penetrance and leads to earlier onset.* This genetic anticipation was first observed in patients with *TERC* mutations[148], and has subsequently been observed in families with mutations in other TBD causing genes[31,153]. The observation that inheriting short telomere length in combination with the disease causing mutation leads to earlier disease onset argues that short telomere length contributes to disease manifestations.
4. *Inherited short telomere length even in the absence of short telomere causing mutations phenocopy to TBD manifestations in families.* This observation has been reported for multiple TBD related genes, and provides convincing evidence that short telomeres are sufficient to cause TBDs[149,150].

Second, there are several lines of evidence that restored telomere length or telomerase function could improve tissue function in TBD patients based on human genetics.

1. *Amongst mixed populations of cells with and without a telomerase defect, cells without a telomerase defect have a competitive growth advantage.* This phenomena is demonstrated by the skewed X chromosome inactivation observed in female carriers of pathogenic DKC1 mutations[151].
2. *Somatic reversion to restore gene function is recurrently observed in the bone marrow of TBD patients.* Examples of this phenomena have been frequently observed in TBD patients, including through the restoration of mutated alleles which has been observed in *TERC* and *DKC1*[31]. These data similarly demonstrate that cells with repaired telomere synthesis function have a strong competitive growth advantage in the hematopoietic system.
3. *Somatic telomerase activating mutations are uniquely common in the blood of TBD patients.* While clonal hematopoiesis is commonly observed with aging in the population[152,153], TBD patients have distinct recurrent mutations which drive clonal hematopoiesis compared with the general population, including mutations in shelterin components POT1 and TERF2IP which contribute to the negative regulation of telomerase activity, as well as TERT promoter mutations[154]. These data suggest that, even in the presence of the detrimental allele, genomic alterations which increase telomerase activity can endow cells with a replicative advantage.

Third, there is genetic evidence for a therapeutic window to safely lengthen telomeres in TBD patients, despite associations between long telomeres and increased cancer risk.

1. *TBD patients with somatic reversion events in their blood have lower rates of myelodysplastic syndrome*[154]. This finding suggests that restoring telomerase activity to

TBD patient cells can lower malignancy risk, potentially by reducing selective pressures promoting the outgrowth of transformed cells.

2. *Genetically determined longer telomere length is associated with increased lifespan in the population*[33]. Additionally, inherited long telomere length is associated with a reduced risk of coronary artery disease and interstitial lung disease[114]. Based on these data, the years of life lost due to a theoretically higher risk of cancer from telomere elongation may be offset by reduced risk of other lethal diseases.

Collectively, these data implicate telomere length insufficiency as the underlying cause of disease in the majority of TBD patients. Based on data from the hematopoietic system, there is strong support for the therapeutic hypothesis that a telomere lengthening drug could improve tissue function. While lifetime exposure to long telomere lengths increases the risk of malignancy, human genetic data indicate there is likely a therapeutic window to treat TBD patients with a therapy that promotes telomere synthesis.

Dissertation Review

Telomere length homeostasis is critical for cellular function and human health. Yet the mechanisms governing telomere length control are incompletely defined. In this dissertation, I perform the first genome-wide evaluation of the genetic control of telomere length in human cells, leading to my identification of dNTP metabolism genes as critical for human telomere length control. I demonstrate that upregulation of dNTP metabolism via salvaged nucleosides promotes telomere lengthening through activation of telomerase, including at doses which did not impact cell growth or cause replication stress. I develop an assay for the rapid assessment of telomerase activity within

human cells and apply this assay to dissect the metabolic regulation of telomere synthesis. Inherited mutations which lead to telomere length insufficiency cause a spectrum of fatal diseases termed the telomere biology disorders (TBDs), for which we lack effective targeted therapies. In this dissertation, I demonstrate that manipulation of dNTP metabolism through four different modalities can rescue telomere lengthening defects in TBD patient derived cells, including: 1) supplementation with thymidine, 2) supplementation with deoxyguanosine combined with the PNP inhibitor ulodesine, 3) inhibition of the dNTPase SAMHD1, 4) overexpression of an efficient deoxnucleoside kinase. By identifying a new aspect of human telomere length control, my work paves the way for further studies investigating the metabolic control of telomerase activity, and may open new avenues to therapeutically manipulate telomerase activity.

Chapter 2: Thymidine nucleotide metabolism controls human telomere length

Attributions

This chapter contains a modified version of an article entitled “Thymidine nucleotide metabolism controls human telomere length.” published in *Nature Genetics* on March 23, 2023 (Mannherz and Agarwal, 2023). Full authorship includes:

William Mannherz[1,2,3] and Suneet Agarwal[1,2,3]*

[1]Division of Hematology/Oncology and Stem Cell Program, Boston Children's Hospital, Boston, MA, USA.

[2]Pediatric Oncology, Dana-Farber Cancer Institute, Boston, MA, USA.

[3]Biological and Biomedical Sciences Program, Harvard/MIT MD-PhD Program, Harvard Stem Cell Institute, Harvard Initiative in RNA Medicine, and Department of Pediatrics, Harvard Medical School, Boston, MA, USA.

I performed the experiments, analyzed the data, and prepared the figures. I conceived of the project, designed experiments, and wrote the manuscript together with Suneet Agarwal. Noah Lampl provided technical assistance on experiments characterizing the long term culture of TYMS knockout cells and fibroblasts which were performed following the publication of the article and have been included here. Ronald Mathieu provided support with flow cytometry experiments. Alejandro Gutierrez and Kimberly Bodaar provided guidance and support with CRISPR/Cas9 screening. Suneet Agarwal oversaw the project.

Abstract

Telomere length in humans is associated with lifespan and severe diseases, yet the genetic determinants of telomere length remain incompletely defined. Here, we performed genome-wide CRISPR/Cas9 functional telomere length screening and identified thymidine (dT) nucleotide metabolism as a limiting factor in human telomere maintenance. Targeted genetic disruption using CRISPR/Cas9 revealed multiple telomere length control points across the dT nucleotide metabolism pathway: decreasing dT nucleotide salvage by nuclear thymidine kinase (*TK1*) deletion or *de novo* production by thymidylate synthase (*TYMS*) knock-out reduced telomere length, whereas inactivation of the dNTPase-encoding gene *SAMHD1* lengthened telomeres. Remarkably, supplementation with dT alone drove robust telomere elongation by telomerase in cells, and dTTP stimulated telomerase activity in a substrate-independent manner *in vitro*. In induced pluripotent stem cells derived from patients with genetic telomere biology disorders, dT supplementation or inhibition of *SAMHD1* promoted telomere restoration. Our results demonstrate a critical role of thymidine metabolism in controlling human telomerase and telomere length, which may be therapeutically actionable in patients with fatal degenerative diseases.

Introduction

Telomeres are repetitive DNA elements flanking linear chromosomes which promote genomic stability[155,156]. Telomere length decreases as cells divide because DNA polymerases cannot fully replicate linear chromosomes[6,7]. When critically short, telomeres initiate cellular senescence, arresting cell division[27]. This shortening is counteracted by telomerase, a reverse transcriptase[12] that uses an RNA template[13], *TERC*, to synthesize new telomeric repeats[16]. In Mendelian randomization studies, long telomeres are associated with increased lifespan[33], while inherited

mutations in genes regulating telomere maintenance are associated with lethal diseases manifesting with pulmonary fibrosis, liver cirrhosis, and bone marrow failure, collectively termed telomere biology disorders[31,157,158]. Despite the importance of telomere length homeostasis for cellular function and health, determinants of human telomere length control are incompletely defined[33].

dNTPs are common precursors for genome replication by DNA polymerases and telomere elongation by telomerase. Disruptions to DNA precursor metabolism can impair genome replication and are associated with genome instability, mitochondrial genetic diseases, and cancer[85,89,159–161]. Telomere synthesis occurs via a unique reverse transcription mechanism involving the ratcheting of an RNA template to generate hexanucleotide (5'-GGTTAG-3') repeats, with distinct dynamics and substrate preferences compared to DNA polymerases[108]. Despite evidence that nucleotide levels influence the enzymatic activity of reconstituted telomerase[71,73,74,162–164], a role for dNTP metabolism in regulating telomere length in humans at a cellular or organismal level has not been directly established. Here, we take advantage of methodologic advances[165,166] to perform the first genome-wide functional screen for human telomere length regulators. We identify dT nucleotide metabolism as a critical regulator of human telomere length, advancing our understanding of cellular metabolic pathways required for genomic integrity and pointing to potential novel therapies for lethal diseases with high unmet need.

Results

CRISPR screening links thymidine flux and telomere length

Fluorescence *in situ* hybridization using a peptide nucleic acid (PNA) telomere repeat probe coupled with flow cytometry (flow-FISH) is a clinically-validated telomere length assay performed on single cells[110,166]. We used flow-FISH as a phenotypic readout for CRISPR/Cas9

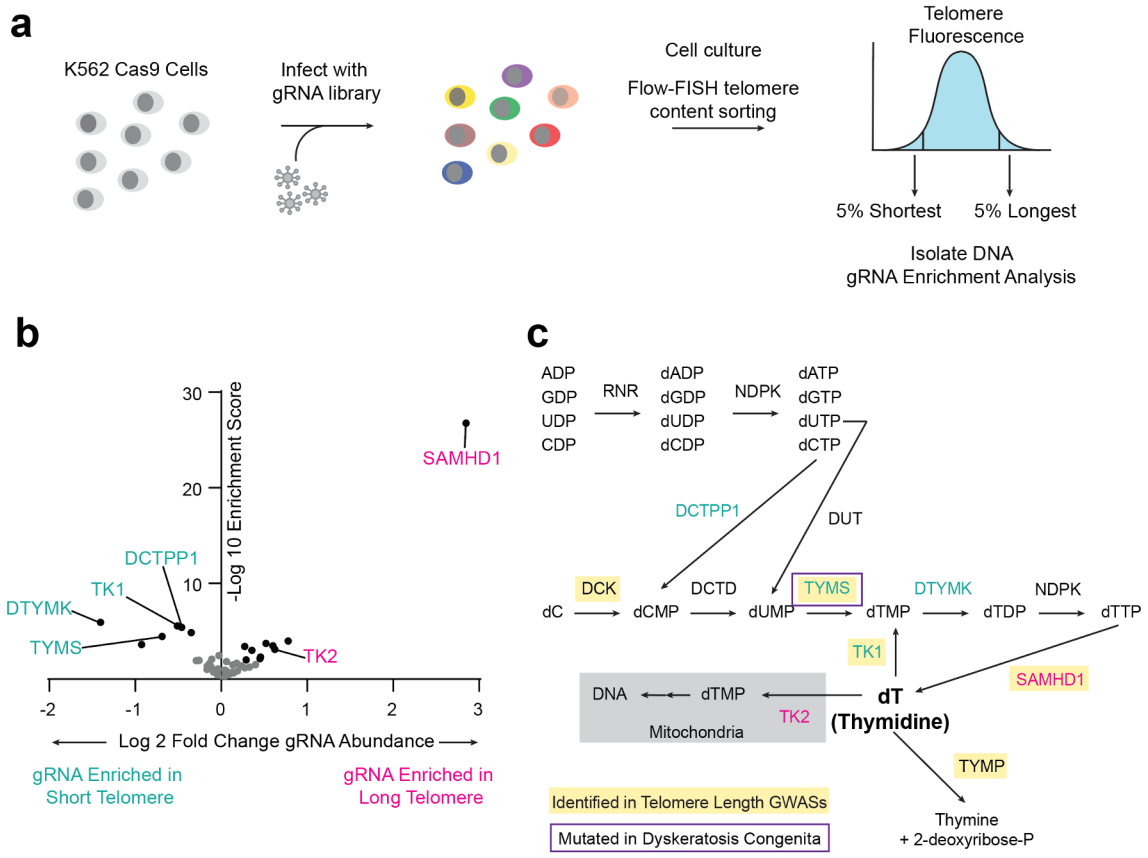
screening in human cells to identify novel genes regulating telomere length (**Fig. 1-1a**). K562 cells expressing SpCas9 (**Figure S1a-c**) were transduced with the Brunello genome-wide gRNA library[165] and cultured for 49 days, followed by isolation of cells harboring the longest and shortest 5th percentiles of telomere length using flow-FISH (**Figure S1d-g**). We isolated gDNA from the sorted populations, performed deep sequencing, and analyzed gRNA representation using the MAGeCK Robust Rank Algorithm (RRA)[167] (**Figure S1h,i**). We found that gRNAs targeting telomerase reverse transcriptase (*TERT*) were enriched in the short telomere population, while gRNAs targeting several components of shelterin, a telomere chromatin protein complex that negatively regulates telomere length[19,54,168,169], were enriched in the long telomere population, including *POT1*, *TERF1,* and *TERF2IP* (*RAP1*). These data validate our CRISPR screening strategy to identify tolerable genetic loss-of-function associated with human telomere length.

Unbiased pathway analysis of screening hits using MAGeCKFlute[170] revealed that gRNAs targeting pyrimidine nucleotide metabolism genes were enriched in the cell population with short telomeres (**Figure S1j**). Recent genome-wide association studies (GWAS) have also implicated nucleotide metabolism genes in telomere length control[33,34], and mutations at the thymidylate synthase (*TYMS*) locus have been newly identified in patients presenting with the telomere biology disorder dyskeratosis congenita[32]. Based on our screening results and the emerging human genetic data, we performed a second round of screening using a custom gRNA library targeting 53 nucleotide metabolism genes. Comparing gRNAs enriched in the sorted long and short telomere populations, we identified several genes implicated specifically in dT nucleotide metabolism (**Figure 1b,c**). In cells with short telomeres, we saw enrichment of gRNAs that disrupted genes predicted to promote dT nucleotide synthesis, including *DTYMK*, *TYMS*, *TK1*[171], and *DCTPP1*[87]. Conversely, gRNAs targeting genes predicted to reduce nuclear dT nucleotide levels, including the

dNTPase *SAMHD1*[92,93,172], were enriched in cells with long telomeres. Taken together, these results point to dT nucleotide levels as a novel regulator of telomere length in human cells.

Figure 2-1. Telomere length CRISPR/Cas9 screening reveals thymidine nucleotide metabolism genes are required for telomere length control. a, Diagram of flow-FISH telomere content screening strategy. Cas9-expressing K562 cells are transduced with a gRNA library, cultured for weeks at split ratios sufficient to maintain library representation, and sorted by flow-FISH to isolate cells with the highest and lowest 5% of telomere fluorescence. **b**, Results of CRISPR/Cas9 screening performed in duplicate, of 53 nucleotide metabolism genes with 10 gRNAs per gene and 200 non-targeting controls. gRNA enrichment was analyzed using the MAGeCK Robust Rank Algorithm (RRA). RRA gene enrichment score vs. $\log_2$ fold change gRNA abundance in high vs. low 5th percentile TelC-A647 fluorescence populations. Black dots represent genes significantly enriched in long or short populations with a false discovery rate < 0.05 calculated by the Benjamini-Hochberg Procedure. **c**, Diagram of thymidine (dT) nucleotide metabolism. Genes identified in recent GWASs[33,34] are highlighted. *TYMS* (boxed) was recently associated with dyskeratosis congenita[32].

Figure 2-1. (Continued)



Thymidine treatment increases telomere length in human cells

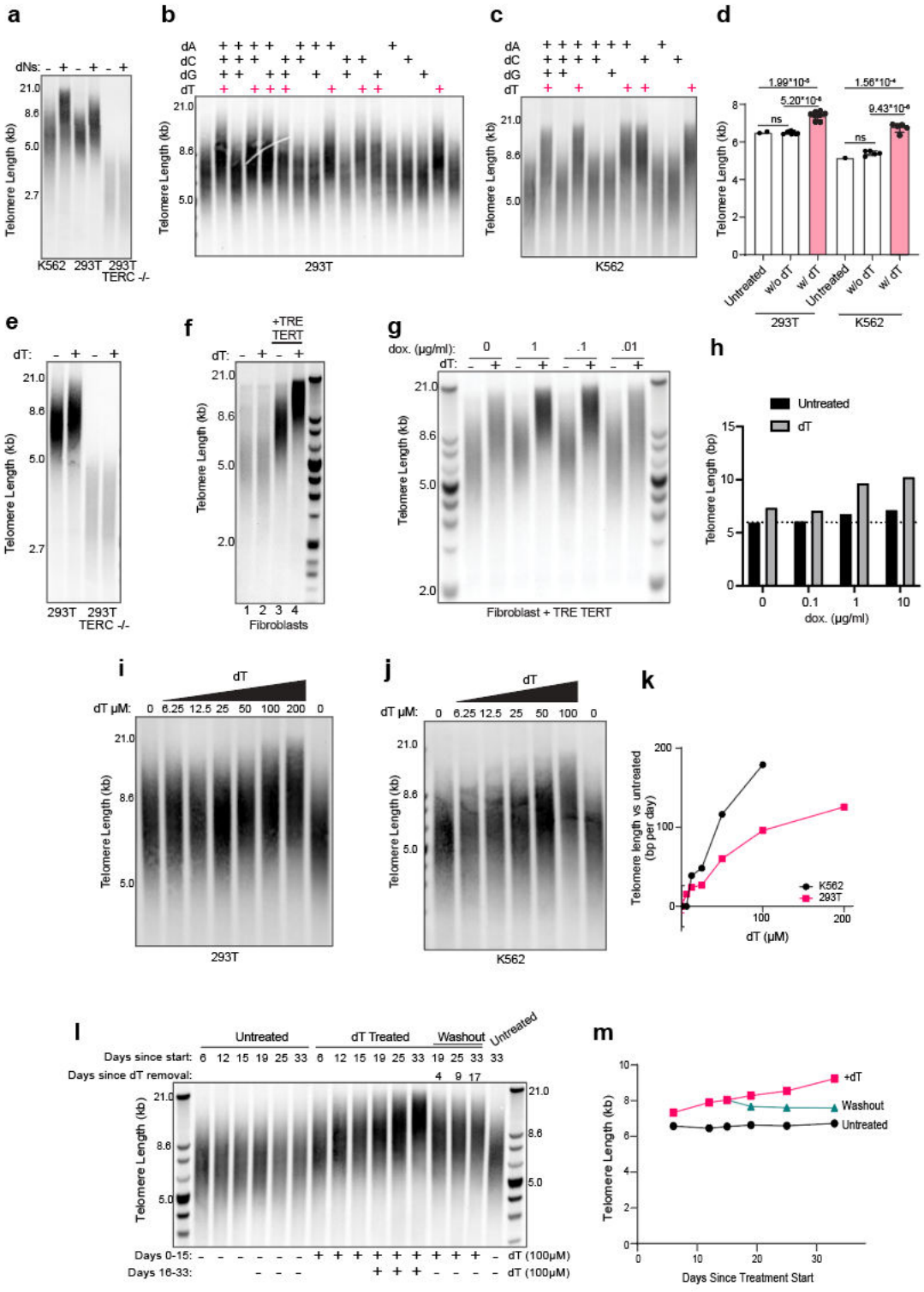
Based on these data, we tested whether manipulation of nucleotides could alter telomere length in human cells. Deoxynucleoside (dN) supplementation can increase cellular nucleotide levels via salvage pathway kinases[171,173]. Remarkably, supplementing K562 or 293T cell culture media with the four canonical dNs drove rapid telomere lengthening by thousands of nucleotides within 8 days (**Figure 2-2a**). When we repeated the experiment in telomerase-negative *TERC*-null 293T cells (**Figure 2-2a** and **S2a-g**), we found no increase in telomere length, indicating that telomerase is required for dN-mediated telomere lengthening. To identify which dNs promote telomere elongation, we treated 293T (**Figure 2-2b**) and K562 cells (**Figure 2-2c**) with dNs individually or in combinations. We found all combinations that included dT promoted telomere lengthening, as did dT alone, while no combination lacking dT elongated telomeres (**Figure 2-2b-d**). Again, dT treatment of telomerase-negative *TERC*-null 293T cells failed to drive detectable telomere elongation (**Figure 2-2e**). Similarly, in fibroblast cells which lack telomerase activity at baseline, dT treatment for had no effect on telomere length, whereas fibroblast cells engineered to express TERT from a doxycycline inducible construct showed increased telomere lengthening from dT after culture for one month, with a greater telomere lengthening effect at higher levels of telomerase expression (**Figure 2-2f-h**). Collectively, these results demonstrate that dT supplementation alone can drive rapid and robust telomere elongation in human cells in a telomerase-dependent manner, and offer an explanation for the genetic data implicating nucleotide biosynthetic pathways in human telomere length regulation.

We next evaluated how treatment with escalating doses of dT impacted telomere length. We found a continuous dose response in telomere elongation after dT treatment up to 200 μM in 293T and 100 μM in K562 cells (**Figure 2-2i-k**). We also confirmed that dT from different

manufacturers, each of >98% purity, promoted telomere elongation similarly (**Figure S3a**). To study the kinetics of telomere length changes after dT treatment and its withdrawal, we performed a time-course in 293T cells and found that dT supplementation gradually and continually increased telomere length, over 33 days (**Figure 2-2l,m**). Withdrawal of dT after 15 days aborted telomere elongation, indicating that the effects of dT on telomere length depend on exposure rather than triggering autonomous telomere lengthening mechanisms (**Fig. 2-2l,m**). These data indicate that dT supplementation promotes gradual, exposure-dependent, and reversible telomere elongation in human cells.

Figure 2-2. Thymidine treatment drives telomerase-dependent telomere lengthening in human cells. Terminal restriction fragment Southern blot (TRF) probed for the telomere repeat of K562, 293T, or *TERC*-null (-/-) 293T cells treated with or without deoxyribonucleosides (dNs; 100 μM each of dA, dC, dG and dT) for 8 days. **b**, TRF of 293T cells treated with 100 μM of the indicated deoxynucleoside(s) for 9 days. Untreated lanes are technical replicates. **c**, TRF of K562 cells treated with 100 μM of the indicated deoxynucleoside(s) for 8 days. **d**, Quantification of **b** and **c** (see Methods). 293T without dT (n = 8 samples) or with dT (n = 8 samples). K562 without dT (n = 5 samples) or with dT (n = 5 samples). P value calculated with One-Way ANOVA using Bonferroni correction for multiple comparisons for each cell line. Data presented as mean +/- s.d.; ns, $P > 0.05$. **e**, TRF of 293T or 293T *TERC*-null cells treated with or without 100 μM of thymidine (dT) for 7 days. **f**, TRF of normal human fibroblasts treated with 100 μM dT as indicated for 6 weeks (lanes 1 and 2) and normal human fibroblasts stably expressing hTERT from a tetracycline response element (TRE) inducible promoter as indicated which were cultured in the presence of 1 μg/ml doxycycline and with treated with 100 μM dT as indicated for one month (lanes 3 and 4). **g,** TRF of fibroblasts expressing TRE-hTERT cultured in the presence of 100 μM dT and doxycycline as indicated for one month. **h,** Quantification of **g** as in **d**. **i**, TRF of 293T cells treated with the indicated dose of dT for 10 days. **j**, TRF of K562 cells treated with the indicated dose of dT for 8 days. **j**, Quantification of **i** and **j**, as in **d**. **i**, 293T cells treated with or without 100 μM of dT for the indicated period of time. On day 15, dT-treated cells were split and continued to be cultured either with or without 100 μM dT for the indicated number of days. Day 33 untreated lanes are technical replicates. **j**, Quantification of **i**. Panels presented in this figure are the results of single experiments.

Figure 2-2. (Continued)

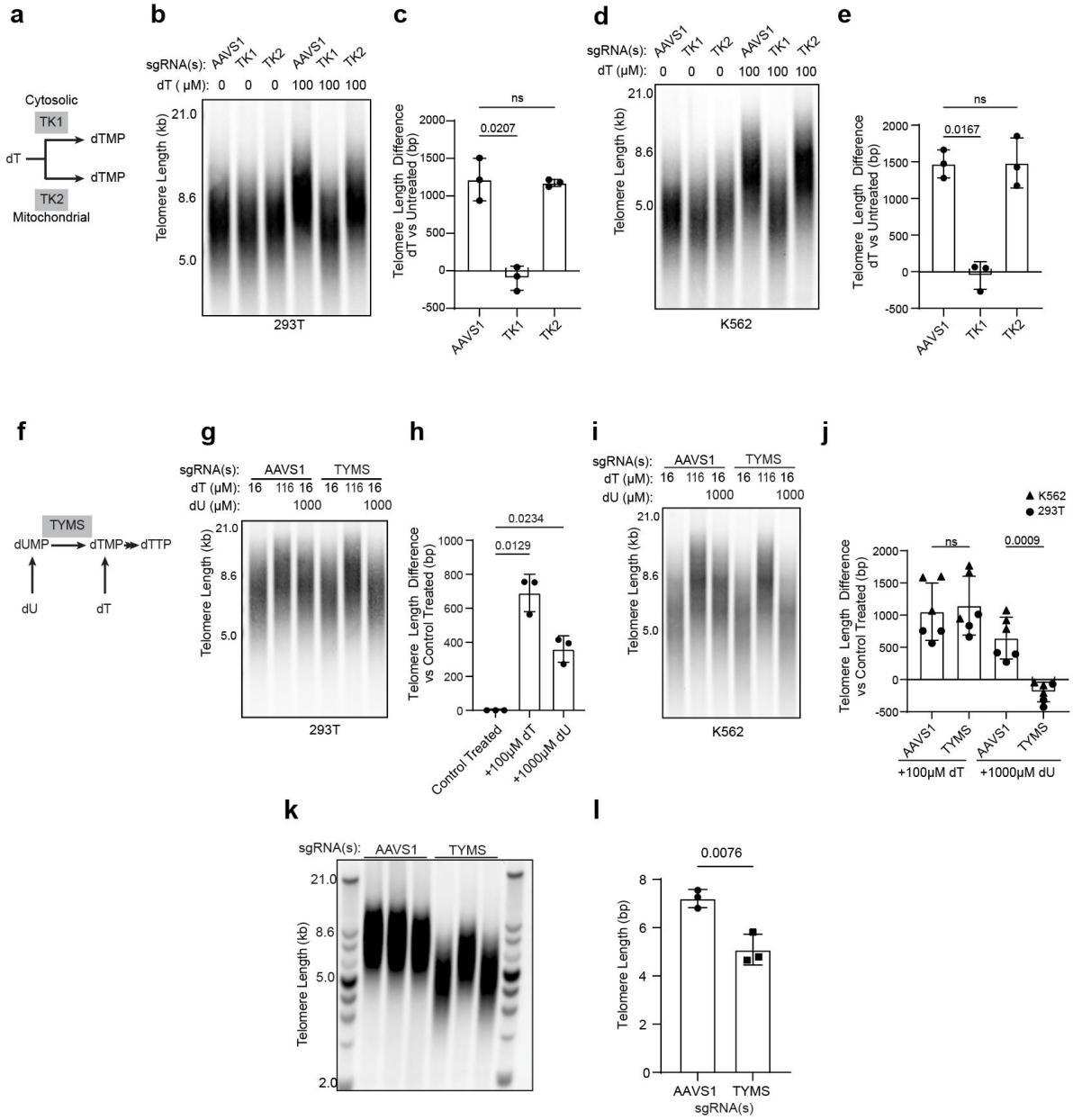


TK1 is required for telomere lengthening by thymidine

dT salvage occurs through distinct pathways to generate dTTP for mitochondrial versus nuclear genome synthesis (**Figure 2-3a**). Thymidine kinase 1 (TK1) acts in the cytosol to generate dTMP available for nuclear genome replication, while thymidine kinase 2 (TK2) acts in mitochondria to generate dT nucleotides for mitochondrial genome synthesis[85]. As telomeres reside in the nuclear genome, we hypothesized that dT-mediated telomere lengthening requires functional TK1 but not TK2. To test this hypothesis, we electroporated 293T or K562 cells with SpCas9 and gRNAs targeting either *TK1* or *TK2*, or with a gRNA targeting the *AAVS1* control locus (**Figure S3b,c**). Consistent with our hypothesis, we found that *TK1*-edited cells showed a complete abrogation of telomere lengthening after dT treatment (**Figure 2-3b-e**), whereas *TK2*-edited cells showed telomere length increases equivalent to control *AAVS1*-targeted cells (**Figure 2-3b-e**) in the presence of dT. Without dT treatment, we found modest telomere length decreases in *TK1* knockout cells (**Figure 2-3b,d** and **Figure S3d**), as anticipated from our screening data. These results indicate that cytosolic phosphorylation of dT to generate dTMP by TK1 is required for telomere lengthening after dT treatment. To assess how dT supplementation alters cellular nucleotide levels, we performed liquid chromatography-mass spectrometry[174] on 293T cells treated with 100 μM of dT for 24 hours and found that dT treatment increased levels of dTMP, dTDP and dTTP (**Figure S3e**). These data are consistent with our genetic data that dT exerts its effects on telomere length by conversion into dT nucleotides.

Figure 2-3. Thymidine nucleotide metabolism genes control thymidine mediated telomere lengthening. **a**, Diagram of dT salvage. **b**, Representative TRF of 293T cells targeted with Cas9 and the indicated sgRNA(s), followed by treatment with the indicated dose of dT for 14 days. **c**, Quantification of **b**. *n* = 3 biological replicates, *P* values calculated using RM One-Way ANOVA with the Geisser-Greenhouse correction and Dunnett's multiple comparison test. **d**, Representative TRF of K562 cells targeted with Cas9 and the indicated sgRNA(s), followed by treatment with the indicated dose of dT for 10 days. **e**, Quantification of **d** as in **c**. *n* = 3 biological replicates. **f**, Diagram of dT and dU salvage. **g**, Representative TRF of 293T cells targeted with Cas9 and the indicated sgRNA(s), followed by treatment with the indicated doses of dT and dU for 10 days. **h**, Quantification of median telomere length in **g** as in **c**. *n* = 3 biological replicates. **i**, Representative TRF of K562 cells targeted with Cas9 and the indicated sgRNA(s), followed by treatment with the indicated doses of dT and dU for 10 days. **j**, Quantification of median telomere length in **g** and **i**. *P* values calculated using RM One-Way ANOVA with the Geisser-Greenhouse correction and Bonferroni's multiple comparison test, *n* = 3 biological replicates for each cell line. Data in **c**, **e**, **h** and **j** are presented as means +/- s.d.; ns, $P > 0.05$. **k**, TRF of 293T cells targeted with the indicated sgRNA, which were cloned and confirmed for editing via Sanger sequencing. n=3 clones per genotype. TRF performed after two months in culture following gene editing. All cells were continuously cultured in the presence of 16 μM dT. **l**, quantification of **k** as in **c**, n=3 clones per genotype.

Figure 2-3. (Continued)



TYMS is required for telomere lengthening by deoxyuridine

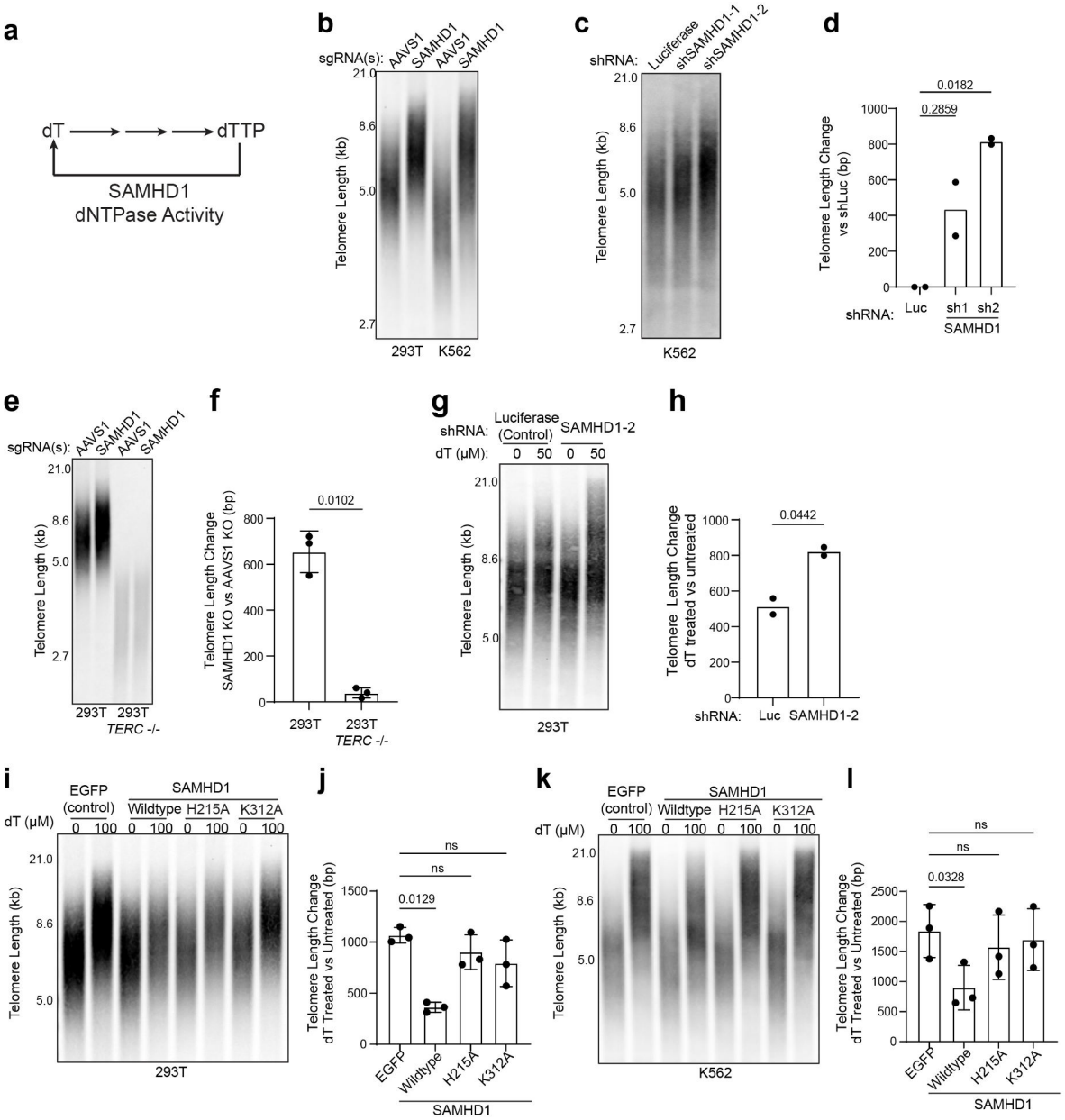
As an alternative to dT salvage, dTMP can be *de novo* synthesized from deoxyuridine monophosphate (dUMP) by TYMS using one carbon transfer from 5,10-methylene-tetrahydrofolate (**Figure 2-3f**). Deoxyuridine (dU) nucleoside can be salvaged via TK1 to form dUMP[171]. Therefore, we tested the impact of dU supplementation in 293T cells and found telomere elongation to a degree similar to dT over the course of 10 days, albeit at 10× the concentration (1 mM) (**Figure S3f**). Folate, however, did not appear to be limiting as its supplementation in 293T cells did not yield telomere elongation (**Figure S3f**). To test whether dU increases telomere length via conversion of dUMP to dTMP by TYMS (**Fig. 2-3f**), we targeted *TYMS* in 293T and K562 cells using CRISPR/Cas9 (**Figure S3g**). *TYMS*-deficient cells required salvaged dT for survival; thus, both *TYMS* edited and control *AAVS1* edited cells were treated with a baseline level of 16 μM of dT. We then treated cells with either 100 μM of additional dT (116 μM total) or with 1 mM of dU for 10 days and evaluated telomere length. We found that *TYMS*-knockout cells remained responsive to increased doses of dT to promote telomere lengthening, while dU could no longer promote telomere lengthening in *TYMS*-deficient cells (**Figure 2-3g-j**). Of note, even in the presence of 16 μM dT, cloned TYMS deficient 293T cells showed reduced telomere length compared with similarly cultured AAVS1 targeted clones (**Figure 2-3k,l**), indicating that defective thymidine de novo synthesis leads to telomere shortening in human cells, and supporting the results from our targeted screening. Collectively, these results demonstrate that dU lengthens telomeres via conversion into dTMP, and that in cells with deficient *de novo* dT nucleotide synthesis machinery due to *TYMS* inactivation, dT supplementation can increase dT nucleotide levels via the salvage pathway to lengthen telomeres.

SAMHD1 restricts human telomere length

SAMHD1 regulates cellular dNTP levels by degrading all four canonical dNTPs, including dTTP, into dNs[92,93,172] (**Figure 2-4a**). This function has been suggested to restrict retroviruses by limiting dNTP pools available for reverse transcription[92,94]. In our screen for telomere length regulators, *SAMHD1* gRNAs drove robust telomere elongation (**Figure 2-1b**). Recent biochemical studies demonstrate that SAMHD1 is enriched at telomeric chromatin[175], and GWAS have associated *SAMHD1* with human telomere length[33]. However, effects of manipulating SAMHD1 on human telomere length have not been shown. We therefore directly evaluated how disruption of *SAMHD1* could impact telomere length homeostasis in human cells lines. We found that deletion of *SAMHD1* by CRISPR/Cas9 was tolerated and lengthened telomeres by thousands of nucleotides in 27 days (**Figure 2-4b** and **Figure S4a**), in line with our screening results. Inhibiting SAMHD1 using shRNA-mediated RNA interference also showed a telomere lengthening effect (**Figure 2-4c,d** and **Figure S4b-e**). In *TERC*-null 293T cells, however, we found no change in telomere length upon *SAMHD1* knockout or knockdown (**Figure 2-4e,f** and **Figure S4e**), indicating that telomere lengthening due to SAMHD1 loss-of-function occurs by a telomerase-dependent mechanism. These results demonstrate that SAMHD1 controls telomere length in human cells.

Figure 2-4. SAMHD1 restricts human telomere length and limits thymidine-mediated telomere elongation. a, Diagram of SAMHD1 dNTPase activity. **b**, TRF of 293T or K562 cells cultured for 27 days following Cas9-sgRNA targeting with the indicated sgRNA(s); results from a single experiment. **c**, Representative TRF of K562 cells cultured for 33 days following infection with shRNA expression constructs targeting luciferase (control) or SAMHD1. **d**, Quantification of telomere length in **c**. *P* value calculated by RM One-Way ANOVA with the Geisser-Greenhouse correction and Dunnett's multiple comparison test, $n = 2$ biological replicates. **e**, Representative TRF of 293T or 293T *TERC* -/- cells cultured for 14 days following Cas9-gRNA targeting with the indicated sgRNA(s). **f**, Quantification of **e**. *P* value calculated using paired two-sided *t* test, $n = 3$ biological replicates. **g**, Representative TRF of 293T cells transduced with the indicated shRNA construct, then supplemented with the indicated dose of dT for 8 days. **h**, Quantification of **g** as in **f**. $n = 2$ biological replicates. **i**, Representative TRF of 293T cells overexpressing EGFP or SAMHD1 of the indicated genotype, and supplemented with the indicated dose of dT for 10 days. **j**, Quantification and statistical analysis of **i** as in **d**..$n = 3$ biological replicates. **k**, Representative TRF of K562 cells manipulated as in **i**. **l**, Quantification and statistical analysis of **k** as in **d**. $n = 3$ biological replicates. Data in **d**, **f**, **h**, **j** and **l** are presented as means; error bars indicate s.d.; ns, $P > 0.05$.

Figure 2-4. (Continued)



Because SAMHD1 is known to degrade dTTP[92,172] (**Figure 2-4a**), we asked whether SAMHD1 restricts the degree of telomere lengthening from dT treatment. Five days after transduction with a *SAMHD1* targeting shRNA, we treated cells with or without 50 μM dT for eight days. We found that the combined effect of *SAMHD1* knockdown and dT treatment produced greater telomere lengthening (823 ± 33 bp) compared to dT treatment alone (514 ± 63 bp) (**Figure 2-4g,h**). SAMHD1 has several proposed functions beyond its dNTPase activity, including contributing to homology directed repair and replication fork progression[176,177]. To investigate whether SAMHD1 dNTPase activity restricts dT-mediated telomere lengthening, we overexpressed two different dNTPase-deficient versions of SAMHD1 in cells[178,179]. We found that overexpression of wild-type SAMHD1 reduced telomere lengthening following dT treatment, compared to control cells overexpressing EGFP. In contrast, overexpression of dNTPase-deficient SAMHD1^{H215A} or SAMHD1^{K312A} variants could not restrict telomere lengthening from dT to the same degree (**Figure 2-4i-l** and **Figure S4f**). Collectively, these data indicate that SAMHD1 dNTPase activity regulates telomere length homeostasis in human cells, and point to dTTP as a downstream metabolite promoting telomere elongation after dT supplementation.

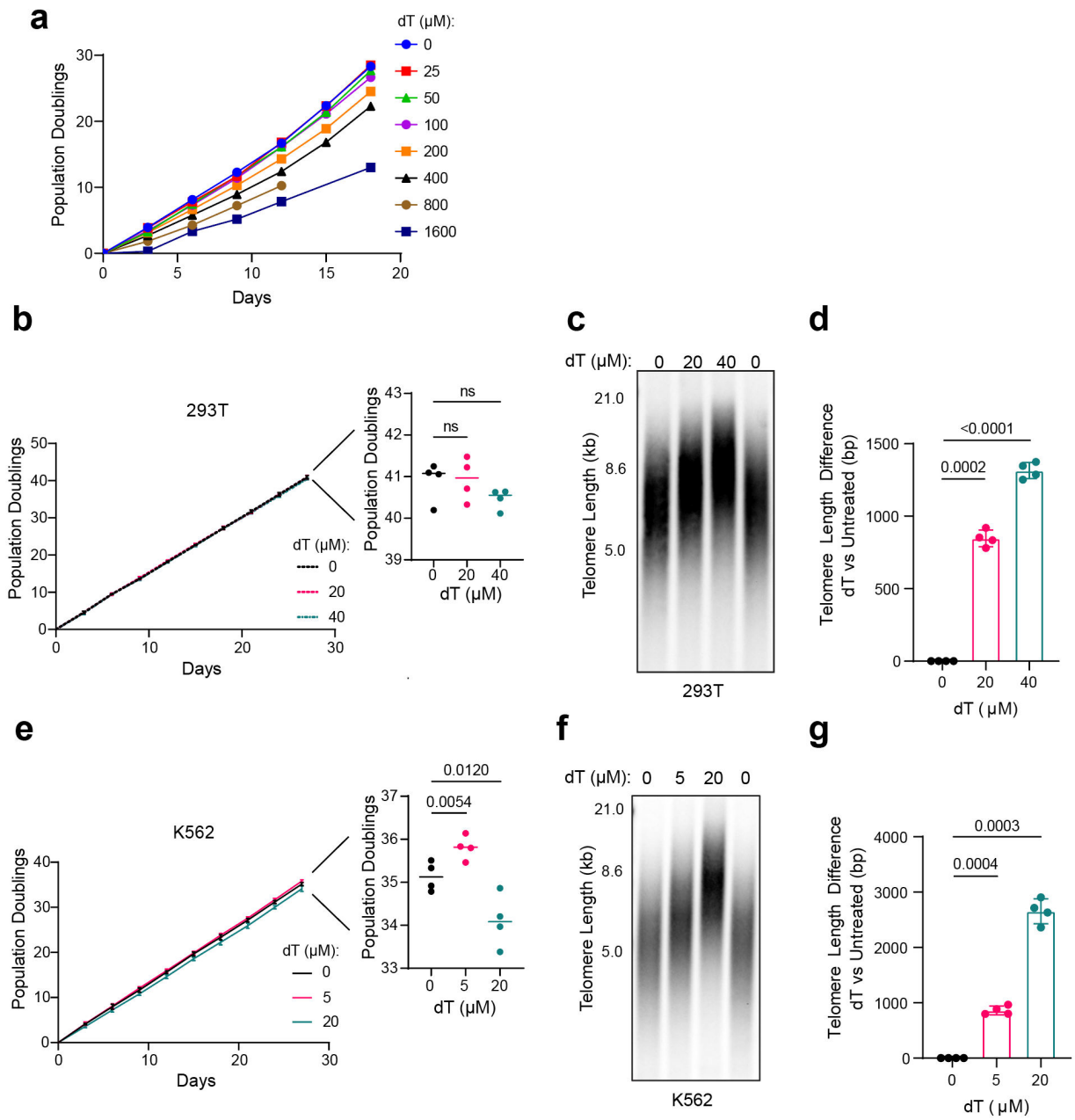
Thymidine elongates telomeres without inhibiting cell growth

dT is commonly used to inhibit cell cycle progression, arresting cells in S phase at doses in the millimolar range[180,181]. We asked whether dT-mediated telomere lengthening could be dissociated from cell cycle effects of dT. When 293T cells were treated with increasing doses of dT, growth was minimally impacted at doses below 100 μM (**Figure 2-5a**). We therefore chose doses with no discernable effects on growth and evaluated their impact on telomere length. We found that

supplementation of 293T cells with 20 μM or 40 μM dT for 34 days drove robust telomere lengthening with undetectable impact on cellular growth (**Figure 2-5b-d**). Similar results were seen in K562 cells treated with low doses of dT for 34 days (**Figure 2-5e-g**). DNA content staining and flow cytometry similarly showed no detectable changes in cell cycle distribution at dT doses below 100 μM in 293T cells and below 12.5 μM in K562 cells (**Figure S5a-d**). These data indicate that the slowing of cell growth is not required for telomere lengthening from thymidine treatment.

Figure 2-5. Telomere lengthening from dT treatment occurs without inhibiting cell growth. **a**, Growth curve of 293T cells treated with the indicated doses of dT. **b**, Growth curves of 293T cells treated with the indicated dose of dT. n = 4 biological replicates, inset graph shows population doublings after 27 days, P value calculated using RM One-Way ANOVA with the Geisser-Greenhouse correction and Dunnett's multiple comparison test. **c**, Representative TRF of 293T cells from **b**, after 34 days of culture in media containing the indicated dose of dT. **d**, Quantification of **c**. n = 4 biological replicates. P values calculated as in **b**. **e**, Growth curves of K562 cells treated with the indicated dose of dT. n = 4 biological replicates, quantification and statistical analysis as in **b**. **f**, Representative TRF of K562 cells from **e**, after 34 days of culture in media containing the indicated dose of dT. **g**, Quantification of **f**. n = 4 biological replicates, P values calculated as in **b**. Data in **b**, **d**, **e** and **g** are presented as means; error bars indicate s.d.; ns, $P > 0.05$.

Figure 2-5. (Continued)



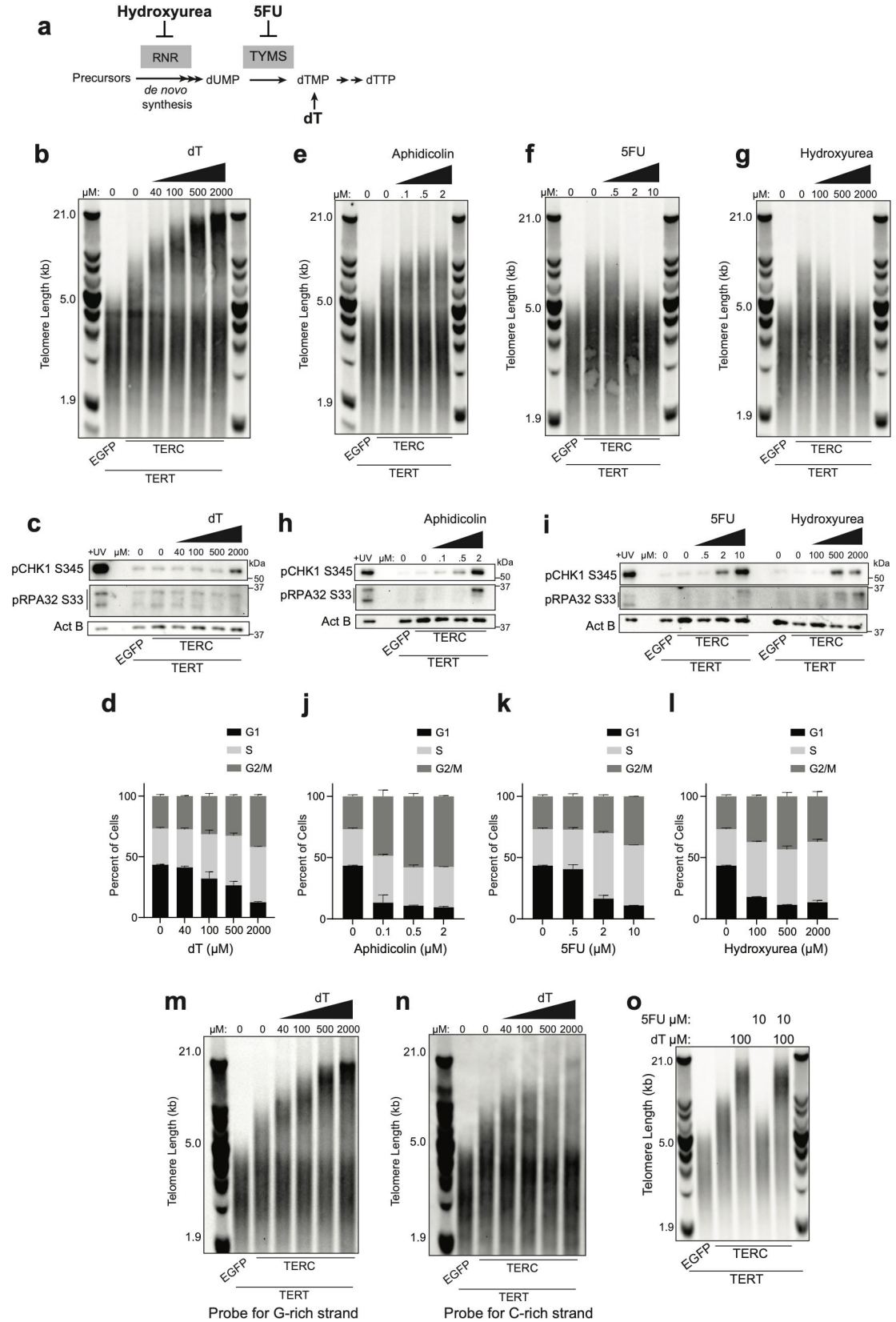
Thymidine elongates telomeres without replication stress

dT supplementation increases levels of dTTP and can reduce dCTP levels, leading to replication stress at high doses. Because replication stress signaling has been implicated in telomerase biology[182–184], we asked whether replication stress induction explained the telomere length increases seen with dT treatment. We first tested whether telomere elongation is a universal response to replication stress-inducing compounds. When we treated 293T cells with aphidicolin, which inhibits DNA polymerases, at doses maximally-tolerated for cell growth, we found telomere elongation after 10 days (**Figure S6a**), as previously observed[184]. However, treatment with hydroxyurea, which blocks deoxyribonucleotide production by ribonucleotide reductase (RNR; **Figure 2-6a**), up to doses permissible for cell growth, did not change telomere length after 10 days (**Figure S6a**). This suggested to us that replication stress induction may not cause telomere elongation in all cases. However, cytotoxicity limited our ability to apply higher doses of replication stress-inducing compounds for time periods long enough to study telomere length changes. To study the relationship between replication stress, dT, and telomere length more acutely, we transfected *TERC*-null 293T cells with expression vectors encoding *TERT* and *TERC*, generating 'super-telomerase' cells[48], which showed telomere elongation within two days (**Figure S6b, lanes 1 and 3**). Remarkably, we found that treatment of super-telomerase cells with dT for only 30 hours robustly increased telomere repeat synthesis in a dose-responsive and telomerase-dependent manner (**Figure 2-6b** and **Figure S6b, lanes 3 and 4**). Of note, this stimulatory effect on telomerase could be observed with only 40 μM dT, far below doses that induce replication stress signaling as measured by immunoblotting for pCHK1-S345 and pRPA32-S33 (**Figure 2-6c**), and below those that significantly impacted cell cycle progression (**Figure 2-6d** and **Figure S6e**). Using this system, we next asked how high-dose treatment with replication stress-inducing agents

such as aphidicolin, hydroxyurea, and the TYMS inhibitor 5FU influence telomere synthesis compared to dT. We found that treatment of super-telomerase cells with aphidicolin for 30 hours drove detectable increases in telomere length, albeit to a lesser extent than dT (**Figure 2-6e**). However, rather than elongating telomeres like dT or aphidicolin, treatment with hydroxyurea or 5FU ablated telomere elongation by telomerase (**Figure 2-6f,g**). Despite the markedly different effects on telomere biology seen at the highest doses of dT, aphidicolin, 5FU, or hydroxyurea, all induced similar levels of replication stress signaling (**Figure 2-6h,i**) and had similar impacts on cell cycle progression (**Figure 2-6j-l** and **Figure S6f-h**). Collectively, these data demonstrate that replication stress signaling induction does not universally promote telomere synthesis and does not explain the telomere lengthening in cells treated with dT at low doses.

Figure 2-6. Induction of replication stress is insufficient to explain telomere lengthening from dT treatment. a, Diagram of the effect of dT, 5FU, and hydroxyurea on dT nucleotide metabolism. RNR, ribonucleotide reductase. **b**, T R F Southern blot of 293T *TERC*-null cells transfected with the indicated expression vectors, cultured for 18 hours, then treated with the indicated dose of dT for 30 hours. Representative blot shown from two biological replicates. **c**, Immunoblot of cells from **b** using the indicated primary antibodies. UV-treated 293T cells used as a positive control. **d**, Cell cycle analysis of cells from **b** measured by DAPI staining and flow cytometry, displaying the percentage of cells in each gate. Data from four biological replicates shown for untreated cells and from two biological replicates shown for treated cells. Error bars indicate standard deviation. **e-g**, TRF Southern blot of 293T *TERC*-null cells transfected with the indicated expression vectors, cultured for 18 hours, then treated with the indicated doses of aphidicolin (**e**), 5FU (**f**), or hydroxyurea (**g**) for 30 hours. Representative blots from two biological replicates. **h,i**, Immunoblot of cells from **e-g**, as in **c**. **j-l**, Cell cycle analysis of cells in **e-g** by DAPI staining and flow cytometry, as in **d**. Data from four biological replicates shown for untreated cells and from two biological replicates shown for treated cells. Untreated samples are the same as in **d**. **m**, TRF Southern blot of 293T *TERC*-null cells transfected with the indicated expression vectors, cultured for 18 hours, then treated with the indicated doses of 5FU and dT for 30 hours. **n**. TRF of 293T *TERC*-null cells manipulated as in **b**. **m**, TRF from **n** was stripped and re-probed using a probe complementary to the telomeric C-rich strand repeat. Data in **d**, **j**, **k** and **l** are presented as means; error bars indicate s.d.; ns, $P > 0.05$. Full-length western blots are provided as source data.

Figure 2-6. (Continued)



Given the rapid extension of G-strand by telomerase observed in dT treated super telomerase expressing cells, we asked whether the telomeric C-strand was similarly extended. Stripping and re-probing blots for C-strand strand telomeric signal revealed that high doses of dT led to an increased accumulation of high molecular weight G-strand signal compared with C-strand signal (**Figure 2-6m,n**), indicative of insufficient C-strand synthesis to keep up with rapid G-strand elongation by telomerase within this brief time window.

Substrate-independent enhancement of telomerase by dTTP

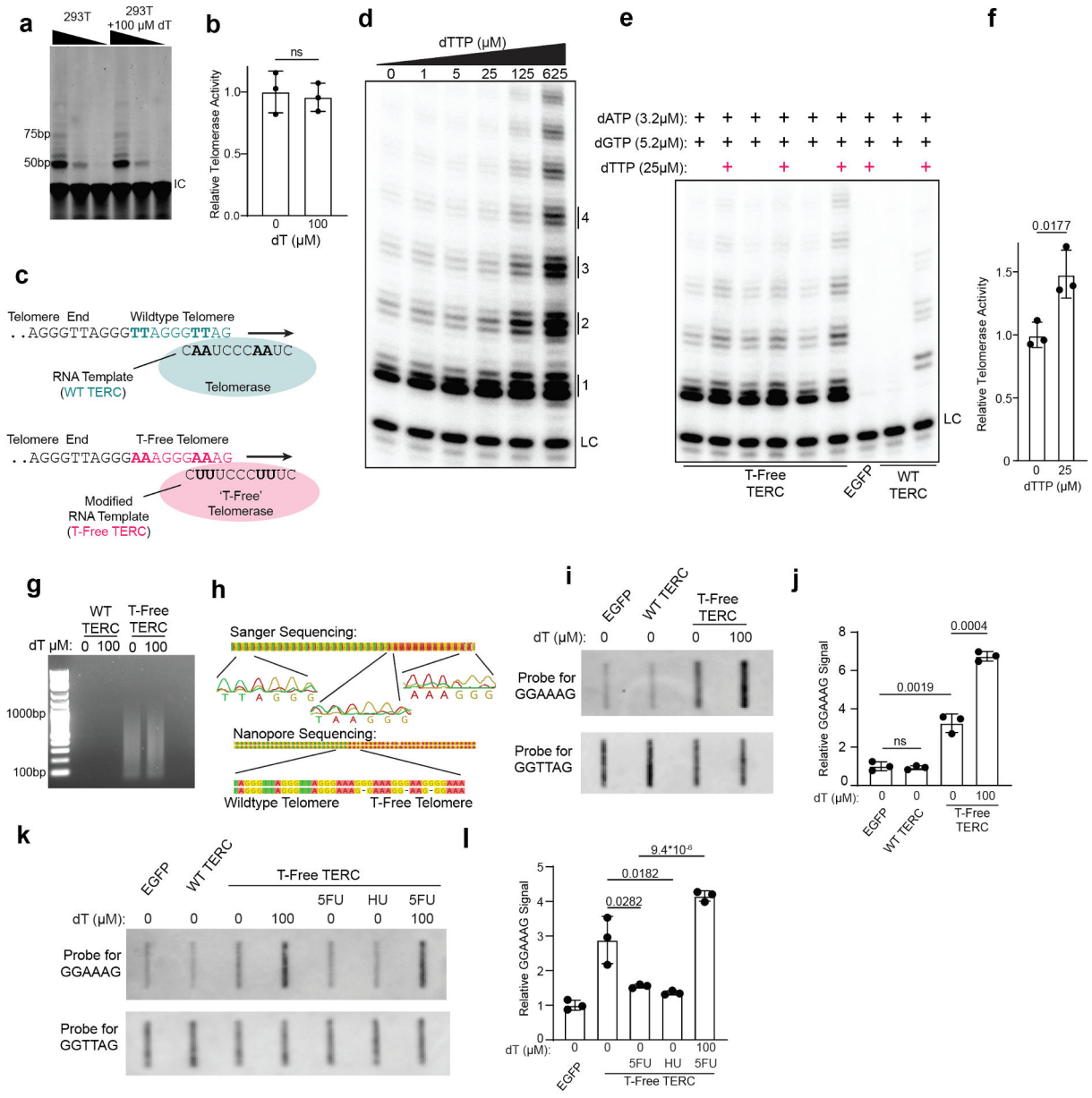
The timeframe and magnitude of the effects of dT and 5FU on telomeres in super-telomerase cells strongly suggested to us that thymidine nucleotides might directly impact telomerase activity. Given that high dose 5FU completely inhibited telomere elongation in super-telomerase cells (**Figure 2-6f**) and acts by inhibiting TYMS to limit *de novo* dTTP production, we asked whether dT supplementation could rescue telomere synthesis following 5FU treatment. Indeed, we found that dT treatment restored telomere elongation despite maximal doses of 5FU (**Figure 2-6o**). These data show that 5FU inhibits telomerase activity by limiting *de novo* thymidine nucleotide production and provide further evidence that thymidine nucleotide synthesis is required for telomerase activity.

The effects of thymidine nucleotides on telomerase activity could be from increasing the quantity of telomerase holoenzymes per cell, or alternatively by enhancing telomerase function. To test the former possibility, we measured the abundance of active telomerase enzymes in cells using the telomeric repeat amplification protocol (TRAP) assay and found no difference in telomerase activity in lysates from 293T cells treated with or without 100 μM dT (**Figure 2-7a,b**). These data indicate that dT treatment does not change the overall quantity of telomerase

holoenzymes in cells. Next, to test the effects of dTTP on telomerase function *in vitro*, we performed the TRAP assay with increasing levels of exogenous dTTP and found enhanced telomerase activity (**Extended Data Fig. S7a,b**). However, because dTTP is a direct substrate for GGTTAG repeat synthesis by telomerase, these experiments could not distinguish substrate-dependent versus substrate-independent effects of dTTP on telomerase activity. To study this further, we engineered a modified *TERC* expression vector with the template region encoding "T-free" repeats (GGAAAG) rather than wild-type (GGTTAG) repeats (**Figure 2-7c**), allowing us to interrogate potential substrate-independent effects of dTTP on telomerase activity. When we tested T-free super-telomerase cell extracts in a modified TRAP assay (**Figure S7c,d**), we found increased T-free telomerase activity with increasing dTTP levels (**Figure 7e-h**). Sequencing T-free telomerase TRAP products demonstrated that thymidine was not represented in the extended products (**Figure 7i-k**). These results confirmed that T-free telomerase does not use dTTP as a substrate, and surprisingly suggested a substrate-independent effect of dTTP on telomerase activity**.** To determine this without the potential confounder of PCR amplification in the TRAP assay, we directly tested the effects of dTTP on immunopurified T-free telomerase, as measured by incorporation of α-^{32}P-dATP on a telomere-repeat oligonucleotide substrate[72]. Remarkably, dTTP enhanced T-free telomerase activity in a dose-dependent manner (**Figure 2-7d**), with levels approximately 50% higher at a concentration of 25 μM (**Figure 2-7e,f**), and with a greater effect on longer telomerase products suggestive of increased telomerase processivity (**Figure S7l**). Taken together, these results demonstrate that dTTP is capable of increasing telomerase activity in a manner independent of its role as a substrate, potentially through an allosteric mechanism.

Figure 2-7. dT nucleotides enhance human telomerase activity independent of dTTP's role as a telomerase substrate. a, Representative TRAP assay of 293T cells treated as indicated for 3 days. **b**, Quantification of **a**. *n* = 3 biological replicates, *P* value calculated using unpaired two-sided *t* test. **c**, Diagram of wildtype and 'T-free' telomerase. **d**, Direct telomerase assay using immunopurification of overexpressed, tagged TERT co-transfected with T-free TERC into 293T *TERC*-null cells. LC: loading control, 16-nt ^{32}P-end labeled oligo. Telomerase repeat products numbered. **e**, Direct telomerase assay using immunopurification of overexpressed, tagged TERT co-transfected with the indicated TERC vector or EGFP as control into 293T *TERC*-null cells. *n* = 3 replicates. **f**, Quantification of **e**. P value calculated as in **b**. **g**, PCR to detect wildtype and T-free telomere junction (see Methods) performed on 293T *TERC*-null cells transfected with the indicated vectors, cultured for 18 hours, then treated with dT as indicated for three days. **h**, Sanger and nanopore sequencing of products from lane 4 in **g**. Sanger trace corresponding to cytosine omitted for clarity. **i**, Slot blot of DNA from 293T *TERC*-null cells overexpressing TERT as well as the indicated vector, cultured for 18 hours, then treated with the indicated dose of dT for 30 hours, performed in technical triplicates. Representative data from one of two biological replicates displayed. **j**, Quantification of GGAAAG signal in **i**. *P* values calculated using unpaired two-sided *t* tests, *n* = 3 technical replicates. **k**, Slot blot of 293T *TERC*-null cells transfected as in **i**, and treated with the indicated dose of dT, 5FU (10 μM), or HU (500 μM) as indicated. Representative data from one of two biological replicates displayed. **l**, Quantification of **k** as in **j**. *n* = 3 technical replicates. Data in **b**, **f**, **j** and **l** are presented as means, error bars indicate s.d.; ns, $P > 0.05$. Full-length gels are provided as source data.

Figure 2-7. (Continued)



Substrate-independent control of telomerase in cells by dT

After observing this substrate-independent effect of dTTP on telomerase activity *in vitro*, we next asked whether dT treatment could enhance T-free super-telomerase activity in cells. When we transfected *TERC*-null 293T cells with TERT and T-free TERC vectors, we detected altered repeat sequences on native telomere ends by PCR (**Figure 2-7g,h**). Southern analysis showed increases in telomerase-dependent GGAAAG signals in response to dT. However, these signals appeared over a range of molecular weights rather than just elongation of pre-existing telomere ends as seen with the native GGTTAG template (**Figure S7m,n**). This might be explained by instability of an unprotected G-rich GGAAAG repeat extension, which likely cannot be bound by POT1, cannot undergo C-strand fill-in due to the requirement for pol-alpha/primase to begin the RNA primer with a purine[185,186] (templated by "C" or "T", now absent from T-free G-rich strand), and cannot efficiently complement the native telomere sequence to form a T-loop, thus potentially subject to nucleolytic cleavage. Nevertheless, to quantify T-free telomerase repeat synthesis in cells, we used slot blotting to measure GGAAAG repeat content in cellular DNA (**Figure 7o-r**) and found a specific increase in GGAAAG repeats in cells overexpressing T-free super-telomerase (**Figure 2-7i,j**). When we treated cells overexpressing wild-type versus T-free super-telomerase with 100 μM dT, we found an increase in GGAAAG repeat content exclusively in cells expressing T-free telomerase (**Figure 2-7i,j** and **Figure 7s,t**). Furthermore, we found that treatment with 5FU or hydroxyurea reduced levels of GGAAAG repeats in T-free super-telomerase expressing cells, and that treatment with dT could rescue the inhibition of GGAAAG repeat synthesis following 5FU treatment (**Figure 2-7k,l**), patterns identical to those found with the native template (**Figure 2-6o**). These findings support a model wherein dTTP increases telomerase activity in human cells by a mechanism independent of its role as a telomerase substrate.

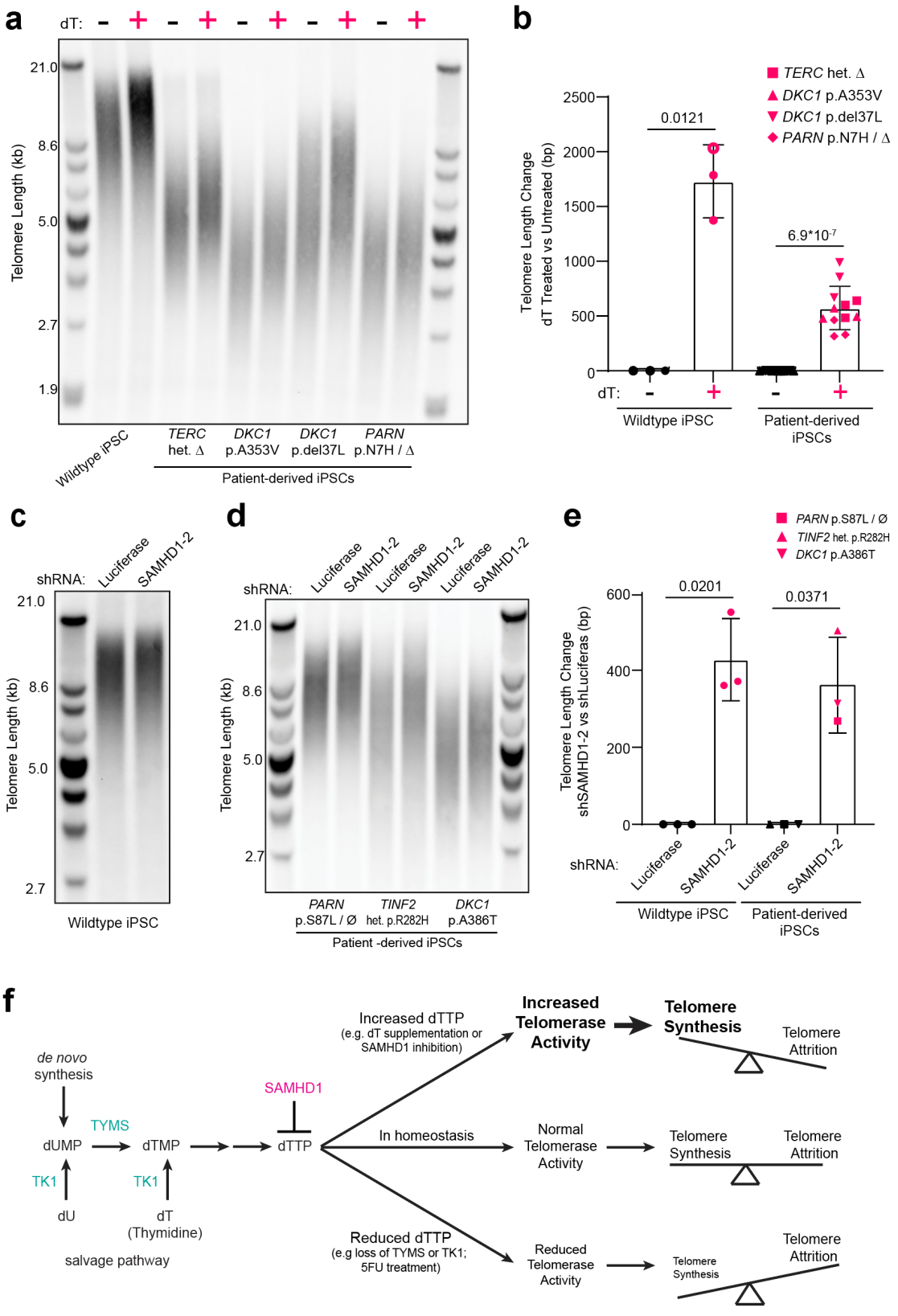
To further characterize the molecular nature of the T-free telomerase products both in the presence and absence of thymidine supplementation, we evaluated how alterations including treatment with ExoI, an exonuclease degrades single stranded DNA from the 3' end, mung bean nuclease, a single stranded DNA endonuclease, and omitting restriction enzymes influenced their size distribution by Southern blotting. We found that omitting restriction enzymes did not significantly change the pattern of T-free repeat distribution, indicating that the majority of these repeats are not genomically associated (**Figure S8a-c**). Treatment with ExoI similarly did not change the distribution pattern while treatment with Mung Bean Nuclease led to a reduction in the molecular weight of the products, indicating these species are likely partially single stranded and circular. When we gel purified high molecular weight DNA to isolate genomically bound T-free telomerase signal, we identified signal intensity at the molecular weight corresponding to the length of the telomeres in these cells, supporting the notion that T-free telomerase repeats are added to the telomere end (**Figure S8a-c**), in line with our PCR-based assessment (**Figure 2-7g,h**). Collectively, these data support the hypothesis described above that 5'-GGAAAG-3' repeats synthesized by T-free telomerase are unstable due to inability to bind POT1, inability to be converted to double stranded DNA due to the requirement for primase to initiate with a purine, and inability to form a T-loop, and are thus cleaved from the telomere end and accumulate as extrachromosomal partially single stranded circles. The relationship between the biogenesis of these products and telomeric circles which occur in ALT positive cancers[187] may be of further interest for investigation.

Thymidine manipulation elongates telomeres in patient iPSCs

Telomere biology disorders (TBDs) are caused by mutations in at least 18 genes[31,32] regulating telomere maintenance. We asked whether treatment with dT or disruption of *SAMHD1* could promote telomere lengthening in induced pluripotent stem cells (iPSCs) derived from patients with TBDs. We first confirmed that dT supplementation for three weeks significantly elongated telomeres in iPSCs from a healthy donor (**Figure 2-8a,b**). We next tested a panel of iPSCs from TBD patients with hypomorphic genetic defects, including mutations in *TERC*, *DKC1* (encoding a component of the telomerase holoenzyme), or *PARN*, which promotes TERC maturation. We found that treatment with 50 μM dT for three weeks produced telomere elongation in all cases (**Figure 2-8a,b**). When we examined the impact of dT treatment on cell cycle progression in iPSCs, we found doses ≤50 μM had minimal effects (**Figure S9a,b**). Assessment of pCHK1-S345 and pRPA32-S33 by immunoblotting revealed no indication of replication stress signaling in iPSCs upon treatment with dT (**Figure S9c**), in line with prior literature[188]. We next evaluated the capacity of stable *SAMHD1* knockdown to alter telomere length in both wild-type iPSCs and patient iPSCs harboring TBD-causing mutations and found telomere elongation across the genotypes tested, including *DKC1*, *PARN,* and *TINF2*, which encodes a telomere shelterin component (**Figure 2-8c-e**). Collectively, these data demonstrate that manipulation of thymidine nucleotide metabolism can restore telomere lengthening in stem cells harboring TBD-causing genetic defects.

Figure 2-8. dT supplementation or SAMHD1 knockdown drives telomere lengthening in iPSCs from patients with telomere biology disorders. a, TRF of iPSCs derived from a healthy donor or from TBD patients harboring mutations in the indicated genes that were treated with or without 50 μM dT for three weeks. Representative blot from three biological replicates. **b**, Quantification of **a**. *P* values calculated using paired two-sided *t* tests. Open circle indicates cells treated with 100 μM dT for three weeks. All other treated cells received 50 μM dT. All data points represent biologically independent samples. Sample size sizes for wild-type iPSC, untreated ($n = 3$) or dT treated ($n = 3$) and for TBD patient-derived iPSCs, untreated ($n = 12$) or dT treated ($n = 12$). **c**, TRF of wild-type iPSCs transduced with the indicated shRNA expression construct and cultured for 26 days. Representative blot from three biological replicates shown. **d**, TRF of iPSCs derived from TBD patients harboring mutations in the indicated genes that were transduced with the indicated shRNA expression construct and cultured for one month. **e**, Quantification of **c** and **d**, as in **b**. All data points represent biologically independent samples. Sample sizes for wild-type iPSCs, shLuciferase ($n = 3$ samples) or shSAMHD1-2 ($n = 3$ samples), and for TBD patient-derived iPSCs, shLuciferase ($n = 3$ samples) or shSAMHD1-2 ($n = 3$ samples). **f**, Model of the relationship between dTTP metabolism and telomere length. Data in **b** and **e** are presented as means, error bars indicate s.d.; ns, $P > 0.05$.

Figure 2-8. (Continued)



Discussion

Impaired telomere length maintenance is associated with reduced lifespan[33] and fatal genetic degenerative diseases[31,157,158,189]. Using phenotypic CRISPR/Cas9 screening in intact cells, we identified dT nucleotide metabolism as a critical pathway controlling human telomere length homeostasis. DNA precursor levels are tightly controlled though a balance of *de novo* synthesis, salvage, and catabolism[85]. Here we demonstrate that telomere length is highly sensitive to changes in dT nucleotide metabolism (**Figure 2-8f** and **Figure S10**): loss of genes in the dT nucleotide synthesis or salvage pathways reduced telomere length, whereas loss of the dNTP degrading gene *SAMHD1* lengthened telomeres. In addition to genetic perturbations, we find that telomere synthesis is highly sensitive to small molecules targeting dT nucleotide metabolism. Supplementing cells with dT drove robust telomere elongation, whereas treatment with 5FU or hydroxyurea, which limit dTTP production, blocked telomere repeat synthesis by telomerase. Collectively, our work, in line with emerging population and Mendelian genetic data[32–34], demonstrates the critical importance of dT nucleotide metabolism in human telomere length control and highlights the additional insights gained from longitudinal functional genetic studies in human cells.

While dTTP is a canonical substrate of human telomerase alongside dATP and dGTP, this striking impact of dT nucleotide metabolism on telomere length in human cells is unexpected given prior studies using reconstituted telomerase[73,74,163,164] and yeast[100,190] indicating that dGTP is rate-limiting for telomerase activity. Here, using a modified telomerase enzyme that no longer uses dTTP as a substrate, we find evidence for substrate-independent enhancement of telomerase activity by dT nucleotides both *in vitro* and in living cells. While we cannot exclude a role for secondary effects of dT on dATP and dGTP levels contributing to telomere length changes in cells,

a substrate-independent, potentially allosteric effect of dTTP on telomerase activity offers a unifying mechanism to explain our genetic, pharmacological, and biochemical findings, that, coupled with recent human genetic data[32–34], firmly establishes a role for dT nucleotide metabolism in telomere length regulation. More specifically, a preponderance of orthogonal evidence, including high-throughput functional genetic screening, 5FU treatment, GWAS, and genetic discovery, collectively implicates *TYMS* as a critical control point, thus revealing a limiting role for *de novo* dT nucleotide production in human telomere length regulation.

Prior work connected replication stress signaling with enhanced telomerase recruitment to telomeres[183] and increased telomere length[182,184]. Our data demonstrate that telomere lengthening from dT can occur at doses that do not result in replication stress or disrupt the cell cycle. Furthermore, we showed that 5FU and hydroxyurea, compounds known to cause replication stress, blocked telomere repeat synthesis by telomerase in our system, rather than extending telomeres. We cannot exclude that replication stress-mediated changes in telomerase recruitment could play a role in telomere elongation at very high dT doses; however, our data clearly demonstrate that modulating dT nucleotides at more physiological levels can impact human telomere length by other means, such as activation of telomerase.

While we show that cell cycle inhibition and replication stress cannot explain telomere lengthening from dT, we find that the high doses commonly used to synchronize cells cause significant changes in telomere repeat synthesis. Several investigations of human telomerase biology have used dT or related compounds like bromodeoxyuridine (BrdU) to facilitate measurements such as the timing of telomere synthesis by telomerase during the cell cycle, and the kinetics of repeat addition by telomerase at a given chromosome end. Our results indicate a

more nuanced interpretation of telomere biology effects may be required when using dT and its analogs for synchronization or labeling in human cells.

Defects of nucleotide synthesis are associated with diseases, including mitochondrial genetic disorders and cancer[85,89,159], and manipulation of nucleotide metabolism is widely used in life-saving therapies, including those for cancer, autoimmune, and infectious diseases[96,191]. Remarkably, we found that supplementation with dT promotes rapid telomere lengthening at low micromolar doses. We observed this effect across various cell lines, including iPSCs derived from patients with TBDs caused by diverse, hypomorphic genetic defects. Based on our findings *in vitro* and in cultured cells, along with promising clinical trials currently underway using oral dT supplementation to treat a mitochondrial genetic disease[97], we propose that there may be a therapeutic window to modulate telomere length via manipulating dT metabolism in patients with a range of genetic degenerative disorders.

dNTP metabolism is commonly considered in relation to DNA replication and repair. Our work uncovers a unique sensitivity of telomerase reverse transcriptase activity to dT nucleotide homeostasis. While dT supplementation alone can inhibit genome replication by DNA polymerases[180] and HIV-1 reverse transcription[192], we found that dT treatment drove robust increases in telomere synthesis by telomerase. These findings expand our understanding of how differences in the common pool of cellular nucleotide substrates driven by genetic variation and other factors can have distinct effects on the various DNA synthesis machineries in the cell. Evolutionary pressures on dNTP metabolism have likely faced a tradeoff between telomere length maintenance, nuclear and mitochondrial genomic integrity, and other forces, including the restriction of endogenous or exogenous retro-elements. Telomere length homeostasis offers a new

lens with which to examine the genetic regulation and evolution of DNA precursor metabolism in humans.

Materials and Methods

Human study participants

Biological samples were procured under Boston Children's Hospital Institutional Review Board approved protocols, after written informed consent in accordance with the Declaration of Helsinki. Patients and patient-derived iPSCs are as described[44,193,194]. The *TINF2* mutant patient presented with dyskeratosis congenita and bone marrow failure in early childhood, consistent with the pathognomonic p.R282H mutation.

Cell culture

K562 cells (ATCC) were grown in RPMI1640 (Gibco) media supplemented with 10% fetal bovine serum. 293T cells (ATCC) were grown in DMEM (Gibco) supplemented with 10% fetal bovine serum, and were subcultured using 0.05% trypsin (Gibco). iPSCs were grown in Essential 8 Media (Life Technologies) supplemented with the ROCK inhibitor Y271632 (Stem Cell Technologies) at 10 μM on plates coated with hES-qualified Matrigel matrix (Corning) and were subcultured using Accutase (Stem Cell Technologies). The *TINF2* mutant iPSC line was derived from bone-marrow derived fibroblasts using the 4-in-1-dTomato lentiviral reprogramming vector (a kind gift from A Schambach) as described[195]. The *PARN* mutant iPSCs were derived and characterized as described[44]. The *DKC1* p.A353V mutant iPSC line was derived and characterized as described[194]. The *DKC1* p.del37L and p.A386T mutant iPSCs were derived and characterized as described[193]. The *TERC* mutant iPSC line was derived and characterized as described[193]. The wild-type iPSC line was derived and characterized as described[44].

Lentiviral transduction of shRNA and overexpression constructs was performed in media

supplemented with protamine sulfate (Sigma Aldrich) at 10 μg/ml for 16 hours. Transduced cells underwent selection with puromycin (Sigma Aldrich) at 2 μg/ml for 3-5 days, or blasticidin (InvivoGen) at 10 μg/ml for 5-10 days. For doxycycline-inducible transgene expression, 1 μg/ml doxycycline (Sigma Aldrich) was used.

Transfections were performed using Lipofectamine LTX with Plus Reagent (Invitrogen) in Opti-Mem (Gibco) according to the manufacturer's instructions. On the evening prior to transfection, two million cells were plated per well of a six well dish, then transfected with 2.5 μg total DNA per well. pXPR_011 was used as the EGFP control vector, pBS U3 TERC 500 was used to overexpress TERC, and PCDNA3.1 3XHA TERT was used to overexpressed TERT. In conditions were TERT was transfected in addition to TERC/EGFP, total DNA input was kept the same and a 5:1 mass ratio of TERC to TERT vector was used. Unless otherwise stated, super-telomerase extracts were generated using cells two days post transfection.

Quantification of cell growth was performed using hemocytometry with Trypan Blue viability staining. For growth curves, 50,000 cells were plated per well in a 12-well dish, or 100,000 cells were plated per well in a 6-well dish. Cells were passaged when sub-confluent, counted using a hemocytometer, and replated at equal numbers in fresh media.

Lentivirus production

293T cells were transfected with psPAX2 and pMD2.G as well as the appropriate transfer vector by calcium phosphate precipitation. Virus-containing media was harvested 48 and 72 hours after transfection. shRNA and overexpression construct virus containing media was filtered with 0.45-μm filters (VWR) and stored at -80 °C. For gRNA libraries, virus containing media was filtered

using 0.45-μm filters and concentrated by ultracentrifugation followed by resuspension in DMEM and storage at -80 °C.

Cas9-expressing cell line generation and validation

K562 cells (ATCC) were transduced with lentivirus containing the Lenti-Cas9-2A-Blast construct followed by selection in 10 μg/ml blasticidin for 10 days. After selection, cells were transduced with the pXPR_011 vector and cultured for two weeks followed by flow cytometry to quantify the percentage of GFP-positive cells on an LSR-II analyzer (BD Biosciences) using BD FACSDiva 8.0.2. Cells were gated on FSC/SSC as described in **Figure S1d** using FlowJo V10.7.1.

gRNA library design and production

For secondary screening using a nucleotide metabolism-focused gRNA library, genes were selected for inclusion based on annotated involvement in nucleotide salvage and deoxyribonucleotide metabolism by Gene Ontology. 10 gRNAs per gene were designed using the Broad GPP sgRNA design tool[165,196]. 200 non-targeting gRNAs sequences were selected from the Brunello gRNA library. Library information including genes targeted and gRNA sequences can be found in **Supplementary Table 1**. A pool of ssDNA encoding the gRNAs flanked by BsmBI recognition sites and overhang sequences for PCR amplification (as described[196]) was synthesized by Twist Bioscience. The library was PCR amplified using Q5 High Fidelity Taq Polymerase (NEB) and cloned into lentiGuide-Puro using Golden Gate cloning[196] with BsmBI-v2 (NEB) and T4 DNA Ligase (NEB) in T4 DNA Ligase buffer (NEB). The library was transformed into chemically competent Stbl3 cells (Invitrogen), which were prepared using the Zymo Mix and Go! E. coli Transformation Kit. Sufficient transformation reactions were performed to attain >40

colonies per gRNA. Library representation was confirmed by PCR amplification using Titanium Taq Polymerase (Takara Bio) followed by next generation sequencing using an Illumina MiSeq instrument and library quantification using the MAGeCK RRA[167] software. Gene-specific and non-targeting gRNA libraries were cloned separately and pooled in appropriate quantities to maximize gRNA representation prior to lentivirus production.

Flow-FISH telomere length and CRISPR/Cas9-based screening

Cas9-expressing K562 cells were plated at 3 million cells per well in 12-well dishes at numbers sufficient for >3,000× library coverage. Cells were spinfected at 931*g* for 2 hours at 30 °C in 1 ml of media per well, in the presence of 10 μg/ml protamine sulfate (Sigma Aldrich). After the spin, 3 ml of fresh media was added and cells were incubated overnight. Virus was removed on day 1. Puromycin selection at 2 μg/ml was performed from days 2-6. Sufficient virus was used to ensure between 20% and 50% of cells were infected. After puromycin selection, cells were cultured at >1,000× library coverage for the amount of time indicated in the figure legend. Flow-FISH was performed using an Alexa-647 conjugated telC-PNA probe (PNA bio) as described[166,197]. Cells were counterstained with DAPI and gated on DAPI low cells and then based on Alexa 647 fluorescence as described in **Figure S1**. Cells were sorted using either a BD FACSARIA II or FACSARIA III. For the Brunello library, 200 million cells on each day were sorted using the above method on day 49 and 50 from the same population of cells. Samples from the two days were treated as replicates for downstream analysis. For the nucleotide metabolism gRNA library experiment, approximately 20 million cells were sorted from two populations that had been infected and cultured separately, and were treated as replicates for downstream analysis. Gates were adjusted throughout the sort such that approximately 5% of cells with the highest and lowest

Alexa-647 fluorescence were collected. DNA from sorted cells was purified by phenol-chloroform extraction using standard procedures. Next, gRNAs were PCR amplified using Titanium Taq Polymerase (Takeda) and primers containing Illumina P5 and P7 binding sites[196]. PCR products were purified using a 1:1 ratio of sample purification SPRI magnetic beads (Beckman Coulter). Pooled, barcoded amplicons were sequenced on an Illumina Next seq using 75bp High Output chemistry. Data analysis and quality control was performed using the MAGeCKFlute pipeline (version 0.5.9.2)[170]. Briefly, FASTQ files were mapped using the count function with the control norm-method. Gene enrichment scores were calculated using the test function comparing the low Alexa 647 vs. high Alexa 647 populations for the nucleotide metabolism targeted library, or high Alexa 647 vs. unsorted and low Alexa 647 vs unsorted populations for the Brunello library, with the MAGeCK Robust Rank Algorithm using paired replicates and non-targeting guides as controls. Unbiased pathway analysis was performed using the hypergeometric test to identify KEGG pathways enriched using the FluteRRA function, which includes *q*-value estimation for false discovery rate control.

Terminal restriction fragment length analysis

Genomic DNA was isolated from cells using the Purelink Genomic DNA mini kit (Invitrogen). 1-3 µg of gDNA was digested with RsaI (NEB) and HinfI (NEB) for 2-3 hours at 37 °C and loaded onto a 0.6% agarose gel followed by Southern blotting onto Hybond N+ Membrane (Amersham), then detection using the Telotaggg Telomere Length Assay Kit (Roche) with either the telomeric probe provided in the kit or an GGAAAG complementary probe, which was synthesized as described[198] using the GGAAAG Probe Template oligonucleotide (see below). GGAAAG complementary probe was used at a working concentration of 1 ng/ml of DIG Easy Hyb (Roche).

After hybridization, detection was performed as described in the Telotaggg Telomere Length Assay Kit (Roche). Probed membranes were stripped by briefly rinsing in water then washing twice with 0.2M NaOH, 0.1% SDS at 37 °C with for 15 minutes with shaking followed by hybridized and detection as described above. Where indicated, digestion with Exonuclease I (NEB) was performed at 37°C for 30 minutes in Cutsmart buffer (NEB), and treatment with Mung Bean Nuclease (NEB) was performed at 30°C for 30 minutes in Cutsmart buffer (NEB). When used in combination with Quantification was performed using the WALTER webtool[199]. Statistical analysis performed using Graphpad Prism V9.1.0.

RNA isolation and RT-qPCR

RNA was isolated from cells using Trizol Reagent (Invitrogen). RNA was DNAse treated with the TURBO DNA-free™ Kit (Invitrogen). cDNA was synthesized using the SuperScript™ III Reverse Transcriptase (Invitrogen) using random hexamers (Invitrogen). qPCR was performed using SsoAdvanced Universal SYBR Green Supermix (Bio-Rad) in technical triplicate. Relative expression was quantified using ΔΔCt methodology.

TRAP assay

Cell extracts for TRAP assays were made using TRAPeze™1X CHAPS Lysis Buffer (Roche) supplemented with RNASEin (Promega). Standard TRAP reactions (in **Figure 2-7a** and **Figure S2**) were performed as described[200], with cell input normalized across samples using the Bio-Rad DC assay. TRAP assays were modified to enable unique dNTP concentrations in telomerase reactions from PCR reactions (in **Figure 2-7d,e** and **Figure S7a-f**) as follows: reactions were assembled with 1× TRAP buffer (20 mM Tris-HCl, pH 8.3; 1.5 mM $MgCl_2$; 63 mM KCl; 0.05%

Tween 20; 1 mM EGTA), TS, ACX, TNST, and NT primers as described[200] (see Primers/Oligos below), dNTPs were added at physiologic concentrations (dATP 24 μM, dGTP 5.2 μM, dCTP 29 μM, dTTP 37 μM)[76] unless otherwise mentioned in the figure legend, followed by telomerase extracts. TRAP assays were modified to detect GGAAAG repeats using the following primers: TS GGAAAG, TNST GGAAAG, ACX GGAAAG, and NT (see Primers/Oligos below). After addition of telomerase extracts, reactions were incubated for 30 minutes at 30 °C followed by heat inactivation at 95 °C for 5 minutes. Reactions were purified in order to remove dNTPs using the Oligo Clean and Concentrator Kit (Zymo) and eluted in 15 μl of water. 10 μl of elutate was then used in TRAP PCR reactions along with 1× TRAP buffer, 0.4U Titanium Taq Polymerase, and 50 μM of each dNTP, and PCR was performed as described[200]. PCR products were resolved on 10% polyacrylamide gels (Bio-Rad), stained with Gel Red (Biotium), and imaged on a Bio-Rad Chemi-Doc Touch Imager. Images were quantified for a given lane using ImageJ by measuring the signal of the telomerase repeat sized products divided by the signal of the internal control band for the lane, normalized to the same ratio for the untreated sample(s) in a given experiment[200]. Statistical analysis performed using Graphpad Prism V9.1.0.

Targeted CRISPR/Cas9 gene editing

37 pmol of Alt-R® S.p.Cas9 Nuclease V3 (IDT) and 50 pmol of chemically modified sgRNA(s) (Synthego) were complexed at room temperate for 20 minutes. 200,000-400,000 cells were combined with Cas9/gRNA complexes in 20 μl Buffer R (Thermo Fisher) with Alt-R® Cas9 Electroporation Enhancer (IDT) followed by electroporation using the Neon Transfection System (Thermo Fisher) and the Neon Transfection 10 μl kit. K562 cells were electroporated with three pulses at 1,150 V for 10 ms. 293T cells were electroporated with one pulse of 1,200 V for 30 ms.

CRISPR/Cas9 gene editing efficiency determination

Genomic DNA was isolated from cells using the Purelink Genomic DNA mini kit (Invitrogen) followed by PCR amplification with Q5® High-Fidelity DNA Polymerase (NEB) with the high GC enhancer, followed by either running on a 2% agarose gel or Sanger sequencing. Sanger trace files were analyzed using the Synthego ICE webtool V3.0 to calculate editing efficiency. Editing efficiency was determined using the same DNA used for TRF blotting.

Cell cycle analysis by DNA content staining and flow cytometry

Cells were prepared either for flow-FISH staining as described[166] (for experiments in **Figure S5**) or by ethanol fixation (for data in **Figure 2-6** and **Figures S6** and S**9**), followed by rehydration and counterstaining using DAPI (BD Biosciences) and analysis on an LSR-II or Fortessa analyzer (BD Biosciences) using BD FACSDiva 8.0.2. Cells were gated on FSC/SSC as described in **Extended Data Figure 1d** using FlowJo V10.7.1.

Immunoblotting

For immunoblots in **Figure 2-6** and **Figure S8**, cells were lysed in RIPA buffer (150 mM NaCl, 1% Triton X-100, 0.5% sodium deoxycholate, 0.1% SDS, 50 mM Tris pH 8.0) supplemented with HALT protease inhibitor cocktail (Thermo Fisher), quantified using the Bio-Rad DC assay, and 10 µg of lysate was combined with 2× Laemmli sample buffer (Bio-Rad) and run on a 10% SDS-PAGE gel (Bio-Rad) followed by transfer to PVDF membrane (Bio-Rad) using standard procedures. For immunoblots in **Figure S4**, cells were lysed in 1× Laemmli sample buffer (Bio-Rad) and run on a 10% SDS-PAGE gel (Bio-Rad) followed by transfer to PVDF membrane (Bio-

Rad) using standard procedures. Human SAMHD1 was detected using primary antibody from either Abcam ab67820 (**Figure S6a,c**) or Origene OTI3F5 (**Figure S6b**) at 1:500 dilution and horseradish peroxidase conjugated goat-anti-mouse IgG H&L ab205719 at 1:1,000 dilution. pCHK1-S345 was detected using a rabbit monoclonal primary antibody from Cell Signaling Technologies (133D3) at 1:1,000 dilution. pRPA32-S33 was detected using a rabbit primary antibody from Bethyl Laboratories (A300-246A) at 1:1,000 dilution. Rabbit primary antibodies were detected using horseradish peroxidase conjugated goat-anti-rabbit IgG H&L antibody (Bio-Rad, 1706515) at 1:3,000 dilution. Anti-beta-actin antibody directly conjugated to horseradish peroxidase (Santa Cruz Biotechnology C4; sc-47778 HRP) at 1:1,000 was used to quantify relative loading. Imaging was performed using a Bio-Rad Chemi Doc Imager.

Liquid chromatography-mass spectrometry

Extraction of and quantification of polar metabolites was performed as described[174] using HPLC grade methanol (Fisher Scientific). If a given species was detected in multiple ion modes, the mode with the highest average signal in the untreated cells was used for analysis.

Nanopore sequencing

For sequencing of telomere end PCR products, amplicons were purified using the Qiagen PCR Purification kit and sequenced using the Plasmidsaurus amplicon sequencing service. Data from Plasmidsaurus nanopore sequencing and Sanger sequencing were aligned and displayed using Geneious Prime. T-free TRAP products were prepared for nanopore sequencing using the Ligation Sequencing Kit with the Native Barcoding Expansion (Oxford Nanopore Technologies SQK-

LSK109, EXP-NBD104) according to the manufacturer's instructions, except that a ratio of 4:1 of SPRI Purification Beads (Beckman Coulter) was used for all purification steps. Samples were pooled after barcode ligation, adapters were ligated per the manufacturer's instructions, then products were loaded onto a Flongle flow cell (FLO-FLG001). Reads were first analyzed using the high accuracy mode (MinKNOW/Guppy) and reads which had passed quality standards (Q score > 9) from the high accuracy base calling were re-base called using super-high accuracy algorithm (MinKNOW/Guppy). Then, super-high accuracy base-called reads that had Q score > 10 were used for further analysis. FASTQ files were analyzed in MATLAB as follows. Reads containing a match to the TS GGAAAG forward primer and the TAGGGAT portion of the reverse primer reverse complement were extracted and the base pairs between the primer binding sites were analyzed for their base pair composition using Version 1.0 of a custom MATLAB script which has been posted to public repository[201]. Software versions used: Geneious Prime 2019.2.3, MinKNOW 22.05.5, Bream 7.1.3, Configuration 5.1.5, Guppy 6.1.5, MinKNOW Core 5.1.0, MATLAB R2021a. Base pair frequency analysis and plotting in was performed using ggseqlogo[202] with R version 4.1.2.

Telomerase immunopurification

293T *TERC*-null cells were transfected as described above with 3xHA-TERT and TERC/EGFP in 10-cm diameter dishes with reagents scaled up proportional to cell growth area. Two days after transfection, cells were harvested, washed once in PBS, and lysed in TRAPeze™1X CHAPS Lysis Buffer (Roche) supplemented with RNasin Plus (Promega) and HALT protease inhibitor cocktail (Thermo Fisher), followed by incubation on ice for 30 minutes and precipitation of insoluble material by centrifugation. Immunoprecipitation was performed as described in

https://www.colorado.edu/lab/cech/lab-protocols with minor modifications. Briefly, 75 µl of anti-HA magnetic beads (Sigma-Aldrich, SAE0197, mouse IgG1 monoclonal antibody, Clone HA-7, 50% beads by volume) were added to clarified lysates followed by 2 hours incubation at 4 °C while rotating. Prior to addition, beads were prepared by washing four times in 50 mM Tris-HCl pH 8.0, 1 mM $MgCl_2$, 1 mM Spermidine, and 5 mM β-mercaptoethanol. After immunoprecipitation, telomerase bound beads were washed four times with 1 ml of telomerase buffer with 30% glycerol (50 mM Tris-HCl pH 8.0, 50 mM KCl, 1 mM $MgCl_2$, 1 mM Spermidine, 5 mM β-mercaptoethanol, 30% glycerol). After washing, a 50% bead slurry was made with telomerase buffer with 30% glycerol, then beads were aliquoted, snap frozen, and stored at -80 °C.

Direct telomerase assay

Reactions were performed as described in https://www.colorado.edu/lab/cech/lab-protocols with minor modifications. 20 µl reactions were assembled containing 6 µl of immunopurified telomerase, 5.2 µM dGTP, 3 µM dATP, 0.166 µM [α-P^{32}] dATP (3,000 Ci/mmol, Perkin Elmer), 1 µM PAGE purified 3x(TTAGGG) primer (IDT), 50 mM Tris-HCl pH 8.0, 50 mM KCl, 1 mM $MgCl_2$, 1 mM Spermidine, an 5 mM β-mercaptoethanol. dTTP was added as indicated in the figure legend. Reactions were then incubated at 30 °C for 1 hour, then 100 µl of stop buffer (3.6 M ammonium acetate, 10 mg/ml glycogen) was added as well as ^{32}P end-labeled PAGE purified TTAGGGTTAGGGTTAG primer (IDT) followed by the addition of 500 µl ethanol. Products were then incubated at -80 °C for 45 minutes, pelleted, washed with 1 ml 70% ethanol, dried, and resuspended in 10 µl water. Purified products were combined 1:1 with electrophoresis buffer (0.1× TBE, 50 mM EDTA, 0.1% Bromophenol blue, 0.1% Xylene Cyanol, 93% formamide), denatured at 95 °C for 5 minutes, then centrifuged at 18,000*g* for 5 minutes to precipitate insoluble material.

9 µl of samples were then loaded onto 10% acrylamide/7 M urea gels. After electrophoresis, gels were then dried using the Bio-Rad Gel Air Drying System and imaged using phosphorimaging on an Amersham Typhoon 5 Biomolecular Imager (GE Healthcare). End labeling of the loading control primer was performed using T4 PNK (NEB) and γ-^{32}P-dATP 6,000 Ci/mmol (Perkin Elmer). Images were quantified using ImageJ as follows. For total telomerase activity measurement, telomerase product signal in a lane was quantified and normalized to the loading control band signal within the same lane. This ratio was then normalized to the average product to loading control ratio for the 0 µM dTTP lanes. For the analysis of telomerase repeat intensity, the signal of each repeat was quantified and first normalized to the loading control band signal for that lane. Then the ratio of a given repeat to loading control was divided by the corresponding ratio for the 0 µM dTTP lane, yielding a measure of relative repeat intensity, which was plotted for repeats 1-4. Statistical analysis was performed using Graphpad Prism V9.1.0.

Slot blotting

Slot blotting was performed as described[203] with minor modifications. Briefly, DNA concentration was normalized to 20 ng/µl using a nanodrop spectrophotometer. 3.3 µl of DNA was added to 16.5 µl of denaturation solution (0.5 M NaOH, 1.5 M NaCl) and heated to 55 °C for 30 minutes. 495 µl of neutralization solution (0.5 M Tris-HCl, 1.5 M NaCl) was added to denatured DNA and 156 µl of this solution was added in triplicate to different slots on a Bio-Dot SF Apparatus (Bio-Rad) and blotted onto Hybond N+ Membrane (Cytivia). Membrane preparation and washing was performed as described[203]. For samples with paired GGTTAG and GGAAAG slot blots, the above recipe was doubled, and 156 µl was loaded onto parallel membranes in triplicate on each membrane. After

blotting, membranes were hybridized and detected as described above for TRF Southern blots using the probe indicated in the figure. Blots were analyzed using ImageJ. Statistical analysis was performed using Graphpad prism V9.1.0.

shRNA construct cloning

Oligonucleotides encoding shRNAs targeting SAMHD1 or luciferase control were annealed and cloned into the pLKO.1-puro vector using the Quick Ligation™ Kit (NEB).

Expression construct cloning

SAMHD1 expression constructs were cloned using primers with flanking Attb sites used to amplify *SAMHD1* sequence derived from cDNA prepared as described above or EGFP from the pXPR-011 vector using Q5 High Fidelity DNA Polymerase (NEB). Amplicons were cloned into the pCW5a7.1 vector in a single reaction using Gateway™ LR Clonase™ II Enzyme mix (Invitrogen), Gateway™ BP Clonase™ II Enzyme mix, (Invitrogen) and the Gateway™ pDONR™221 Vector (Invitrogen). Point mutations were introduced using the Q5 site directed mutagenesis kit (NEB) and verified using Sanger sequencing. The T-free TERC construct was generated using the Q5 site directed mutagenesis kit (NEB), and verified using Sanger sequencing.

Plasmids

4-in-1-dTomato lentiviral reprogramming vector was a gift from A Schambach. Lenti-Cas9-2A-Blast was a gift from Jason Moffat (Addgene plasmid # 73310). pXPR_011 was a gift from John Doench and David Root (Addgene plasmid # 59702). Human Brunello CRISPR knockout pooled library in lentiGuide-Puro was a gift from David Root and John Doench (Addgene #73178).

lentiGuide-Puro was a gift from Feng Zhang (Addgene plasmid # 52963). pLKO.1 - TRC cloning vector was a gift from David Root (Addgene plasmid # 10878). pCW57.1 was a gift from David Root (Addgene plasmid # 41393). psPAX2 was a gift from Didier Trono (Addgene plasmid # 12260). pMD2.G was a gift from Didier Trono (Addgene plasmid # 12259). pBS U3-hTR-500 was a gift from Kathleen Collins (Addgene plasmid # 28170). pCDNA-3xHA-hTERT was a gift from Steven Artandi (Plasmid #51637).

Data Availability

gRNA library sequencing data and T-free TRAP sequencing data used for analysis have been deposited in the Sequence Read Archive (SRA) and are available under BioProject PRJNA851386 (https://www.ncbi.nlm.nih.gov/sra/PRJNA851386).

Code Availability

The MATLAB script used to analyze the T-free TRAP sequencing data has been posted to a public repository[201]. Version 1.0 was used in this manuscript (https://doi.org/10.5281/zenodo.7607615).

Table 2-1.

Compound	Supplier	Catalog #	Purity	Note
Thymidine	Sigma Aldrich	T1895	≥99%	Default source used
Thymidine	Santa Cruz Biotechnology	CAS 50-89-5	>98%	Referred to as manufacturer 2 in Extended Data Figure 3a
Thymidine	MP Biochemicals	MP219475401	>99.9%	Referred to as manufacturer 3 in Extended Data Figure 3a
Deoxyuridine	Sigma Aldrich	D5412	>98.5%	Thymidine free according to manufacturer
Deoxyadenosine	Sigma Aldrich	D8668	≥99%	
Deoxyguanosine	Sigma Aldrich	D0901	≥99%	
Deoxycytidine	Thermo Scientific	AC226720010	≥99%	
Folic Acid	Sigma Aldrich	F8758	>97%	
Hydroxyurea	Thermo Scientific (Acros Organics)	AC151680050	≥97.5%	
5-Fluorouracil (5FU)	Sigma Aldrich	F6627-1G	≥99%	
Aphidicolin	Sigma Aldrich	A0781	>98%	

Table 2-1. Small Molecules Used in this Study

Table 2-2.

Oligonucleotides and primers	
Name	**Sequence (5' to 3')**
shSAMHD1-1 oligo 1	CCGGCCCTGAAGAAGATATTTGCTTCTCGAGAAGCAAATATCTTCTTCAGGGTTTTTG
shSAMHD1-1 oligo 2	AATTCAAAAACCCTGAAGAAGATATTTGCTTCTCGAGAAGCAAATATCTTCTTCAGGG
shSAMHD1-2 oligo 1	CCGGGCCATCATCTTGGAATCCAAACTCGAGTTTGGATTCCAAGATGATGGCTTTTTG
shSAMHD1-2 oligo 2	AATTCAAAAAGCCATCATCTTGGAATCCAAACTCGAGTTTGGATTCCAAGATGATGGC
shLuciferase oligo 1	CCGGCGCTGAGTACTTCGAAATGTCCTCGAGGACATTTCGAAGTACTCAGCGTTTTTG
shLuciferase oligo 2	AATTCAAAAACGCTGAGTACTTCGAAATGTCCTCGAGGACATTTCGAAGTACTCAGCG
SAMHD1 K312A SDM F	TGATGTGGACgcaTGGGATTATTTTG
SAMHD1 K312A SDM R	ATGCCATTTCTTTTATTAGATAC
SAMHD1 H215A SDM F	GCCATTTTCTgccATGTTTGATGGAC
SAMHD1 H215A SDM R	CCATGACCGAGATCATGAC
P5 Lenti Guide Puro Seq	ATGATACGGCGACCACCGAGATCTACACTCTTTCCCTACACGACGCTCTTCCGATCT[s]TTGTGGAAAGGACGAAACACCG
P7 Lenti Guide Puro Seq	CAAGCAGAAGACGGCATACGAGATNNNNNNNNGTGACTGGAGTTCAGACGTGTGCTCTTCCGATCTTCTACTATTCTTTCCCCTGCA
TERC qPCR Fw	GGGAGGGGTGGTGGCCATTTTT
TERC qPCR Rv	CACCGCGAAGAGTTGGGCTCTG
GAPDH qPCR Fw	CAGTCTTCTGGGTGGCAGTGA
GAPDH qPCR Rv	CGTGGAAGGACTCATGACCA
SAMHD1 qPCR Fw	TCACAGGCGCATTACTGCC
SAMHD1 qPCR RV	GGATTTGAACCAATCGCTGGA
ACTB qPCR FW	ATGATGATATCGCCGCGCTCGT
ACTB qPCR RV	TGCCGTGCTCGATGGGGTACTT
AAVS1 sgRNA	CUCCCUCCCAGGAUCCUCUC
TK1 sgRNA 1	AAGGCACAGGACACACUGUU
TK1 sgRNA 2	GCAGCUUCUGCACACAUGAC
TK1 sgRNA 3	ACUGAGCAAUCUGGAAGCGA
TK2 sgRNA 1	CCAAGACGCGCGUUACCGGG
TK2 sgRNA 2	GCCGGGAAGUCGCGGGAGCC
TK2 sgRNA 3	CUCGCCCGGCUAUGCUGCUG
TYMS sgRNA 1	CGCCCGCCGCGCCAUGCCUG
TYMS sgRNA 2	CGAGCCGCGUCCGCCGCACG
TYMS sgRNA 3	CGUCAGGAAGGACGACCGCA
SAMHD1 sgRNA 1	AAAGCCACCGCGCCUGAGGA
SAMHD1 sgRNA 2	UCUGCGGAAGGGGUGUUUGA
SAMHD1 sgRNA 3	CUUGGAGGGCUGCUCGGAAU
TK1 FW	AAAGCCCAAAAGCATCCCCT
TK1 RV	TCTGCCCTGCTCTTTTCTGG
TK2 FW	ATCCCAGAACCAAAGCCGAG
TK2 RV	AAATGCGACCGGGTCTCTTT
TYMS FW	TGCTGCTGGCTTAGAGAAGG
TYMS RV	GTAAGGCGAGGAGGACGATG
SAMHD1 Gateway Cloning F	GGGGACAAGTTTGTACAAAAAAGCAGGCTTAGCCGCCACCATGCAGCGAGCCGATTCCG
SAMHD1 Gateway Cloning R	GGGGACCACTTTGTACAAGAAAGCTGGGTATCACATTGGGTCATCTTTAAAAAGCTG
EGFP Gateway Cloning F	GGGGACAAGTTTGTACAAAAAAGCAGGCTTAGCCGCCACCATGGTGAGCAAGGGCGAGG
EGFP Gateway Cloning R	GGGGACCACTTTGTACAAGAAAGCTGGGTATTAGGACTTGTACAGCTCGTC
GGAAAG SDM FW	gaaagACAAAAAATGGCCACCACCC
GGAAAG SDM RV	cctttcTGAGAAGGGCGTAGGCGC
TS	AATCCGTCGAGCAGAGTT
GGAAAG TS	AATCCGTCGAGCAGAGAA
ACX	GCGCGGCTTACCCTTACCCTTACCCTAACC
GGAAAG ACX	GCGCGGCTATCCCTATCCCTATCCCTTTCC
TNST	AATCCGTCGAGCAGAGTTAAAAAGGCCGAGAAGCGAT
GGAAAG TNST	AATCCGTCGAGCAGAGAAAAAAAGGCCGAGAAGCGAT
NT	ATCGCTTCTCGGCCTTTT
GGTTAG Junction FW	CGGTTTTTTAGGGTTAGGGTTAGGGTT
GGAAAG Junction RV	GCGCGGCTTTCCCTTTCCCTTTCCCTTT
TERC-Null Geno FW	GCGAAGAGTTGGGCTCTGTCA
TERC-Null Geno RV	TCATCAGGATTCAGGCTATCACCC
GGAAAG Probe Template	/5Phos/AAAGGGAAAGGGAAAGGGAAAGGGAAAGGGAAAGGGAAAGGGTAG ATA GTT GAG AGT C
Universal Priming	/5Phos/GACTCTCAACTATC+T+A
	Note: [s] refers to additional 0-8 bp spacers to diversify library during sequencing as described[25]. +N indicates locked nucleic acid.

Table 2-2. Oligonucleotides Used in this Stud

Chapter 3: Metabolic constraint of human telomere length by nucleotide salvage efficiency

---

Attributions

This chapter contains a modified version of a manuscript entitled “Metabolic constraint of human telomere length by nucleotide salvage efficiency”. Full authorship includes:

William Mannherz[1,2,3,4], Noah Lampl[1,2,3], Suneet Agarwal[1,2,3,4]

[1]Division of Hematology/Oncology and Stem Cell Program, Boston Children's Hospital; Boston, MA, USA.

[2]Pediatric Oncology, Dana-Farber Cancer Institute; Boston, MA, USA.

[3]Harvard Stem Cell Institute, Harvard Initiative for RNA Medicine, and Department of Pediatrics, Harvard Medical School; Boston, MA, USA

[4]Biological and Biomedical Sciences Program, Harvard/MIT MD-PhD Program, Harvard Medical School; Boston, MA, USA.

I performed the experiments, analyzed the data, and prepared the figures. I conceived of the project, designed experiments, and wrote the manuscript together with Suneet Agarwal. Noah Lampl provided technical assistance. Suneet Agarwal supervised the project.

Abstract

Human telomere length is tightly regulated and associated with diseases at either extreme, but how these bounds are established remains incompletely understood. Here, we developed a rapid telomere synthesis assay and found that nucleoside salvage bidirectionally constrains human telomere length. Metabolism of deoxyguanosine (dG) or guanosine via purine nucleoside phosphorylase (PNP) to form guanine ribonucleotides strongly inhibited telomerase and shortened telomeres. Conversely, salvage of dG to its nucleotide forms via deoxycytidine kinase drove potent telomerase activation, the extent of which was controlled by the dNTPase SAMHD1. Circumventing limits on salvage by expressing *Drosophila melanogaster* deoxynucleoside kinase or augmenting dG metabolism using the PNP inhibitor ulodesine robustly lengthened telomeres in human cells, including those from patients with lethal telomere diseases. Our results provide an updated paradigm for telomere length control, wherein telomerase reverse transcriptase activity is actively and bidirectionally constrained by the availability of its dNTP substrates in a manner that may be therapeutically actionable.

Introduction

The ends of linear chromosomes are capped by hexameric repeat sequences termed telomeres, which are required for genomic integrity[155,156]. During genome replication, a terminal portion of telomeres is lost due to the inability of DNA polymerases to completely replicate linear chromosomes[6,7]. Loss of telomere sequence to a critically short length causes DNA damage signaling leading to cellular senescence and exit from the cell cycle[27]. In self-renewing cells, the telomerase reverse transcriptase (TERT) compensates for telomere shortening by synthesizing new 5'-GGTTAG-3' repeats using the telomerase RNA template (TERC) and dNTP substrates[13,16,72,204].

In prevailing models of human telomere length regulation, the expression, abundance, and recruitment of telomerase are regarded as the critical factors counter-acting telomere attrition and thus determining cellular self-renewal capacity in health and disease[21].

In the human population, telomere length normally declines throughout life and has well-defined upper and lower boundaries[110,111,166], deviation from which at either extreme is linked to lethal diseases. Shorter telomere length is associated with reduced lifespan by mendelian randomization[33], and germline mutations in the telomerase components and related genes which result in short telomeres lead to a spectrum of fatal degenerative diseases termed telomere biology disorders (TBDs)[157] characterized by premature stem cell exhaustion. Conversely, long telomeres are associated with increased risks of various malignancies in the general population by mendelian randomization[33,114], and rare germline mutations that lead to long telomeres predispose patients to melanoma, chronic lymphoblastic leukemia and other cancers[115,116,120,121]. Despite these associations, the cellular mechanisms constraining human telomere length remain incompletely defined.

Nuclear dNTPs pools serve as common substrates for genome replication by DNA polymerases and reverse transcription by telomerase, and as such have generally been assumed to be sufficient for telomere lengthening capacity in cells. However, an emerging body of genetic and functional data suggests that dNTP metabolism impacts human telomere biology. Genetic variation in dNTP metabolism genes has been linked with telomere length by GWAS[33,34], and germline mutations at the thymidylate synthase (*TYMS*) locus have been found to cause dyskeratosis congenita, the prototypical TBD[32]. Despite these and other[205,206] clear genetic associations, the mechanisms and extent to which nucleotide metabolism controls telomerase activity in human

cells are not well understood, in large part due to barriers in eliciting measurable changes in telomere length after acute perturbations in the native cellular context.

Here, we developed a rapid and robust human cell-based assay to dissect the metabolic regulation of telomerase reverse transcription. We reveal that nucleotide salvage efficiency bidirectionally controls telomerase activity and telomere length in human cells, to a degree as strong as that observed from manipulating core telomerase components. Overcoming limits on nucleotide salvage by deoxynucleoside kinase over-expression rapidly increased telomere length in human cell lines, and was effective in primary cells as well as cells derived from patients with TBDs. Our findings revise the prevailing model of human telomere length regulation by demonstrating significant constraints on telomerase reverse transcriptase activity due to nucleotide salvage efficiency and dNTP levels, in a manner that may be modifiable for therapeutic benefit.

Results

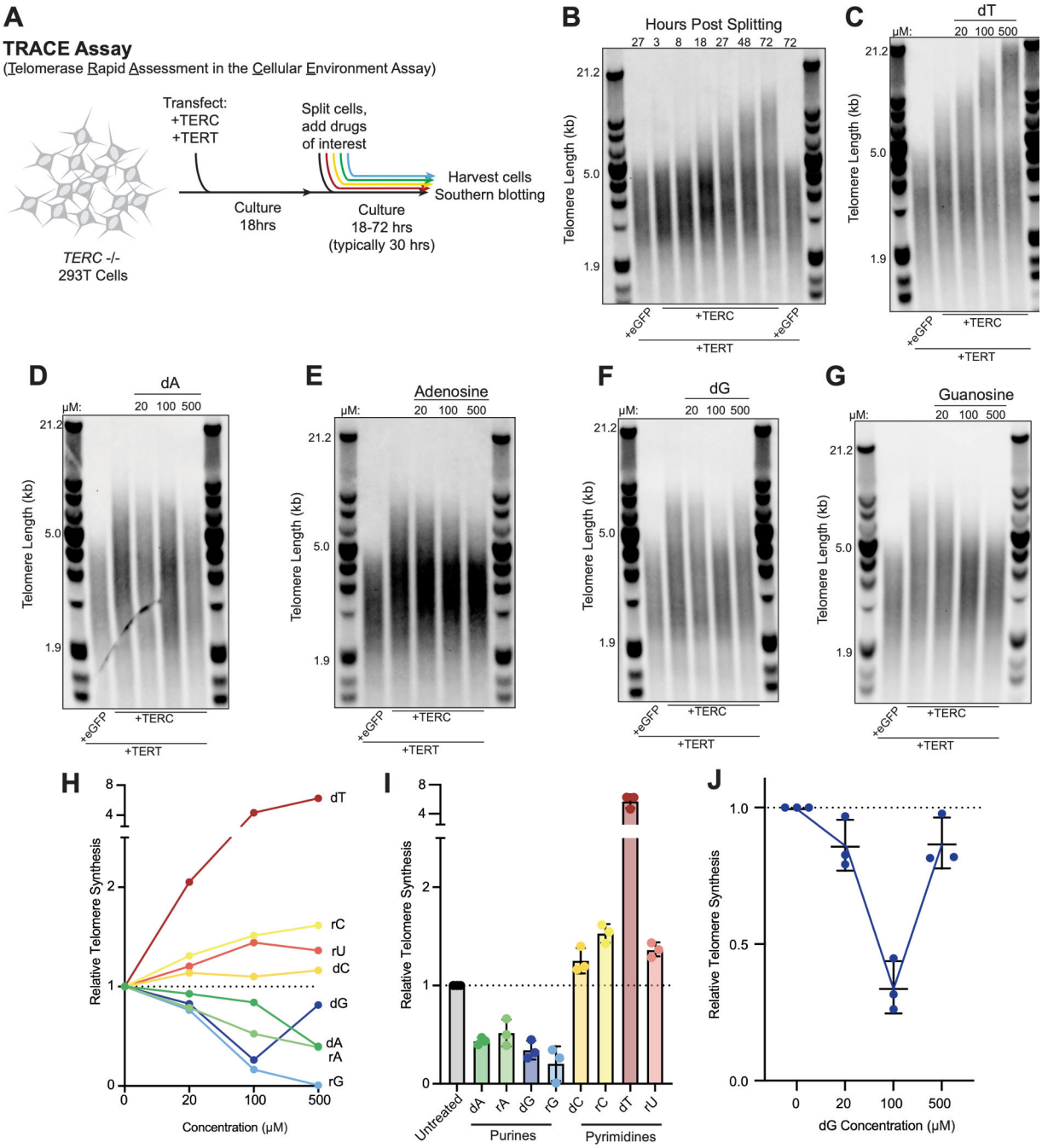
TRACE - a rapid human cell-based telomerase assay

The absence of rapid, high-throughput assays to study telomerase activity in its native cellular setting has been a major barrier to assessing the impact of metabolic perturbations and identifying therapeutically useful targets. Current telomerase assays either rely on measuring telomere length changes in cells after continuous culture for several weeks, or measuring enzymatic telomeric repeat addition in cell lysates using exogenous dNTPs and primers, potentially obscuring critical aspects of telomerase regulation. To overcome these barriers, here we establish a method for Telomerase Rapid Assessment in the Cellular Environment, or TRACE (**Figure 3-1a**), wherein telomerase-null 293T cells[206] are transfected with vectors encoding TERC and TERT[48], leading to telomerase-mediated telomere lengthening detectable by Southern blot in less than 48 hours

(**Figures 3-1b, and S11a,b)**. To evaluate how TRACE responds to small molecules, we applied the telomerase inhibitor BIBR1532[207] for 30 hours in the assay and found dose dependent decreases in telomere synthesis (**Figure S11c,d**). To study the capability of TRACE to read out genetic impairment of telomerase components, we performed the assay using expression vectors encoding TBD-associated mutations in TERT[208,209] or TERC[210] and found that these pathogenic variants impaired telomere synthesis (**Figure S11e-h**). Collectively, these data demonstrate that the TRACE assay can rapidly read out small molecule and genetic modulation of telomerase activity in human cells.

Figure 3-1. Metabolite screening by TRACE assay reveals purine nucleoside supplementation inhibits telomerase activity in human cells. (A) Diagram of TRACE assay. (B) Terminal restriction fragment Southern blot (TRF) from TRACE assay performed as follows: *TERC*-/- 293T cells were transfected with the indicated expression vectors, cultured for 18 hours, then split and harvested at the indicated timepoints after splitting. (C-G) TRFs from TRACE assay where cells were transfected as in (B). 18 hours after transfection, cells were split and supplemented as indicated for 30 hours prior to harvesting. (H) Quantification of TRACE assays from (C-G), and (S1I-K), displayed as the relative telomere synthesis compared to untreated cells. (I) Quantification of TRACE assay performed as in c. Cells were treated with the indicated compounds at the following doses: dG, 100 μM; all other compounds, 500 μM. Experiment performed in biological triplicate. Includes data from (C-H) and (S1I-K). (J) Quantification of data from (F) performed in biological triplicate. (I-J) Data are presented as means; error bars indicate s.d. rC, cytidine; rU, uridine; dC, deoxycytidine; dA, deoxyadenosine; rA, adenosine; rG, guanosine.

Figure 3-1. (Continued)



Purine nucleosides inhibit telomerase

We next utilized the TRACE assay to evaluate how the manipulation of nucleotide metabolism impacts telomerase activity. We supplemented cells with individual deoxynucleosides (dNs) and ribonucleosides (rNs) at a range of concentrations and found that pyrimidines drove telomerase activation in a dose dependent manner (**Figures 3-1c and S11i-k)**, most robustly thymidine (dT) consistent with prior results[206]. In contrast, purine nucleoside supplementation caused telomerase inhibition, with the guanine nucleosides guanosine and deoxyguanosine (dG) inhibiting telomerase activity more potently than adenosine and deoxyadenosine (dA) (**Figure 3-1d-i**). Interestingly, dG inhibited telomerase activity to a greater degree at 100 μM than at 500 μM (**Figure 3-1j**), showing a dose dependent, non-linear relationship between telomerase activity and dG supplementation. Collectively, these results demonstrate that augmentation of purine metabolism via nucleoside supplementation can inhibit telomerase activity in human cells.

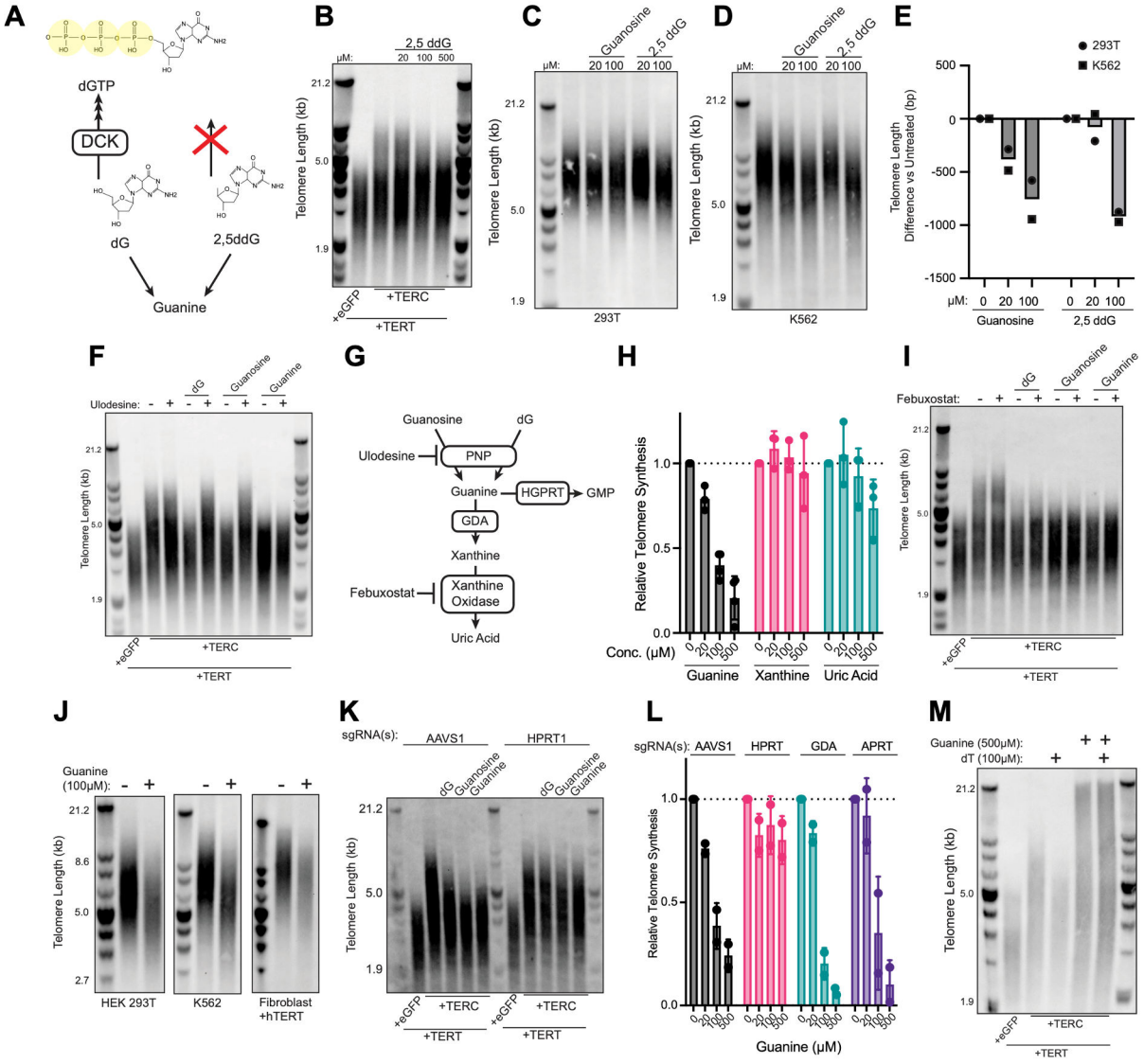
PNP is required for telomerase inhibition by guanosine and deoxyguanosine

We next investigated which metabolites of guanosine and dG mediate telomerase inhibition. First, because dG might undergo 5'-phosphorylation by deoxycytidine kinase (DCK), we tested if supplementation of 2',5'-dideoxyguanosine (2,5ddG), a dG analog which cannot be directly phosphorylated by DCK (**Figure 3-2a**), would also inhibit telomerase activity. Similar to the effects of guanosine and dG, we saw a dose dependent inhibitory effect of 2,5ddG supplementation in the TRACE assay (**Figure 3-2b**). To evaluate the effects on telomere length in cells without telomerase overexpression, we treated 293T cells and K562 cells with either 2,5ddG or guanosine, and saw dose dependent telomere shortening after 21 days in culture (**Figure 3-2c-e**). These results indicate that phosphorylation of dG by DCK to form dG nucleotides is not responsible for dG's

telomerase inhibitory effect. Furthermore, they validate the TRACE assay's ability to identify non-natural compounds that result in telomere shortening when applied to cells with endogenous levels of telomerase expression.

Figure 3-2. Metabolism of guanosine nucleosides by PNP and HGPRT to form guanine ribonucleotides inhibits telomerase activity and shortens telomeres. (A) Schematic of metabolic pathways for dG and 2,5ddG. (B) TRF from TRACE assay performed as follows: *TERC*-/- 293T cells were transfected with the indicated expression vectors, cultured for 18 hours, then split and cultured in the indicated doses of 2,5ddG for 30 hours. (C and D) TRF Southern blot of 293T cells or K562 cells cultured in the presence of the indicated compounds and doses for 21 days. (E) Quantification of (C and D). (F) TRF from TRACE assay performed as in (B). Doses of compounds: ulodesine, 1μM; dG, 100μM; guanosine, 500μM; guanine, 500μM. (G) Schematic of guanine nucleoside salvage and catabolism. (H) Quantification of TRF from TRACE assay performed as in (B) with the indicated doses of guanine, uric acid, and xanthine. See (Figure S2) for corresponding representative TRFs. Experiment performed in biological triplicate. (I) TRF from TRACE assay performed as in (B). Doses of compounds: febuxostat, 100μM; dG, 100μM; guanosine, 500μM; guanine, 500μM. (J) TRF of indicated cells cultured with or without 100μM supplemented guanine for three weeks. Representative TRF shown from three biological replicates. See Figure S2 for quantification.(K) TRF from TRACE assay performed on *TERC*-/- 293T targeted with the indicated sgRNA(s). Assay performed as in (B). dG, 100μM; guanosine, 500μM; guanine, 500μM. Representative TRF shown from two biological replicates. (L) Quantification of TRF from TRACE assay performed using *TERC*-/- 293T targeted with the indicated sgRNA(s). Assay performed as in (B). See Figure S2 for corresponding representative TRFs. Experiment performed in biological duplicate. (M) TRF from TRACE assay performed as in (B) Representative TRF shown from two biological replicates. (H and L) Data are presented as means and error bars indicate s.d.

Figure 3-2. (Continued)



Both guanosine and dG nucleosides are catabolized by purine nucleoside phosphorylase (PNP) to yield guanine and the associated sugar. We thus asked whether treatment with PNP inhibitors would rescue telomerase inhibition from guanine nucleoside supplementation in the TRACE assay. When we applied the PNP inhibitor ulodesine[211], we found that telomerase activity was no longer inhibited by guanosine or dG, whereas ulodesine alone had no effect (**Figure 3-2f**). These results pointed to a common downstream catabolite, and consistent with this, we found that guanine itself strongly inhibited telomerase activity in the TRACE assay in a manner that could not be reversed by ulodesine (**Figure 3-2f**). Similar results were obtained using the structurally distinct PNP inhibitor forodesine[212] (**Figure S12a**). These data support a model wherein telomerase inhibition by guanine nucleosides results from their common catabolism by PNP to form guanine.

Guanine ribonucleotides inhibit telomere lengthening in human cells

Guanine can be further catabolized into xanthine by guanine deaminase (GDA) followed by conversion into uric acid by xanthine oxidase (**Figure 3-2g**). We asked if telomerase inhibition from purine nucleosides could be due to the accumulation of the guanine degradation products xanthine or uric acid. To test this hypothesis, we compared the effects of directly supplementing cells with guanine, xanthine, or uric acid in the TRACE assay. Whereas guanine supplementation potently inhibited telomerase activity, xanthine and uric acid had minimal effects at doses up to 500 μM (**Figures 3-2h and S12b-d**). As a complimentary approach to evaluate whether the accumulation of guanine catabolic products drives telomerase inhibition, we tested the xanthine oxidase inhibitor febuxostat[213] in the TRACE assay and found it was unable to rescue telomerase activity from treatment with either dG, guanosine, or guanine (**Figure 3-2i**). Together, these findings suggest that guanosine and dG supplementation drive telomerase inhibition via the

accumulation of guanine, rather than its downstream degradation products. To study these effects under conditions with physiologic telomerase expression, we treated unmanipulated 293T or K562 cells with 100 μM guanine for 21 days and found reproducible telomere shortening (**Figures 3-2j and S12e**). To test this in diploid primary cells, we treated normal human fibroblasts in which TERT was stably expressed with guanine for 21 days, and similarly observed inhibition of telomere lengthening (**Figures 3-2j and S12e**). Collectively, these results indicate that conversion of guanosine and dG into guanine causes telomerase inhibition, and show that guanine supplementation shortens telomeres in human cells.

Guanine can be salvaged by hypoxanthine-guanine phosphoribosyltransferase (HGPRT) to generate GMP (**Figure 3-2g**). We thus asked if guanine salvage into cellular ribonucleotide pools via HGPRT is required for telomerase inhibition after guanine supplementation. Using CRISPR/Cas9, we generated *HPRT1* deficient *TERC*-/- 293T cells and verified efficient on-target gene inactivation (**Figure S12f**). We similarly used CRISPR/Cas9 to generate *TERC*-/- 293T cells deficient for *APRT*, encoding adenine phosphoribosyltransferase which converts adenine to AMP, and *GDA* encoding guanine deaminase which catabolizes guanine to xanthine (**Figure 3-2g**). The *AAVS1* safe harbor locus was targeted as a control. Using the TRACE assay we found that, relative to *AAVS1*-targeted cells, telomerase activity in *HPRT1*-targeted cells was minimally inhibited by guanosine, dG or guanine (**Figures 3-2k and S12h**). In comparison, telomerase inhibition by guanine in *GDA*- or *APRT*-targeted cells was similar to control cells (**Figures 3-2l, S12h,i**). Taken together, these data support a model where treatment with guanosine, dG, or guanine leads to salvage of guanine by HGPRT to form guanine ribonucleotides, which in turn results in telomerase inhibition.

Guanine supplementation has been shown to reduce nucleotide levels including ATP as well as the telomerase substrates dGTP and dTTP downstream of its salvage into ribonucleotide pools[214,215]. ATP is an allosteric activator of ribonucleotide reductase (RNR)[82] which is the rate-limiting enzyme in the *de novo* dNTP synthesis pathway. Therefore, the depletion of ATP levels and subsequent inhibition of RNR and dNTP production offer a potential explanation for the downregulation of telomerase activity following guanine supplementation (**Figure S12j**). To test this, based on prior work showing dT augments dTTP and dGTP production[216] and dT supplementation upregulates telomerase activity[206], we asked if the inhibitory effect of guanine treatment could be rescued by increasing dT nucleotide salvage. Using the TRACE assay, we found that dT supplementation could fully rescue cells from the telomerase inhibitory effects of guanine treatment (**Figure 3-2m)**. Taken together, our results indicate that the inhibitory effects of guanine occur due to depletion of dNTP pools downstream of GMP accumulation.

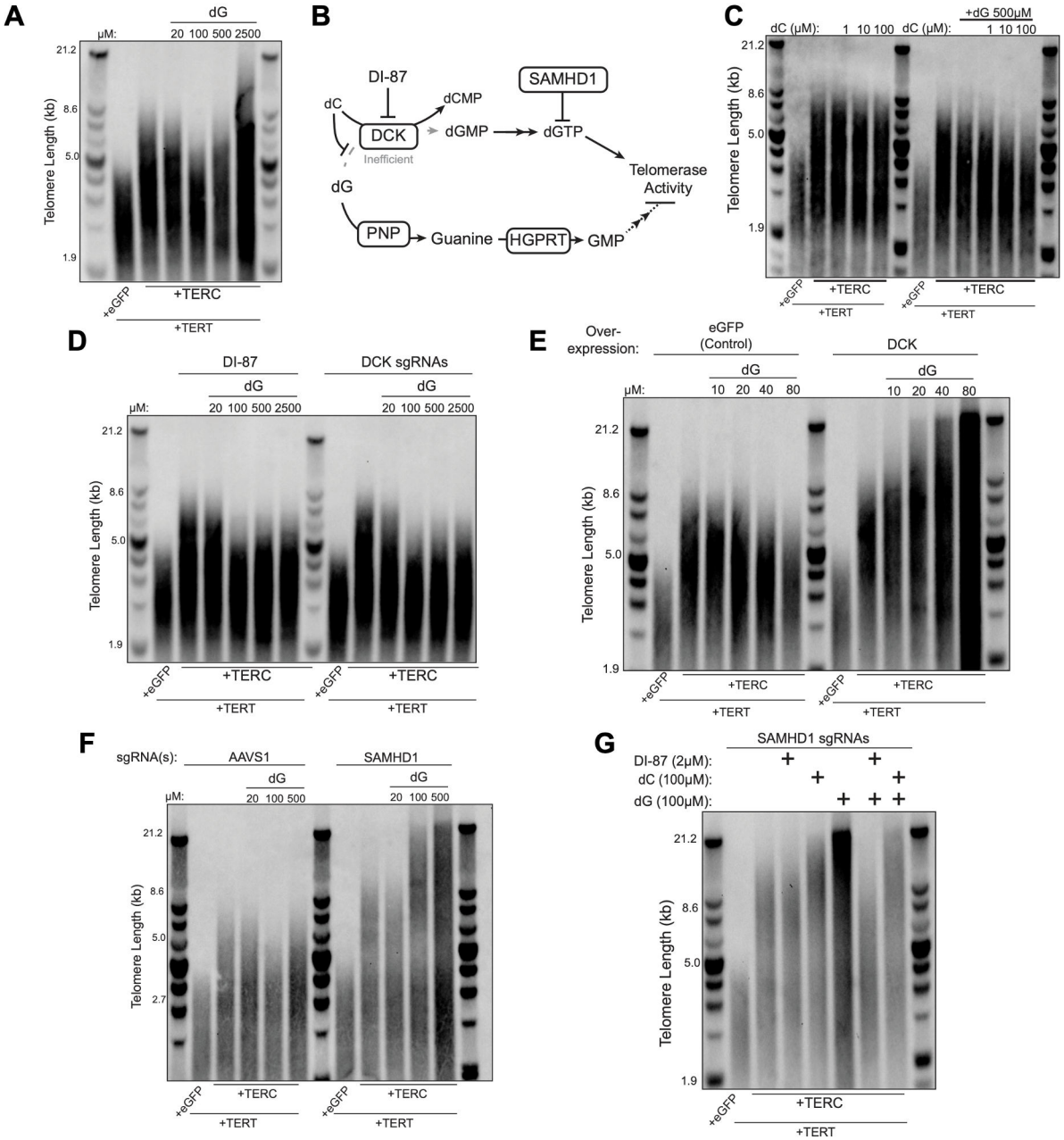
DCK inefficiently salvages dG to promote telomerase activation

In the TRACE metabolite screen, we found that dG supplementation had a non-linear effect on telomerase activity, with 100 μM dG inhibiting telomerase activity to a greater degree compared to 500 μM dG (**Figure 3-1h**). We repeated this analysis using a broader dG dose range, and again found that while 100 μM dG strongly inhibited telomerase activity, 500 μM had a smaller inhibitory effect, and 2.5 mM dG increased telomere synthesis above baseline (**Figure 3-3a)**. Given dGTP is a telomerase substrate, we wondered if salvage of excess dG by DCK into dG nucleotides could underlie the increased telomerase activity observed with high dose dG, potentially counteracting the inhibitory effects on telomerase from the "default" pathway of dG breakdown into guanine (**Figure 3-3b**). To address this question, we used a series small of

molecule and genetic approaches to alter DCK function. DCK is known to prefer dC as a substrate compared with dG[217], and dC supplementation has been shown to inhibit dG salvage by DCK[218] (**Figure 3-3b**). Thus, we first asked if dC supplementation could block a potential telomerase activating effect of high dose dG. Using the TRACE assay, we found that while dC itself had a minimal effect on telomerase activity, the addition of dC to 500 μM dG led to shorter telomeres than 500 μM dG alone (**Figure 3-3c**), consistent with the notion that substrate competition at the level of DCK blocks telomerase stimulation from dG nucleotide salvage. Next, we applied the DCK inhibitor DI-87[219] to cells treated with increasing doses of dG in the TRACE assay. In comparison to the effects of dG alone, we found reduced telomerase activity at 500 μM and 2.5mM dG in the presence of DI-87 (**Figure. 3-3d**). Similarly, when we inactivated *DCK* in *TERC*-/- 293T cells using CRISPR/Cas9 (**Figure S13a**) we found that dG no longer stimulated telomerase activity at high doses (**Figure 3-3d**). Finally, given DCK is inefficient at phosphorylating dG, we asked if increasing cellular DCK activity would enable dG-dependent telomerase activation at lower doses. We generated DCK overexpressing *TERC*-/- 293T cells for use in the TRACE assay and found that dG could now promote telomerase activation at doses as low as 20 μM, with strong activation at 80 μM. In contrast, eGFP-expressing control cells remained inhibited by dG at 40 and 80 μM doses (**Figure 3-3e**). These findings rigorously demonstrate that dG at high levels can be salvaged by DCK to form deoxyguanosine nucleotides that effect net telomerase activation, on a backdrop where dG is otherwise metabolized via guanine into guanosine ribonucleotides that cause telomerase inhibition. Collectively, these results indicate that dG nucleotide salvage capacity and pathway choice dictate the net effect of dG on telomerase activity in human cells.

Figure 3-3. Salvage of dG nucleotides via DCK activates telomerase in a manner modulated by the dNTPase SAMHD1. (A) TRF Southern blot of TRACE assay from *TERC*-/- 293T cells transfected with the indicated expression vectors, cultured for 18 hours, then split and cultured in the indicated doses of dG for 30 hours. A representative blot is shown from two biological replicates. (B) Schematic of dG salvage pathways. (C) TRF Southern blot of TRACE assay performed as in (A) where cells were treated with dG and dC as indicated. (D) TRF Southern blot of TRACE assay performed as in (A) using either *TERC*-/- 293T cells (left), or TERC-/- 293T cells which had been targeted with sgRNAs targeting *DCK* (right). Cells were treated with DI-87 at 2μM and with dG as indicated. A representative blot is shown from two biological replicates. (E) TRF Southern blot of TRACE assay performed as in (A) using *TERC*-/- 293T cells overexpressing eGFP or DCK. Cells were treated with dG as indicated. (F) TRF Southern blot of TRACE assay performed as in (A) using *TERC*-/- 293T cells targeted with sgRNA(s) against *AAVS1* or *SAMHD1*. Cells were treated with dG as indicated. A representative blot is shown from two biological replicates. (G) TRF Southern blot of TRACE assay performed as in (A) using *TERC*-/- 293T cells targeted with sgRNAs against *SAMHD1*. Cells were treated with DI-87, dC, and dG as indicated.

Figure 3-3. (Continued)



SAMHD1 restricts telomerase activation from salvaged dG nucleotides

Salvage of dG into nucleotides by DCK could be promoting telomerase activity at the mono-, di-, or triphosphate levels. The dNTPase SAMHD1 restricts cellular deoxyribonucleotide *tri*phosphate levels including dGTP and is a negative regulator of telomere length[205,206] (**Figure 3-3b)**. To determine if dG salvage acts at the nucleotide triphosphate level, we asked what impact SAMHD1 disruption would have on telomerase activation after dG supplementation. We thus used SAMHD1 deficient *TERC*-/- 293T cells[206] in the TRACE assay and evaluated the effects of dG treatment. Unlike the strong telomerase inhibition from 100 μM dG seen in control cells, we found that SAMHD1 deficient cells showed robust telomerase activation at the same dose, an effect that increased further using 500 μM dG (**Figure 3-3f**). In contrast, when we applied guanosine or guanine to SAMHD1 deficient cells, we found that telomerase activity was inhibited to a similar degree compared to cells in which SAMHD1 was intact (**Figure S13b**). These results suggest that the telomerase activation seen after dG salvage by DCK is not only mediated by dGTP, but potently restricted by SAMHD1. To verify that the dG dependent telomerase activation in the absence of SAMHD1 was occurring via DCK salvage, we tested the effect of inhibiting DCK and found that DI-87 strongly inhibited telomerase activation in SAMHD1 deficient cells after dG treatment (**Figure 3-3g**). Similarly, we found that dC, which competes with dG as a DCK substrate, also restricted the telomerase activation from dG in SAMHD1 deficient cells (**Figure 3-3g**). These results indicate that the dNTPase SAMHD1 restricts telomerase activation from dG nucleotide salvage downstream of DCK and provide further support for a model where net dGTP accumulation promotes telomerase activity.

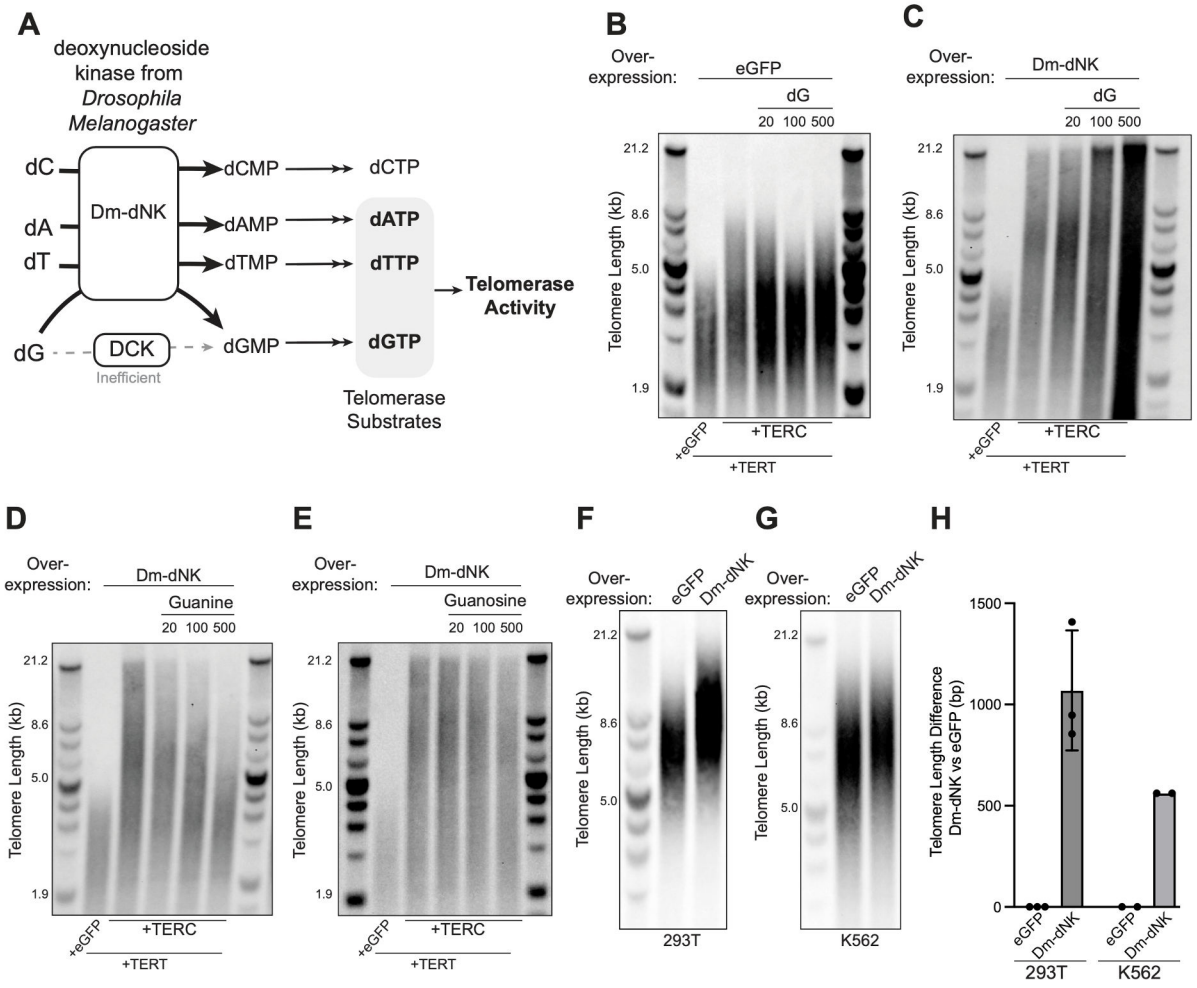
Nucleoside salvage efficiency limits telomerase activity and telomere length

Given the strong activation of telomerase from dG when we overexpressed DCK, which is relatively inefficient at phosphorylating dG, we wondered if altering cellular metabolism to drive more efficient deoxynucleoside salvage could further promote telomerase activity. The *Drosophila melanogaster* deoxynucleoside kinase (Dm-dNK) is a highly efficient kinase with broad specificity and eight-fold more activity on dG than DCK[79,81,220] (**Figure 3-4a**). Thus we generated Dm-dNK expressing *TERC*-/- 293T cells and applied the TRACE assay in the setting of dG. Surprisingly, we found Dm-dNK expressing cells showed higher baseline telomerase activity compared to control eGFP expressing cells without added dG, indicating that overexpressing Dm-dNK and increasing cellular nucleoside salvage capacity is sufficient to promote telomerase activity even in the absence of exogenous nucleoside supplementation (**Figure 3-4b,c**). When we applied dG to Dm-dNK expressing cells we found a further dose dependent enhancement of telomerase activity increasing up to 500 μM dG (**Figure 3-4c**). In contrast to the striking telomerase activation from dG supplementation, treatment with guanosine or guanine continued to show inhibitory effects telomere synthesis, albeit to a lesser degree, consistent with the specificity of Dm-dNK for dNs (**Figures 3-4d,e**). We next asked whether overexpressing Dm-dNK could promote telomere lengthening in long term culture of human cells without telomerase overexpression. When we infected cells with Dm-dNK overexpression constructs and compared them with eGFP expressing control cells, we found Dm-dNK overexpression led to robust telomere lengthening in 293T cells over 25 days of culture (**Figures 3-4f,h**). Whereas a similar level of Dm-dNK expression (driven by a CMV promoter) was not well tolerated in K562 cells, use of a doxycycline-inducible Dm-dNK expression construct also showed telomere lengthening compared to controls (**Figures 3-4g,h**). Taken together, these findings indicate that deoxynucleoside salvage capacity is limiting for

telomere synthesis in human cells, and can be manipulated to increase telomerase activity and drive telomere lengthening.

Figure 3-4. Expression of an efficient deoxynucleoside kinase from Drosophila melanogaster promotes telomerase activity from dG treatment and lengthens telomeres. (A) Schematic of Dm-dNK activity. (B-E) TRF Southern blot of TRACE assay from *TERC*-/- 293T cells overexpressing either eGFP or Dm-dNK which were transfected with the indicated expression vectors, cultured for 18 hours, then split and cultured in the indicated doses of dG, guanine, or guanosine for 30 hours. (F) TRF Southern blot of 293T cells which were transduced with lentivirus for constitutive overexpression of eGFP or Dm-dNK and cultured for one month. A representative blot is shown from three biological replicates. (G) TRF Southern blot of K562 cells which were transduced with lentivirus for doxycycline inducible overexpression of eGFP or Dm-dNK and cultured for one month in the presence of 1μg/ml of doxycycline. A representative blot is shown from two biological replicates. (H) Quantification of (F and G). Data are presented as means and error bars indicate s.d.

Figure 3-4. (Continued)

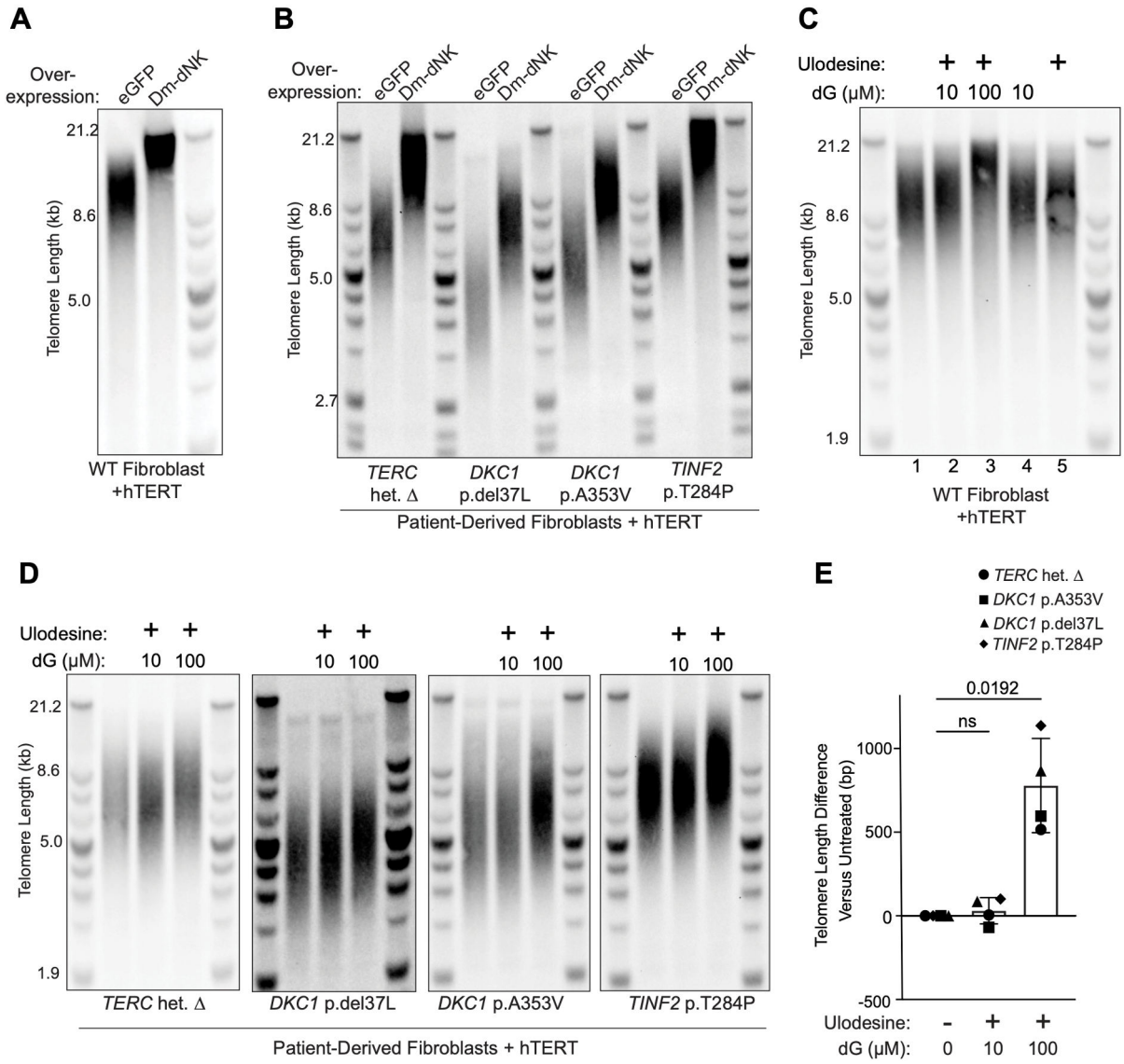


Manipulating deoxynucleoside salvage drives telomere lengthening in cells from TBD patients

TBDs are caused by hypomorphic mutations in the core telomerase components and other telomere maintenance genes. Based on our findings showing overexpression of Dm-dNK could promote telomere lengthening, we asked if the expression of Dm-dNK could overcome genetic defects in telomere synthesis and yield telomere lengthening in cells from TBD patients. To address this question, we utilized a panel of fibroblasts from TBD patients carrying pathogenic mutations in *TERC*, *DKC1* which encodes a member of the telomerase holoenzyme, or *TINF2* which encodes a component of the telomere shelterin complex. We first determined that ectopic expression of Dm-DNK robustly increased telomere length in normal human skin fibroblasts stably expressing TERT (**Figure 3-5a**). Next, we overexpressed Dm-dNK in TBD patient fibroblasts expressing TERT, and found that overexpression of Dm-dNK drove striking increases in telomere length by thousands of base pairs after three weeks in culture (**Figure 3-5b**). These data indicate that deoxynucleoside salvage capacity limits telomere length in human diploid cells, and that augmenting dNTP salvage restores telomere length in cells from patients with TBDs.

Figure 3-5. Manipulation of deoxynucleotide salvage by expressing Dm-dNK or treatment with dG plus ulodesine drives telomere lengthening in fibroblasts from patients with TBDs. (A) TRF Southern blot from TERT expressing fibroblasts from a healthy donor overexpressing eGFP or Dm-dNK as indicated and cultured for five weeks. (B) TRF Southern blot from TERT expressing fibroblasts from TBD patients harboring mutations in the indicated genes overexpressing eGFP or Dm-dNK as indicated and cultured for one month. (C) TRF Southern blot from TERT transformed fibroblasts from a healthy donor which were treated with 1μM ulodesine and dG as indicated for three weeks. (D) TRF Southern blot from TERT transformed fibroblasts from TBD patients harboring mutations in the indicated genes which were treated with 1μM ulodesine and dG as indicated for three weeks.(E) Quantification of median telomere length from (D). Statistical significance determined using paired two-sided t-test. Error bars indicate standard deviation.

Figure 3-5. (Continued)



Next, based on our findings that the pathway by which dG is metabolized influences telomerase activity in a bidirectional manner, we hypothesized that shifting the balance towards deoxynucleoside salvage rather than catabolism using small molecules would drive telomere elongation in long term culture. To test this hypothesis in primary human cells, we treated normal fibroblasts stably expressing TERT with the PNP inhibitor ulodesine. We also tested ulodesine in combination with supplemented dG, because treatment of human subjects with PNP inhibitors has been shown to increase serum dG levels[221]. We found that, while treatment with either ulodesine or with dG alone did not lead to detectable changes in telomere length, the combination of ulodesine with 100 μM dG led to robust telomere lengthening after 21 days in culture (**Figure 3-5c**). We next asked if the combination of treatment with ulodesine and dG could promote telomere lengthening in cells derived from patients with TBDs. Remarkably, we found that treatment with the combination of ulodesine and 100 μM dG for three weeks drove telomere lengthening across all mutant genotypes tested (**Figure 3-5d and 3-5e**). Collectively, these findings indicate that deoxynucleotide salvage limits telomere lengthening in human cells, and that genetic and small molecule-based manipulation of deoxynucleoside salvage can promote telomere restoration in the setting of TBD-causing genetic defects.

Discussion

Telomere length must be kept within a tight window to maintain human health. Genetic dysregulation of telomere length homeostasis leading to either aberrantly short or long telomeres predisposes to lethal diseases. Telomere length is generally considered to be governed by the expression and abundance of telomerase, and the recruitment of telomerase to the chromosome end by shelterin proteins[21]. Here, we reveal that reverse transcription by telomerase in human cells

is constrained by the availability of dNTP substrates for 5'-GGTTAG-3' repeat synthesis. Based on our findings, we propose an updated model for the regulation of telomerase reverse transcription, wherein modulation of nucleotide synthesis and salvage plays an active, critical role in human telomere length homeostasis in normal and disease states. While strategies to therapeutically target canonical regulators of telomerase – expression, abundance, recruitment – have met with limited success to date, our findings suggest that well-trodden paths of pharmacologically manipulating nucleotide synthesis or salvage could lead to new treatments for genetic telomere diseases and other degenerative disorders.

This work was stimulated by several emerging lines of human genetic evidence implicating nucleotide metabolism in telomere length control[32–34], hitherto lacking mechanistic explanations consistent with prevailing models of telomere length control. Independent genetic and functional studies have converged on thymidine metabolism as the central player in the regulation of human telomerase activity and telomere length[32,206]. These findings appear to contrast prior studies using purified telomerase showing that dGTP rather than dTTP plays a dominant role in the control of enzymatic activity[71–74]. Here, we sought to comprehensively determine the relationship between nucleotide metabolism and telomerase reverse transcriptase activity in intact human cells and developed the TRACE assay. Unlike prior methods, TRACE enables detection of telomere length changes in human cells within hours and can be applied to study the impact of metabolic perturbations on telomerase reverse transcriptase activity. We were thus able to screen nucleoside metabolites for their effects on telomere synthesis and identified a bidirectional and limiting role of guanine nucleoside salvage in telomerase regulation. Our findings indicate that the low efficiency of dG phosphorylation by DCK restricts dG nucleotide accumulation and limits telomerase activation from dG supplementation. In the TRACE assay, very high doses of dG were

able to overcome this inefficiency and promote telomerase activation. Furthermore, increasing the efficiency of dG salvage by DCK overexpression yielded potent telomerase activation. These data indicate that dGTP accumulation drives strong telomerase activation in human cells, in line with the effects of dGTP levels on purified human telomerase[71,73,74] and in yeast cells[100]. These results are also consistent with recent observations of negative regulation of telomere length by the dNTPase SAMHD1, which preferentially degrades dGTP[205,206]. Along these lines, the sensitivity of telomerase to dGTP may contribute to the telomerase activation seen after dT supplementation[206]. dTTP has been shown to allosterically act on RNR to increase dGTP production[82]. The upregulation of dGTP after dT treatment may offer an explanation for the surprising finding that telomere repeat synthesis is stimulated by dT supplementation even when telomerase is modified to no longer use dTTP as a substrate[206]. Of note, the efficiency of dT salvage by TK1 is orders of magnitude higher than the efficiency of dG salvage by DCK[79–81], potentially explaining the more robust effect of dT than dG supplementation on telomere elongation in cells. Together, under this model, our findings provide a mechanism for human GWAS data linking the cytosolic deoxynucleoside kinases TK1 and DCK with telomere length[34], acting at the level of nucleoside salvage efficiency. Overcoming normal human physiologic limits on salvage capacity by overexpressing a highly efficient deoxynucleotide kinase from *Drosophila melanogaster* drove robust telomere lengthening, including cells derived from TBD patients. In sum, these findings reveal that deoxynucleoside salvage efficiency actively constrains telomere synthesis by telomerase under physiological conditions, and can be manipulated to overcome impaired telomere maintenance in the setting of TBD-causing genetic defects.

In addition to revealing the importance of deoxynucleoside salvage capacity for telomerase regulation, we also surprisingly found that guanine or guanine nucleoside supplementation led to

telomerase inhibition, and guanine treatment drove telomere shortening across multiple cell types including cancer cell lines. Guanine supplementation has been found to deplete dNTPs including dTTP and dGTP[214,215]. While the mechanism underlying dNTP depletion from guanine supplementation has not been established, guanine salvage into ribonucleotides pools has been shown to reduce ATP levels in human cells[214,215]. ATP is an allosteric activator of ribonucleotide reductase (RNR)[82] which is the rate-limiting enzyme in the *de novo* dNTP synthesis pathway, including the telomerase substrates dGTP and dTTP. Based on this model, we hypothesized that guanine could be inhibiting telomerase by reducing dNTP levels, and asked if upregulating dNTP synthesis could rescue telomerase inhibition in guanine treated cells. We found that augmenting dNTP production by supplementing with dT could fully rescue cells from guanine-mediated telomerase inhibition. These results support a model whereby guanine salvage inhibits telomerase by limiting dNTP availability for telomere synthesis. More broadly, our data showing that dG nucleoside supplementation bidirectionally controls telomerase activity can be unified under a model wherein the dNTP substrates required by telomerase are either increased or decreased, depending on net dG metabolism into guanosine deoxyribonucleotides versus ribonucleotides.

Telomerase activation is a critical step in tumorigenesis in many cancers, and effective anti-neoplastic telomerase inhibitors have been long-sought after but remain largely elusive. dNTP levels are elevated in most cancers[76] by means including the upregulation of the rate limiting thymidine salvage enzyme TK1. Similarly, deoxynucleoside kinases are expressed in many viruses which cause human disease including the oncogenic viruses Epstein-Barr virus and Human Herpesvirus-8[222] which also upregulate telomerase activity as part of their progression[223]. It has been proposed that the increased dNTP levels in cancer cells enables efficient genome replication and frequent cell divisions. Based on our data, it is also possible that elevated dNTP levels provide

a selective advantage to tumor cells by lifting a metabolic constraint on telomere synthesis by telomerase. Several nucleotide analog chemotherapy drugs are known to inhibit dNTP synthesis such as gemcitabine, clofarabine, and 5-fluorouracil, and we therefore speculate that telomerase inhibition may contribute to their anti-tumor activity. The intersection between nucleotide metabolism and telomerase activity offers a new avenue to examine how cellular self-renewal limits are bypassed in chronic viral infections and tumorigenesis, and how this may be interrupted therapeutically.

Manipulation of dNTP metabolism also plays an essential role in the treatment of a variety of disorders beyond cancer, such as purine synthesis inhibitors azathioprine and mycophenolate mofetil in autoimmune disorders, uridine monophosphate in patients with CAD deficiency and deoxypyrimidines in patients with TK2 deficiency. Based on the robust telomere lengthening we observed from overexpressing Dm-dNK as well as from using ulodesine plus dG in primary human cells from patients with genetically-diverse TBDs, our data suggest that strategies to shift deoxynucleoside metabolism towards dNTP accumulation could be a promising therapeutic strategy to augment telomerase activity in TBDs. PNP inhibitors have been shown to be well-tolerated, and to increase serum dG levels and cellular dGTP levels[224,225], and thus based on our data, may be able to promote telomere lengthening as a single agent.

Nuclear dNTP pools serve as common substrates for genome replication by DNA polymerases and for telomere synthesis by telomerase, yet these DNA synthesis machines must perform fundamentally different tasks. While replicative DNA polymerases copy billions of base pairs of sequence with high fidelity within hours during S phase of the cell cycle, telomerase activity is tightly tied to the rate of telomere attrition which is estimated to be ~50-100 base pairs per cell division at each chromosome end[27,30]. Additionally, unlike replicative DNA polymerases,

telomerase has no defined endpoint for telomere repeat synthesis once it has begun. Tight regulation of TERC and TERT expression and control of telomere end accessibility by the shelterin and CST complexes have long been proposed to explain the homeostatic limit of human telomere length[226]. However, in our recent[206] and present work collectively, we have overcome this limit through manipulation of dNTP levels using four different approaches: thymidine supplementation, dG supplementation plus PNP inhibition, SAMHD1 inactivation, and deoxynucleoside kinase overexpression. Nuclear dNTP pool homeostasis is under competing selective pressures including the need to maintain genome fidelity and to restrict the proliferation of DNA viruses, retroviruses, and selfish genetic elements. Given the extreme sensitivity of cellular telomerase activity to changes in dNTP metabolism that we observed in this study, we propose that selective pressures on cellular dNTP levels may have shaped telomere length homeostasis throughout evolution. Conversely, the need to maintain reverse transcription by telomerase may contribute to the lower bound of tolerable dNTP levels: further reductions of dNTPs can cause diseases of telomerase insufficiency, as seen in patients with inherited *TYMS* locus mutations who develop dyskeratosis congenita[32]. We expect that this telomerase-inclusive perspective will offer new insights on how competing constraints on nucleotide flux have impacted cellular metabolism and genome integrity throughout evolution.

Materials and Methods

Human Subjects

Biological samples were procured under Boston Children's Hospital Institutional Review Board-approved protocols, after written informed consent in accordance with the Declaration of Helsinki. The patient with mutation of the *TINF2* gene presented with dyskeratosis congenita and bone marrow failure in early childhood, consistent with the mutation leading to the p.T284P amino acid change in the 'hot spot' region of *TINF2,* a site where mutations are frequently associated with the TBD dyskeratosis congenita.

Cell Models

293T cells (American Type Culture Collection, ATCC) were cultured in Dulbecco's Modified Eagle Medium (DMEM, Gibco) supplemented with 10% fetal bovine serum, MEM Non-Essential Amino Acids (Gibco), L-glutamate (Corning), and penicillin/streptomycin (Corning) and subcultured using trypsin (Gibco). K562 cells (American Type Culture Collection, ATCC) were cultured in RPMI 1640 supplemented with 10% fetal bovine serum, MEM Non-Essential Amino Acids (Gibco), L-glutamate (Corning), and penicillin/streptomycin (Corning). Fibroblasts cells were cultured in Dulbecco's Modified Eagle Medium (DMEM, Gibco) supplemented with 15% fetal bovine serum, MEM Non-Essential Amino Acids (Gibco), L-glutamate (Corning), and penicillin/streptomycin (Corning) and subcultured using trypsin (Gibco). The normal human fibroblast line NHSF2 was a gift from A. Klingelhutz, University of Iowa. The TBD patient fibroblasts with the DKC1 del37L (GM01774)[43] mutation were obtained from the Coriell Cell Repository. The TBD patient fibroblasts with the DKC1 A353V mutation have been described[194].

The TBD patient fibroblasts with the *TERC*$^{+/-}$ 821 base pair deletion have been described[193]. The TBD patient fibroblasts with the TIN2 p.T284P mutation were generated by culturing punch biopsies under glass coverslips until fibroblast outgrowths were apparent. All fibroblast lines were infected with pCW57.1 TERT lentivirus, selected in puromycin, and cultured in the presence of 1μg/ml doxycycline (Sigma-Aldrich) during experimental perturbations.

Lentivirus production and transduction

293T cells were transfected with psPAX2 (plasmid 12260; Addgene) and pMD2.G (plasmid 12259; Addgene) in addition to the appropriate transfer vector using Lipofectamine 2000 (Invitrogen) per the manufacturer's instructions. Lentivirus containing media was harvested 48 and 72 hours after transfection, filtered using 0.45 μM filters (VWR International), and stored at -80°C until use. Lentiviral transduction was performed via spinfection at 931G for 2 hours in media supplemented with protamine sulfate (Sigma-Aldrich) at 10μg/ml. 24 hours after removal of virus containing media, cells were selected using blasticidin (InvivoGen) at 10μg/ml for 5-10 days or puromycin (Sigma-Aldrich) at 1μg/ml for 4-7 days.

TRACE Assay

On the evening prior to transfection, *TERC*-/- 293T cells were plated at $0.75*10^6$ cells per ml of media into a six well plate. The following day, cell media was replaced approximately one hour prior to transfection. Transfection was performed as follows. For each well of a six well plate, 8 μl of Lipofectamine 2000 (Invitrogen) was mixed with 150ul of Opti-MEM serum free media (Gibco) and incubated for 5 minutes. In a separate tube, 416ng pcDNA-3xHA-TERT and 2083 ng of either pBS-U3-TERC or pMAX-eGFP as indicated were mixed into 150 μl of Opti-MEM. These

two solutions were then combined, mixed gently, and incubated for 5 minutes followed by dropwise addition to cells. 18 hours after transfection, cells were split into treatment conditions and cultured for 30 hours unless otherwise indicated. Cells were then harvested and pellets were stored at -80°C until DNA isolation and terminal restriction fragment length analysis (described below).

Terminal Restriction Fragment Length Analysis

DNA was isolated from cell pellets using the Pure Link Genomic DNA Miniprep kit (Invitrogen). 0.5-3 μg of DNA was digested with RsaI (NEB) and HinfI (NEB) for 2 hours at 37°C. DNA was then separated by electrophoresis on a 0.6% agarose gel followed by Southern blotting onto Hybond-N+ membrane (Amersham). Detection was performed using the TeloTAGGG Telomere Length Assay Kit (Roche) using the provided probe at the recommended concentration or a probe complimentary to the C-rich strand of the telomere synthesized as described[198] using the CCCTAA-probe oligonucleotide (See Oligonucleotides, below). Where indicated, Southern blots were stripped using two washes with 0.2M NaOH and 0.1% sodium dodecyl sulfate (SDS) at 37°C for 15 mins with shaking followed by detection as described above. Telomere length quantification was performed with the WALTER webtool (v2.0) [199]. TRACE assay experiments were quantified using ImageJ (Version 2.9.0/1.54f) as follows: First, calculate the ratio (R) of signal above 5kb (largely newly synthesized telomere) to below 5kb (largely pre-existing telomere signal for TERC-/- 293T cells) for each sample. Then, to calculate background normalized ratios (Rb), for each sample expressing TERC, subtract R for eGFP expressing cells on the same blot (removing background signal contribution) from sample R. Then, to calculate the relative telomere synthesis for a given sample, divide the Rb of experimental samples by the untreated control sample on the

same blot (normalizing relative to untreated). Statistical analysis was performed using GraphPad Prism (version 10.0.0).

CRISPR/Cas9 gene editing

Gene editing was performed using the Neon™ Transfection System 10 µL Kit (Invitrogen) by complexing 37 pmol Alt-R S.p. Cas9 Nuclease V3 (IDT) and 50 pmol chemically modified sgRNA(s) (Synthego) at room temperature for 20 minutes followed by addition of 200,000 cells suspended in 20 µl buffer R (Thermo Fisher Scientific) with Electroporation Enhancer (IDT). The cell mixture was electroporated using a Neon Transfection System (Thermo Fisher Scientific) using the following settings: HEK 293T, 1200V, 30ms, 1 pulse; K562 1150 V, 10ms, 3 pulses. After electroporation, cells were plated into normal media. Editing efficiency was evaluated by isolating genomic DNA from cells at least 3 days after electroporation followed by PCR amplifying the target locus. PCR products were visualized by electrophoresis on a 2% agarose gel.

Recombinant DNA Cloning

Constructs to express variants in TERT associated with TBDs were generated from the pCDNA-3xHA-hTERT vector using the Q5 site directed mutagenesis kit (NEB) and were verified by Sanger sequencing.

The DCK expression construct was cloned from 293T cell cDNA into the pLX304 backbone (plasmid 25890; Addgene) by Gibson assembly using the HiFi DNA assembly mix (NEB). The final construct expresses DCK with a C-terminal fusion to a V5 epitope tag which is present in the pLX304 backbone and the sequence was verified by Sanger sequencing. The cDNA was

synthesized by isolating RNA from cells using TRIzol Reagent (Invitrogen), then treating RNA with TURBO DNA-free Kit (Invitrogen). Complementary DNA was synthesized using SuperScript III Reverse Transcriptase (Invitrogen) with oligo-dT priming (Invitrogen).

The PLX304-eGFP construct was generated by PCR amplifying the eGFP sequence from the pXPR_011 vector (plasmid 59702; Addgene) using attB-flanked primers followed by Gateway cloning (Invitrogen) according to the manufacturers protocol into the pLX304 backbone. The final construct expresses eGFP with a C-terminal fusion to the V5 epitope tag which is present in the pLX304 backbone. The sequence was verified by Sanger sequencing

The CMV driven Dm-dNK expression construct pLX304 Dm-dNK V5 was cloned from the pOpen-dromedNK plasmid Project (plasmid 165579; Addgene) into the pLX304 backbone by Gibson assembly using the NEB HiFi DNA assembly mix. The final construct expresses Dm-dNK with a C-terminal fusion to a V5 epitope tag which is present in the pLX304 backbone. The sequence was verified by Sanger sequencing

The doxycycline inducible Dm-dNK expression construct was generated by isolating the insert from the pLX304 Dm-dNK V5 using SacI (NEB) and SalI (NEB), and ligating it into the pCW57.1 backbone (plasmid 41393; Addgene) which had been digested with NheI (NEB) and SalI (NEB) using Quick Ligase (NEB) generating pCW57.1 Dm-dNK V5. The sequence was verified by Sanger sequencing. The blasticidin resistant version of this vector used in Figure 4 was generated by digesting pCW57.1 Dm-dNK V5 with NotI and SpeI and ligating the Dm-dNK containing fragment into the pCW57-MCS1-P2A-MCS2 (Blast) vector (plasmid 80921; Addgene) which had also been digested with NotI and SpeI using Quick Ligase (NEB).

The doxycycline inducible eGFP expression construct was generated by PCR amplifying the eGFP sequence from the pXPR_011 vector using attB-flanked primers followed by Gateway

cloning (Invitrogen) according to the manufacturers protocol into the pCW57.1 backbone. The sequence was verified by Sanger sequencing. The blasticidin resistant version of this vector used in Figure 4 was generated by digesting pCW57.1 eGFP with NotI (NEB) and SpeI (NEB) and ligating the Dm-dNK containing fragment into the pCW57-MCS1-P2A-MCS2 (Blast) vector which had also been digested with NotI (NEB) and SpeI (NEB) using Quick ligase (NEB).

All PCR reactions required for molecular cloning were performed using the Q5 polymerase (NEB).

Oligonucleotides

sgRNAs were purchased from Synthego, all other oligonucleotides were synthesized by IDT.

Table 3-1.

REAGENT or RESOURCE	SOURCE	IDENTIFIER
Chemicals, peptides, and recombinant proteins		
Thymidine	Sigma Aldrich	T1895
Deoxyadenosine	Sigma Aldrich	D8668
Deoxyguanosine	Sigma Aldrich	D0901
Deoxycytidine	Thermo Scientific	AC226720010
Uridine	Sigma Aldrich	U3003
Cytidine	Sigma Aldrich	C4654
Guanosine	Sigma Aldrich	G6264
Adenosine	Sigma Aldrich	A4036
BIBR1532	Sigma Aldrich	5088390001
2,5 ddG	Biosynth	ND08406
Guanine	Sigma Aldrich	51030
Ulodesine	MedChemExpress	HY-19480
Forodesine	Sigma Aldrich	SML3378
Febuxostat	Sigma Aldrich	SML1285
Uric acid	Sigma Aldrich	U2625
Xanthine	Sigma Aldrich	X7375
DI-87	MedChemExpress	HY-133141
Experimental models: Cell lines		
Human: 293T TERC -/-	Mannherz and Agarwal[206]	NA
Human: HEK293T	ATCC	Cat. No. CRL-1573; RRID:CVCL_0045
Human: K562	A gift from Dr. Stuart Orkin	Cat. No. CCL-243; RRID:CVCL_0004
Human: Normal (NHSF2) fibroblast	Westin et al.[227]	NA
Human: TERC+/- 821 base pair deletion patient fibroblast	Agarwal et al.[193]	NA
Human: DKC1 del37L patient fibroblast	Wong and Collins[43]	Coriell Cell Repository GM01774
Human: DKC1 A353V patient fibroblast	Paulsen et al.[194]	NA
Human: TINF2 T284P patient fibroblast	This study	NA

Table 3-1. Chemicals and cell lines.

Table 3-2.

REAGENT or RESOURCE	SOURCE	IDENTIFIER
Recombinant DNA		
pBS U3-hTR-500	Fu and Collins.[228]	Addgene 28170
pCDNA-3xHA-hTERT	Venteicher et al.[229]	Addgene 51637
pmaxGFP	Lonza	NA
pHIV7/SF-U3-TER-500	Agarwal et al.[193]	NA
pHIV7/SF-U3-TER-500 G319A	Boyraz et al.[210]	NA
pcw57.1 TERT Puro	Reilly et al[230]	NA
pLX304 eGFP	This study	NA
pLX304 DCK	This study	NA
pLX304 Dm-dNK	This study	NA
pCW57.1 eGFP (Blast)	This study	NA
pCW57.1 Dm-dNK (Blast)	This study	NA
pCDNA-3xHA-hTERT K570N	This study	NA
pCDNA-3xHA-hTERT T567del	This study	NA
Software and algorithms		
ImageJ	NIH	2.9.0/1.54f
Prism 10	GraphPad	10.0.0

Table 3-2. Recombinant DNA and software.

Table 3-3.

Supplemental Table 1. Oligonucleotide Sequences	
Name	**Sequence**
TERT_SDM_K570N_FW	CGTTTCAAAAcAACAGGCTCTTTTTC
TERT_SDM_K570N_RV	TGGTCTCCGTGACATAAAAG
TERT_SDM_T567del_FW	GTCACGGAGAcgTTTCAAAAGAAC
TERT_SDM_T567del_RV	ATAAAAGAAAGACCTGAGC
AAVS1 sgRNA	CUCCCUCCCAGGAUCCUCUC
HPRT1 sgRNA 1	UCUUGCUCGAGAUGUGAUGA
HPRT1 sgRNA 2	UAAAUUCUUUGCUGACCUGC
HPRT1 sgRNA 3	AAAAUCUACAGUCAUAGGAA
HPRT1 FW	AGGCATGGGGTCTCACTATA
HPRT1 RV	GCTTTGATGTAAAGTACTAGTGAATATGT
APRT sgRNA 1	UCCGCCUCUGCGCGCGCCGA
APRT sgRNA 2	GGCCGCAUCGACUACAUCGC
APRT sgRNA 3	AUGGCGGCGCGGAAGGAGGC
APRT FW	AAGGACGCCTGCACAGC
APRT RV	CCAGGCGTGGTATTCAGGTG
GDA sgRNA 1	CGCCAGGGGCGGCAUCUGAG
GDA sgRNA 2	GUGAUCCCGCAGCACCUCCA
GDA sgRNA 3	GGGGUCGAGCGCACUCCGAC
GDA FW	TAAGCGGGGGCAGGACAA
GDA RV	CACTGCTCCCGACTTCTGG
DCK sgRNA 1	GACGCAAGGCUGGGGUGUCG
DCK sgRNA 2	GCAGCUUCUCUUGGGCGGGG
DCK sgRNA 3	AUCAAGAAAAUCUCCAUCGA
DCK FW	AAAGTCAAACCCCGACACCC
DCK RV	TTCAAAGCGCGCCTCACA
pLX304-DCK Gibson Insert FW	GTCGGGATCAGCCGCCATGGCCACCCCGCCCAAG
pLX304-DCK Gibson Insert RV	TAGGCTTACCCAAAGTACTCAAAAACTCTTTGACCTTTTC
pLX304-DCK Gibson Backbone FW	GAGTACTTTGGGTAAGCCTATCCCTAACCCTC
pLX304-DCK Gibson Backbone RV	CCATGGCGGCTGATCCCGACAGTTAGCCAG
eGFP attB FW	GGGGACCACTTTGTACAAGAAAGCTGGGTATCAACTTTTAGTT GCTTTTGATGGGC
eGFP attB RV	GGGGACAAGTTTGTACAAAAAAGCAGGCTTAGCCGCCACCATG GTGAGCAAGGGCGAGG
Dm-dNK Gibson Insert FW	CGGGATCAGCCGCCATGGCGGAAGCAGCAAGCTG
Dm-dNK Gibson Backbone RV	TGCTTCCGCCATGGCGGCTGATCCCGACAGTTAGCCAG
Dm-dNK Gibson Insert RV	GGATAGGCTTACCGCGTGCAACACGCTGACG
Dm-dNK Gibson Backbone Fw	TGCACGCGGTAAGCCTATCCCTAACCCTC
C-Rich-Strand Probe Template	/5Phos/TTAGGGTTAGGGTTAGGGTTAGGGTTAGGGTTAGGGTTA GGGTAGATAGTTGAGAGTC
Universal Priming	/5Phos/GACTCTCAACTATC+T+A
Note: /5Phos/ represents 5’ phosphorylation. +N represents locked nucleic acid.	

Table 3-3. Oligonucleotides.

Chapter 4: Discussion

In this thesis, I developed rapid and high throughput methods to study telomere length and telomerase activity in human cells. By performing the first genome-wide assessment of human telomere length regulating genes, I identified nucleotide metabolism as a pathway critical for human telomere length homeostasis. I found that telomere length control by nucleotide metabolism is telomerase dependent, and propose this occurs by altering the dNTP substrates available for reverse transcription by telomerase. Augmenting dNTP levels via supplementation of thymidine nucleoside, inhibition of the dNTPase SAMHD1, supplementation of deoxyguanosine plus the PNP inhibitor ulodesine, or overexpression of the *Drosophila melanogaster* deoxynucleoside kinase (Dm-dNK) promoted robust telomerase activation and telomere lengthening in human cells, including cells from patients with lethal telomere biology disorders (TBDs). In contrast to the known pathways governing telomere length in humans, nucleotide metabolism has been therapeutically manipulated to treat diseases for decades and may offer a path forward for the treatment of the telomere-related diseases. My findings provide mechanistic insight into the recent associations between nucleotide metabolism genes, telomere length, and human disease, and establish nucleotide metabolism as a critical, active determinant of telomerase activity in human cells.

Rapid and high throughput methods for studying telomere length within the cellular environment

Combining Flow-FISH and CRISPR/Cas9 for high throughput telomere length screening: Pooled CRISPR/Cas9 screens offer a powerful approach to investigate genotype-phenotype associations in human cells[231]. Flow-FISH is a hybridization based method to quantify telomere repeat content in cells that is clinically used in conjugation with flow cytometry to measure human telomere

length[110,111,166]. Here, I used high throughput Flow-FISH telomere length screening to perform the first genome-wide screen for telomere length regulating genes in human cells. My screen was robust as indicated by the identification of known telomere length regulating genes, including enrichment of sgRNAs targeting TERT in cells with short telomeres and sgRNAs targeting POT1, TERF1 in cells with long telomeres. Based on the enrichment of pyrimidine nucleotide metabolism pathway genes as hits in my genome-wide screen, I performed a targeted screen focused on the nucleotide metabolism pathway which identified SAMHD1 and several thymidine nucleotide metabolism genes as telomere length regulators, setting the stage for my subsequent studies.

Changes in telomere length accumulate with time leading to some additional variables to consider when designing telomere length Flow-FISH screening experiments compared with other screening phenotypes. As telomere length changes can accumulate with each cell division, extending culture time following gRNA library introduction can improve signal to noise ratio. With longer time in culture, precautions to maintain gRNA diversity should be taken, namely increasing the cells maintained during culture to prevent loss of library diversity with cell splitting. Telomere length can drift over time in some cell lines, and this should be taken into account while interpreting results, as perturbations which alter cell growth rate could be misinterpreted as having telomere length altering effects. Selection of a cell line known to have stable telomere length is preferable when designing a telomere length Flow-FISH CRISPR/Cas9 screen. I found telomere length Flow-FISH assays invaluable for identifying and dissecting the relationship between nucleotide metabolism and telomere length homeostasis. Future studies of telomere length control pathways could consider pathway-specific telomere length Flow-FISH CRISPR/Cas9 screening as a powerful initial approach to rapidly profile genes across a pathway or complex. Applying Flow-FISH based telomere length assessment to other pooled genetic screening approaches, such

as assessment of gene variant libraries or CRISPR base editing libraries could prove invaluable for high-throughput investigation of telomere length control.

TRACE enables rapid telomerase activity measurement in human cells: Most assays of telomerase activity require either evaluation of cells after culture for weeks or investigate telomerase from cellular extracts using exogenously supplied dNTPs and oligonucleotide substates, which could obscure telomerase-relevant biology, and makes assessment of the effects of cellular metabolic perturbations challenging. To address these challenges, I developed the Telomerase Rapid Assessment in the Cellular Environment (TRACE) assay, which enables robust and reproducible measurement of genetic and small molecule perturbations to telomerase activity in less than two days. I applied TRACE to rapidly screen cellular nucleosides for their effects on telomerase activity and to evaluate the bidirectional control of telomerase by guanine nucleosides. This assay led me to identify both natural (guanine) and non-natural (2,5-ddG) small molecules which inhibit telomerase and shorten telomeres when applied to cells. The rapid readout of TRACE makes it well suited to study perturbations which can restrict cell growth in long term culture. This feature enabled us to discover the non-linear relationship between telomerase activity and deoxyguanosine (dG) supplementation, where at very high doses dG can be salvaged by DCK to promote telomerase activity. The high doses of dG needed to observe this activation inhibited cell growth and would have been difficult to study without the TRACE assay's rapid readout. The TRACE assay relies on overexpression of the telomerase catalytic components TERT and TERC and is therefore not well suited for study of telomerase biogenesis. Additionally, the high levels of cellular telomerase in the TRACE assay could obscure aspects of telomerase regulation. Despite these limitations, the TRACE assay can enable rapid profiling of key aspects of telomerase

regulation, and may be particularly valuable going forward in the study of the metabolic control of telomere synthesis.

Nucleotide metabolism controls human telomere length

My work has identified dNTP metabolism as a critical and modifiable pathway governing telomere length homeostasis in human cells. Based on my findings, I propose that nucleotide metabolism perturbations alter human telomere length by controlling telomerase activity at the level of its dNTP substrates: dGTP, dTTP, and dATP. Here, I summarize the five distinct means I uncovered by which manipulation of nucleotide metabolism can impact telomere length, and discuss their anticipated effects on dNTP pools:

1. *Impairment of thymidine synthesis genes drives telomerase inhibition and telomere shortening.* In my targeted telomere length Flow-FISH screen focused on the nucleotide metabolism pathway, I identified four genes involved in thymidine synthesis which had gRNAs enriched in the short telomere population, indicating loss of these genes drives telomere shortening: TYMS, the rate limiting enzyme for *de novo* thymidine nucleotide synthesis; TK1, the enzyme which salvages thymidine in the cytosol; DTYMK, which converts dTMP to dTDP; and DCTPP1, which degrades dCTP to generate dCMP, which can be further metabolized to dTTP[87]. I further validated these findings through targeted CRISPR/Cas9 genome editing of *TK1* and *TYMS* which drove telomere shortening in long term culture, validating my screening hits. Collectively, these data indicate that impaired dTTP synthesis reduces telomere length in human cells.
2. *Supplementation with thymidine increases telomere length in human cells*. Thymidine supplementation increases cellular dTTP levels which can secondarily increase dGTP

levels and dATP levels while depleting dCTP levels via allosteric regulation of ribonucleotide reductase by dTTP[78,216]. I found that supplementation of cell culture media with thymidine drove telomere lengthening in several cell lines, including 293T cells, K562 cells, fibroblasts expressing TERT, and iPSCs including both wildtype and TBD patient derived iPSCs. Thymidine supplementation increases dTTP accumulation in the nucleus via the salvage pathway kinase TK1[90], and I found that loss of TK1 prevented telomere lengthening from thymidine treatment, indicating that nuclear accumulation of thymidine nucleotides mediated the telomerase activation from thymidine treatment. Similarly, deoxyuridine treatment increased telomere length in a manner that required TYMS, the enzyme which converts dUMP to dTMP, providing further support for the notion that increased thymidine nucleotide levels leads to telomere lengthening. I found telomere lengthening from dT treatment was negatively regulated by the dNTPase activity of SAMHD1, suggesting that the telomere lengthening effects from dT occur at the triphosphate level. Collectively, these observations indicate that thymidine mediated increases in dTTP as well as potentially secondary increases in dGTP and dATP, stimulates telomere elongation in human cells.

3. *Guanine nucleoside supplementation bidirectionally controls telomerase activity and telomere length.* My findings indicate that supplementation with low-dose deoxyguanosine or with guanosine leads to telomerase inhibition via catabolism by PNP to form guanine followed by incorporation of into ribonucleotide pools through HGPRT. Guanine treatment and has been shown to reduce the levels of dTTP and dGTP when applied to cells[214,215] which may occur via inhibition of RNR. I found that thymidine treatment rescued telomerase inhibition from guanine treatment, suggesting that guanine inhibits telomerase

activity by depletion of dNTPs. Guanine treatment led to telomere shortening in long term culture of several cell lines including fibroblasts expressing hTERT, K562 cells and 293T cells. Conversely, I found that supplemented deoxyguanosine can inefficiently be converted via DCK to deoxyguanosine nucleotides at high doses leading to telomerase activation. Overexpressing DCK or the *Drosophila melanogaster* deoxynucleoside kinase (Dm-dNK) sensitized cells to telomerase activation from deoxyguanosine, indicating that conversion into deoxyguanosine nucleotides promotes telomerase activation. Inhibition of the dNTPase SAMHD1 also sensitized cells to telomerase activation from deoxyguanosine. In fibroblast cells expressing hTERT, including cells derived from TBD patients, supplementation with deoxyguanosine in combination with the PNP inhibitor ulodesine drove telomere lengthening. Collectively, these data indicate that the salvage of deoxyguanosine to form dGTP increases telomere length, while flux of guanine nucleosides into ribonucleotide pools via HPRT leads to telomere shortening, potentially via inhibition of RNR leading to reductions in dGTP and dTTP levels.

4. *Increasing cellular nucleoside salvage capacity by overexpressing Dm-dNK increases telomere length. Drosophila melanogaster* deoxynucleoside kinase (Dm-dNK) is active on all four canonical deoxynucleosides and is highly efficient compared with the human deoxynucleoside kinases[220]. I found that overexpression of Dm-dNK increased telomerase activity and telomere length even in the absence exogenous supplemented deoxynucleosides. Telomere lengthening from Dm-dNK was particularly robust in fibroblasts expressing hTERT, including fibroblasts from TBD patient cells. Expressing Dm-dNK in human cells has been shown to increase the levels of cellular dNTPs, in

particular dTTP[232], supporting the notion that elevation of dNTP levels promotes telomere elongation in human cells.

5. *Impairment of the dNTPase SAMHD1 drives telomere elongation and sensitizes cells to telomere synthesis effects from thymidine and deoxyguanosine treatment.* The dNTPase SAMHD1 is a major negative regulator of cellular dNTP levels[93], and I found that inhibition of SAMHD1 led to robust telomere elongation in numerous settings. sgRNAs targeting *SAMHD1* were highly enriched in cells with long telomeres in my telomere length CRISPR/Cas9 screening, and targeted inactivation of SAMHD1 via CRISPR/Cas9, or shRNA knockdown drove telomere elongation in cells including 293T cells, K562 cells, and iPSCs derived from healthy donors or from patients with TBDs. Further, I found that loss of SAMHD1 sensitized cells to the telomere lengthening effects of thymidine, and to the telomerase activating effects of deoxyguanosine, suggesting that these deoxynucleosides promote telomerase activity at the triphosphate level. SAMHD1 has roles beyond its dNTPase activity, however I found that while telomere lengthening from thymidine treatment was restricted in cells overexpressing wildtype SAMHD1, overexpression of dNTPase deficient SAMHD1 failed to prevent telomere lengthening from thymidine. Taken together, these data indicate that the loss of SAMHD1 dNTPase activity lengthens telomeres in human cells.

These findings collectively support a model where telomere length homeostasis is maintained within a tight window by dNTP levels, and show that both genetic and small molecule manipulations of dNTP metabolism can lead changes in telomere length across diverse human cell types. Together, my findings indicate that upregulation of dNTP levels, in particular dTTP and dGTP, increases telomere length in human cells.

Recent human genetic studies have additionally associated dNTP metabolism genes with telomere length. These include GWAS studies linking variation in dNTP genes with human telomere length measured in the blood, based on data from the UK Biobank[33,34]. Targeted examination of whole exome sequencing data from a DC patient registry identified eight families with mutations at the TYMS locus[32], indicating that inherited defects in a dNTP metabolism gene can cause TBDs. Collectively, these human genetic data, combined with my findings as well as a complementary recent study investigating telomere lengthening in cells from SAMHD1 deficient patients[205] demonstrate that dNTP metabolism is a critical determinant of telomere length homeostasis in humans.

The telomerase substrate-level control model to explain the link between dNTP metabolism and telomere length.

How could alterations in dNTP metabolism influence telomere length? Here I propose a unified model where dNTP metabolism controls telomere length via substrate level regulation of telomerase 5'-GGTTAG-3' repeat synthesis. This hypothesis is based on the above data as well as the following observations about the relationship between dNTPs, dNTP metabolism, and telomerase activity:

Telomere lengthening from manipulation of dNTP metabolism requires telomerase. My findings indicate that the effect of dNTP metabolite changes on telomere length occurs via alterations of the specific activity of telomerase based on several lines of evidence. First, I found that, in contrast to wildtype 293T cells, telomerase deficient *TERC* -/- 293T cells showed no changes in telomere

length from thymidine treatment or from inhibition of SAMHD1. The telomerase dependent nature of telomere length changes from SAMHD1 inhibition were recently verified by another group[205]. Similarly, I found that fibroblast cells, which do not express TERT at baseline, showed no telomere length changes from thymidine exposure, whereas fibroblast cells engineered to express TERT showed robust telomere lengthening from thymidine treatment. These data support a model where manipulation of dNTP metabolism alters the rate of telomere synthesis by telomerase.

Purified telomerase enzymatic activity is sensitive to changes in dNTP levels within the physiologic range: The concentrations of the telomerase substrates dTTP, dGTP and dATP have been known to influence the enzymatic activity of purified telomerase since the first biochemical description of a human telomerase activity[72]. While early experiments studying telomerase generally used high, non-physiological concentrations of dNTPs, recent studies using more physiologic dNTP levels have similarly found that changes in any of telomerase's substrates can alter telomerase activity, and indicate that the processivity of telomere repeat synthesis is most sensitive to changes in dGTP levels[64,71,77]. Collectively, these data demonstrate that alterations of the telomerase substrate dNTPs within a physiologic range influence telomerase reverse transcriptase activity.

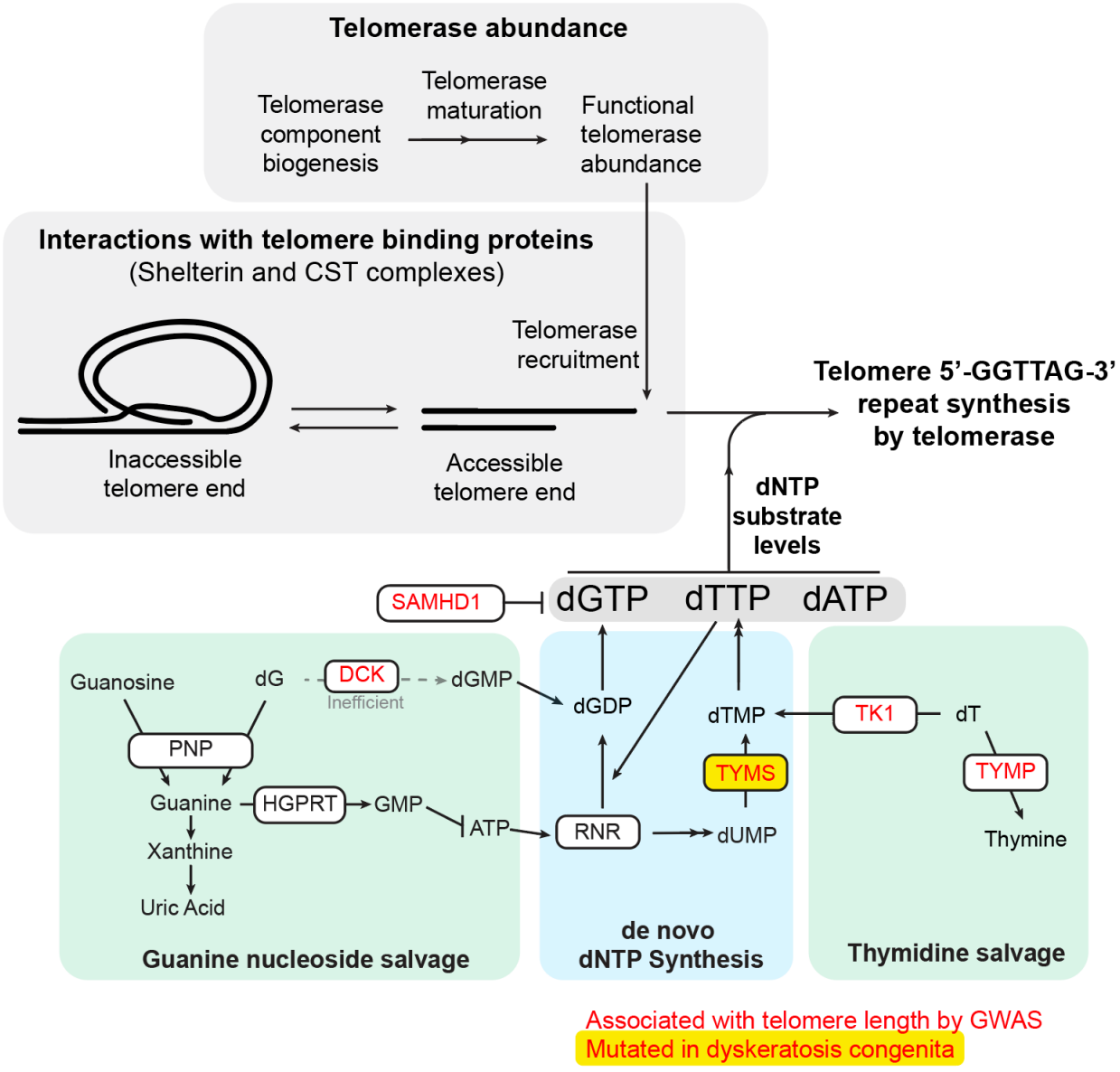
dNTP metabolism manipulations increase the specific activity of telomerase in human cells: Telomerase activation could be explained by an increase in the abundance of telomerase, so I asked if manipulation of dNTP metabolism impacted the levels of telomerase in the cell. I found that the addition of 100 μM thymidine to 293T cells more than doubled the rate of telomere synthesis (In the absence of telomerase, I found 293T cells telomeres shorten by 57 +/- 21 bp per day, while treatment with 100 μM thymidine caused to ~90bp per day telomere lengthening compared with

untreated cells. Thus, telomerase lengthens telomeres by ~147 bp per day in the presence of 100 μM thymidine vs ~57 bp per day untreated cells). However, the same dose of thymidine did not lead to a detectable change in the abundance of active telomerase enzyme as measured by the TRAP assay. Together, these data indicate that changes in the abundance of telomerase do not explain the telomere lengthening effects from thymidine treatment, and suggest that manipulation of dNTP metabolism influences the specific activity of telomerase. Along similar lines, I found that fibroblasts with higher telomerase expression showed greater increases in telomere length following thymidine treatment, a finding consistent with the hypothesis that dT supplementation increases the number of telomere repeats synthesized by each telomerase enzyme. In further support of this notion, in the TRACE assay, where telomerase is highly overexpressed, diverse manipulation of dNTP metabolism can cause dramatic changes in telomere synthesis by telomerase within a minimal timeframe of drug exposure. For example, splitting cells into cultures 100 μM thymidine promotes telomerase activation within only 30 hours by nearly four-fold. Further increases in telomere synthesis can be observed in the setting of cells which lack SAMHD1 or overexpress either DCK or Dm-dNK. In these cells, high dose dG can lead to increases in total cellular telomeric repeat content by more than 10-fold with only 30 hours. Telomerase can also be rapidly inactivated by manipulating dNTP metabolism, for example treatment with 5FU, which inhibits TYMS, effectively ablates telomerase activity over 30 hours of treatment in a manner which could be completely rescued by bypassing the dTTP synthesis block using thymidine. Given the tight time window of exposure to these compounds, a secondary effect of dNTP metabolism manipulation on the abundance of telomerase appears unlikely to explain the observed results. Instead, an increase of the specific activity of telomerase offers a more likely mechanism.

In the substrate-level control model (**Figure 4-1**), following telomerase assembly, recruitment, and binding the telomere end, homeostatic levels of dNTPs promote telomere repeat synthesis by telomerase within a physiologic window. Deviations in dNTP substrate levels from this baseline in either direction lead to an alteration of telomerase activity. Reduction of dNTP-substrate levels inhibits telomerase activity and causes net telomere shortening. Conversely, increased dNTP substrate levels promote telomerase activity leading to telomere elongation.

Figure 4-1. An updated model of human telomere length regulation. To date, most data indicate that human telomere length is regulated by (1) the abundance of telomerase holoenzyme and (2) its interplay with telomere binding proteins. Based my findings and emerging human genetic data, I propose a revised model encompassing a third critical dimension of telomere length regulation in human cells: control of dNTP substrate levels available for telomere 5'-GGTTAG-3' repeat synthesis by telomerase. dNTP substrate accumulation is limited by salvage efficiency including (a) deoxyguanosine (dG) metabolism by DCK, and (b) thymidine (dT) conversion to dTTP via TK1. dTTP can enhance dGTP production by allosteric binding to RNR. Overcoming salvage constraints through dG or dT supplementation or by augmenting kinase activity robustly increases telomerase activity and telomere length. Conversely, guanine nucleoside metabolism via PNP and HGPRT to form guanosine ribonucleotides decreases telomere length, potentially by inhibiting RNR and depletion of dNTPs. Mutations that impair dTTP de novo synthesis lead to reduced telomerase substrate levels and impaired telomerase activity, as observed in patients with TYMS locus mutations who develop dyskeratosis congenita. The dNTPase SAMHD1 limits the accumulation of telomerase dNTP substrates and restricts telomerase activity. My model provides a mechanistic framework for the recent association between genetic variation in dNTP metabolism genes and telomere length in states of health and disease[32–34].

Figure 4-1. (Continued)



Consideration of alternative mechanisms by which dNTP metabolism could influence telomere length homeostasis

dNTP metabolism contributes to several cellular processes that are relevant for telomere homeostasis including nuclear genome replication and repair. In addition to the substrate level control model, I have considered and tested alternative explanations for how dysregulation of dNTP homeostasis could lead to telomere length changes:

Cell cycle timing disruption: Thymidine supplementation has been used to synchronize cells in S phase of the cell cycle, which is understood to occur via elevated dTTP levels allosterically inhibiting the production of dCTP via RNR[216]. As telomerase has been shown to synthesize telomere repeats during S phase of the cell cycle[68,233,234] it appeared possible that lengthening S phase could extend the time available for telomere synthesis by telomerase and thereby promote telomerase activity. To test this hypothesis, I asked whether doses of thymidine which do not impact the cell cycle still alter telomere synthesis. I found that low dose thymidine which had no detectable effects on cell growth over one month still drove telomere lengthening in 293T cells. Further, I found that a low dose of thymidine simultaneously increased the growth rate of K562 cells and increased telomere length over one month of culture. These data indicate that slowing of cell cycle progression is not sufficient to explain the telomere length changes observed from thymidine.

Replication stress signaling: Replication stress signaling can be triggered by insufficient dNTP levels during S phase leading to replication fork stalling, accumulation of single stranded DNA, and activation of the ATR kinase[235]. Telomeres are known to be particularly prone to replication stress, which may be due to their repetitive sequences, binding of both proteins and RNA, and tendency to form G quadruplexes when single stranded[184,236]. The connection between

replication stress and telomere length homeostasis is nuanced. Several studies have found telomeric replication stress can drive telomere trimming[237,238] while other literature suggests replication stress signaling may increase the localization of telomerase to telomeres[183]. Furthermore, treatment with aphidicolin, a compound which induces replication stress by inhibiting DNA polymerase alpha[239], has been shown to increase telomere length in long term culture[184], a finding which I replicated. At high doses, thymidine treatment is understood to induce replication stress by depleting dCTP levels via allosteric regulation of RNR by dTTP[216,240]. I asked whether replication stress could contribute to the telomere lengthening from thymidine treatment. I found that low doses of thymidine which had no detectable effects on replication stress signaling or on cell cycle progression still promoted robust increases in telomere synthesis, suggesting that replication stress signaling is not necessary for telomerase activation by this pathway. Furthermore, I showed that compounds which induce replication stress and arrest cells in S phase via dNTP depletion, namely the TYMS inhibitor 5FU and the RNR inhibitor hydroxyurea, inhibited telomerase activity rather than activating it, indicating that the induction of replication stress is not sufficient for telomerase activation. While I cannot exclude that replication stress signaling could contribute to telomere lengthening from high dose thymidine, my findings suggest that replication stress signaling is likely not a major factor contributing to telomerase activation from lower doses of thymidine. Of note, treating cells with the replication stress inducing compound aphidicolin has been shown to increase levels of dNTPs[241], potentially by reducing their consumption by stalling DNA polymerase activity, or by elevated replication stress signaling, which has been associated with increased RNR activity[242–244]. Based on my findings, dNTP pool increases may offer an alternative explanation for why aphidicolin treatment increases telomere length.

Allosteric effect of nucleotides on telomerase: One hypothesis that I considered might be underlying the robust telomerase activation from thymidine supplementation was that dTTP might be allosterically activating telomerase. I tested this hypothesis by altering the telomerase RNA template to encode 5'-GGAAAG-3' repeats (termed T-free telomerase). I then evaluated how dTTP levels altered the enzymatic activity of T-free telomerase both using the TRAP assay[36], and by directly visualizing telomerase extension products using radiolabeled nucleotide substrates (termed the direct telomerase assay). I found that dTTP stimulated T-free telomerase activity in these assays, suggestive of an allosteric effect. Upon further examination of this phenomena using the direct telomerase assay, I found that in addition to dTTP, other nucleotide triphosphates that are also not substrates of T-free telomerase could cause a similar activating effect, including ATP, and ATP also stimulated wildtype telomerase activity (not shown). Future work is needed to identify the mechanisms underlying the activating effect I observed, for example whether it is related to allosteric action on telomerase itself, whether it is mediated through another factor copurifying with the enzyme, or by another means.

I also attempted to study the relevance of this apparent allosteric effect of dTTP on telomerase activity in human cells by expressing T-free telomerase, supplementing thymidine, and measuring the accumulation of T-free telomerase repeats. I found that supplementation with thymidine increased T-free repeat synthesis, suggesting that dTTP accumulation can promote telomerase activity even when it does not serve directly as a substrate for repeat synthesis by telomerase. However, dTTP accumulation has been shown to act allosterically on RNR to increase dATP and dGTP production[78,216]. In light of my results demonstrating that elevated dGTP synthesis increases telomerase activity in human cells, as well at the extensive literature showing that telomerase enzymatic activity is highly sensitive to dGTP levels[71,73,74,77], an accumulation of dGTP

from thymidine treatment offers a straightforward explanation for the T-free telomerase activation I observed in cells. Additionally, my finding that ATP appears to have a similar activating effect as dTTP on T-free telomerase enzymatic activity in direct telomerase assays also argues against the notion that an allosteric activating effect of dTTP plays a dominant role in telomerase activation in cells from thymidine treatment. Cellular ATP levels are ~100 times higher that dTTP levels[76], and thus would be expected to tonically activate telomerase by this mechanism at baseline. Further, salvage of supplemented thymidine to produce dTTP consumes ATP, and would not be expected to alter total cellular nucleotide triphosphate levels. Collectively, my findings in human cells are consistent with a model where dNTP metabolism perturbations alter telomere length via changes in the substrate-level regulation of telomerase activity.

Alterations of C-strand synthesis by CST: dT supplementation is known to deplete dCTP levels via allosteric inhibition of RNR by dTTP[216], which has been proposed to explain why thymidine treatment arrests cells in S phase of the cell cycle[216]. dCTP is not required for telomere repeat synthesis by telomerase, however it is required for telomeric C-strand fill in by the CST-Polα/Primase complex. Disruption of the C-strand fill in machinery via depletion of CTC1 or STN1[58,59], or by genetic[138,245] or small molecule[184] Polα inhibition leads to telomere elongation by telomerase, potentially by increasing the accessibility of the G-strand overhang to telomerase binding. It is conceivable that the depletion of dCTP from high dose thymidine supplementation could therefore contribute to the telomerase activation from dT by inhibiting C-strand fill in. I did observe an increase in the ratio of telomere G-strand signal to C-strand signal at high molecular weights in the TRACE assay using high doses of dT, which could be explained by increased G-strand synthesis by telomerase, active inhibition of C-strand fill in via dCTP depletion, or a combination of both processes. Along these lines, one could envision that strong activation of

telomerase activity via elevated dNTP pools could lead to rapid increases in the length of the G-strand telomere overhang which could dilute the cellular G-strand overhang binding factors that restrict telomerase activity such as POT1 or CST, thus causing a positive feedback effect on telomerase activity. Of note, loss of SAMHD1 elevates all dNTP levels including dCTP[93,205], and I found that SAMHD1 depletion drove robust telomerase-dependent telomere lengthening, a finding which has also been observed by another group[205]. Therefore, the inhibition of C-strand fill in via dCTP depletion does not appear necessary for telomerase activation from dNTP metabolism manipulation. Going forward, a detailed examination of the relative contributions of substrate-level telomerase activation and impaired C-strand fill in to changes in telomere synthesis from manipulation of dNTP metabolism could be of interest.

Why thymidine?

Given the current human population genetic data[32–34], there appears to be an enrichment of thymidine metabolism genes associated with telomere length, including TYMP, TK1, and TYMS. It should be noted that other pyrimidine metabolism genes including DCK and CDA, as well as SAMHD1, which contributes to the restriction of all dNTP levels, have been associated with human telomere length by GWAS as well[33,34]. Furthermore, I found that supplemented thymidine drives telomere lengthening across many cell types which express TK1, while supplementation with the other nucleosides had minimal effects on telomere length over 10 days of culture in 293T and K562 cells. These data raise the question of why thymidine metabolism appears so critical for telomere length homeostasis when dGTP has been identified as more important than dTTP for the activity of purified telomerase as discussed above.

My data indicate that the low efficiency of dG phosphorylation by DCK restricts dG nucleotide accumulation and telomerase activation from dG supplementation. In the TRACE assay, I found that very high doses of dG were able to overcome this inefficiency and promote telomerase activation. In line with this finding, I found that DCK overexpression sensitized cells to telomerase activation from dG. Furthermore, in addition to being inefficiently salvaged by DCK, I found that dG can also be broken down by PNP to form guanine which, followed by subsequent salvage by HGPRT to generate guanosine ribonucleotides, inhibits telomerase activity and shortens telomeres. Thus, dG supplementation can bidirectionally influence telomere length depending on its metabolic shunting. In contrast, I found that that thymidine is efficiently salvaged by TK1 to promote telomerase activation and telomere lengthening even at low doses. The efficiency of its incorporation into deoxyribonucleotide pools provides a simple explanation for why thymidine stands out in these experiments. Additionally, dTTP is known to allosterically regulate RNR to increase dGTP synthesis[216], therefore alterations which impact dTTP levels may lead to concordant changes in dGTP levels which also influence telomerase activity.

As for the apparent lack of genetic association between dGTP metabolizing genes with human telomere length, it should be noted that both SAMHD1 and DCK can participate in deoxyguanosine nucleotide metabolism, and that SAMHD1 inhibition increases dGTP levels to a relatively higher degree compared with the other dNTPs[93]. Additionally, there are no deoxyguanosine nucleotide specific metabolizing genes which have been described in humans. In contrast, there are several genes specific to thymidine metabolism. Finally, as the manipulation of thymidine metabolism has been found to have minimal effects on ribonucleotide pools[214], dysregulation of thymidine metabolism may be more tolerable compared with mutations which

impact dGTP metabolism while simultaneously causing dysregulation of guanine ribonucleotide metabolism.

Why telomeres?

Nuclear dNTPs pools are common precursors for telomerase activity as well as for DNA replication, begging the question of why patients with inherited TYMS deficiency present with a telomere biology disorder phenotypes[32] rather than manifestations common in patients with inherited defects in the nuclear DNA replication machinery who present with disorders characterized by short stature such as the microcephalic primordial dwarfisms (MPDs)[246].

One potential contributing factor to the apparent sensitivity of telomerase to dNTP metabolism deficiency is the relatively high Km values of dNTP utilization by telomerase (4-120 μM)[71] compared with the replicative DNA polymerases (0.2-10 μM)[75] relative to the cellular dNTP levels (5-40 μM)[76]. Another contributing factor for why telomerase may be uniquely sensitive to alterations in dNTP metabolism could be the fundamental differences in the task of telomere synthesis compared to DNA replication. The rate of telomere synthesis must be tightly linked to the rate of telomere attrition to maintain telomere homeostasis, and even small changes in telomerase activity could become magnified over successive cell divisions. Thus, alterations in dNTP substrate levels which fractionally alter telomerase activity could lead to large changes in telomere length over time. In contrast with telomerase, DNA polymerases and have a defined endpoint: the completion of genome replication. As the duration of S phase is influenced by numerous factors in addition to dNTP levels such as the presence of DNA damage and histones[247], the rate of cell division may be less sensitive to small changes in dNTP levels compared with telomerase. This high sensitivity of telomerase activity to small alterations of dNTP homeostasis

is exemplified by my finding that low-dose thymidine treatment can robustly increase telomere length without altering the detectable rate of cell growth over the course of one month of treatment.

Telomeres, nucleotides, and human disease

dNTP metabolism dysregulation has been observed in multiple disorders including cancer, viral infections, and inherited genetic diseases. My results demonstrate that telomerase is highly sensitive to changes in dNTP metabolism. Here I discuss how the dysregulation of telomerase activity may contribute to these disorders based on my findings.

Cancer: dNTP levels have been shown to be commonly elevated in cancer cell lines compared with non-transformed cell lines[76]. This could be partially explained by an increased fraction of cells in S phase of the cell cycle when dNTP levels are highest[85]. Others have proposed that upregulation of dNTP levels may actively drive tumorigenesis by promoting genome instability[85]. Based on my results, an alternative explanation for this association could be that increased dNTP levels promote telomere synthesis by telomerase. One avenue to study this possibility could be evaluating tumors harboring somatic mutations in the dNTPase SAMHD1. Somatic SAMHD1 mutations are found recurrently in cancers including chronic lymphocytic leukemia (CLL), where these mutations have been hypothesized to promote mutagenesis and inflammation[248]. Given my data and others[205] showing SAMHD1 strongly restricts telomerase activity in human cells, it appears possible that SAMHD1 mutations may alternatively be selected for in these cancer because of their telomerase activating effects. Inhibitors of dNTP metabolism have been widely used to treat cancer, including 5FU, gemcitabine, and clofarabine[96], and based on my findings, the inhibition of telomerase activity from these compounds could potentially contribute to their anti-tumor efficacy.

Viral infections: Viruses which require DNA synthesis as part of their lifecycle have been shown to manipulate human cellular dNTP metabolism by diverse mechanisms. For example, several oncogenic viruses including Epstein-Barr virus and HHV8 (Kaposi sarcoma Herpesvirus) are known to encode thymidine kinases[222]. These viruses have also been shown to upregulate telomerase activity as part of disease progression[223]. Based on my findings, the upregulation of thymidine synthesis in these viruses may promote telomere lengthening and contribute to viral progression. The dNTPase SAMHD1 is a restriction factor for several DNA viruses and retroviruses including HIV[94,249,250]. SAMHD1 has been proposed to inhibit viral replication by suppressing dNTP levels available for DNA synthesis[94]. Several viruses employ strategies to counteract SAMHD1[251], including lentiviruses which encode proteins that induce the proteasomal degradation of SAMHD1[252], as well as EBV which expresses BGLF4 to phosphorylate and inactivate SAMHD1[253]. Based on my findings, increased telomerase activity from inhibition of SAMHD1 could enable enhanced replication of virally infected cells. Along similar lines, the innate cellular antiviral response involves upregulation of interferons, and SAMHD1 has been identified as an interferon response gene[244,254]. Chronic viral infections[255] and interferon alpha treatment[256] have both been associated with shortened telomeres in clinical studies. This telomere shortening in patients with chronic interferon signaling has been proposed to result from increased cell turnover[255] as well as downregulation of telomerase expression[257]. Based on my findings, the increased expression of SAMHD1 downstream of interferon signaling could also contribute to a telomere shortening in this setting via degradation of dNTPs and inhibition of telomerase.

Aicardi-Goutières Syndrome: Inherited mutations in SAMHD1 lead to Aicardi-Goutières Syndrome[254], a severe autoinflammatory disease understood to be cause by an accumulation of cytosolic nucleic acids which trigger a chronic antiviral response[258]. The source of the cytosolic

nucleotides triggering viral responses in these patients is thought to be endogenous retroelements such as LINE1[258]. SAMHD1 has been shown to limit LINE1 activity, potentially via depleting dNTP levels and thereby inhibiting LINE1 reverse transcription[259]. In support of the hypothesis that increased retroelement activity is the underlying cause of disease, treatment with reverse transcriptase inhibitors has shown promise patients with AGS[260]. I found that loss of SAMHD1 led to telomere elongation in several cell lines. In strong support of my findings, another group showed that SAMHD1 inhibition lengthens telomeres in cells expressing telomerase, and that AGS patient fibroblast have increased telomere elongation with exposure to telomerase[205]. While a systematic evaluation of the telomere length in these patients has not been performed, one study examining UK Biobank data showed that rare inherited predicted loss of function mutations in SAMHD1 are associated with increased telomere length[33]. Collectively, these data suggest that AGS patients with SAMHD1 mutations may have long telomeres. AGS is rare and identified patients are generally young and face high mortality rates, thus an evaluation of complications from overly long telomeres such as predisposition to cancer is challenging[261], however one AGS patient with a germline SAMHD1 mutation was reported with early onset CLL (diagnosed at age 24)[248]. A tissue specific analysis of telomere length in these patients may shed light on where dNTP restriction by SAMHD1 plays a role in telomere length control.

dNTP metabolism in patients with telomere biology disorders

Defective dNTP synthesis driven by inherited mutations at the TYMS locus have been recently identified as causing the TBD dyskeratosis congenita (DC)[32]. My data results suggest that lack of dTTP synthesis leads to reduced dNTP substrate levels for telomerase causing impaired telomerase activity and reduced telomere length, offering an explanation for the short telomere length

observed in these patients. While sample sizes are small, it is interesting to note that the TYMS mutant DC patients reported have a relatively higher rate of early onset mucocutaneous findings and relatively lower rate of hematopoietic failure compared with a typical DC presentation. Based on our model, TYMS mutations lead to reduced telomere synthesis via the substrate-level control of telomerase activity, a manner distinct from the other known TBD genes. The relative dependence of a tissue on *de novo* dTTP synthesis via TYMS compared with salvaged dTTP synthesis via TK1 could therefore contribute to differences in tissue specific DC phenotypes observed in TYMS mutant patients compared with other DC patients. Going forward, it will be worthwhile to monitor disease progression in these patients in order to characterize what other TBD manifestations they may develop.

By linking dNTP metabolism telomere length homeostasis, my work may also have implications for the management of TBD patients. For example, my findings raise questions about the safety of administering compounds which inhibit dNTP synthesis to patients with TBDs, including immunosuppressive agents such as methotrexate and antineoplastic agents such as 5FU, as these compounds may inhibit telomerase activity could accelerate disease progression. Furthermore, it would be interesting to examine whether inherited mutations in other dNTP metabolism genes including *DCK, TK1*, *DTYMK*, *DCTD*, *DCTPP1*, *DUT*, *RRM1*, and *RRM2* could cause TBDs as well. Of note, two families with mutations in *DUT*, the gene which converts dUTP to dUMP and thereby promotes dTTP synthesis[262], have been identified as presenting with skin abnormalities similar to those seen in DC patients as well as bone marrow failure and diabetes[32,95]. My model raises the hypothesis that impaired dTTP production in patients with DUT deficiency could lead to reduced telomerase activity, potentially contributing to the overlapping manifestations between these patients and DC patients. Furthermore, as somatic variants predicted

to increase telomerase activity are recurrently found in the blood of TBD patients[154], it may be of interest to examine TBD patients for somatic mutations in genes which negatively regulate telomere length via restricting dNTP pools, for example the dNTPase encoding gene *SAMHD1*.

Therapeutic prospects to promote telomerase activity via dNTP metabolism to treat the TBDs

Therapeutic manipulation of nucleotide metabolism has been used for decades to treat conditions ranging from gout, to inborn errors of metabolism, to autoimmune disease, to cancer. These therapies include supplementation with native metabolites as well as nucleoside analogs, and other small molecules[96,97,191,263]. The prospect of manipulating dNTP metabolism to therapeutically control telomerase activity is an exciting avenue of further research opened by my investigations. Here, I will discuss promising therapeutic opportunities guided by my findings:

Thymidine (dT): I found that supplementation with dT led to telomerase activation and telomere lengthening in several human cell lines, including cells derived from TBD patients. dT has been investigated therapeutically in humans, initially in the 1970s for the treatment of cancer[264], and later for the treatment patients with mitochondrial DNA depletion caused by inherited mutations in *TK2*, which encodes the mitochondrial thymidine kinase[265]. A mouse model of TK2 deficiency developed by Michio Hirano and colleagues was found to recapitulate many disease features, and became a useful model to study strategies for the treatment of TK2 deficient patients[266]. TK2 salvages dT and deoxycytidine (dC) in the mitochondria to form dTMP and dCMP. Hirano and colleagues therefore tested supplementing dTMP plus dCMP in their mouse model and found increased mitochondrial DNA levels and prolonged lifespan[267]. The authors also found that dTMP and dCMP are rapidly dephosphorylated following supplementation and noted that that dT

and dC were likely the bioavailable compounds. Further investigation has shown that dT plus dC supplementation[268], or dT supplementation alone leads to similar benefits in the TK2-mutant mouse model[269]. Based on these promising findings, oral dTMP and dCMP began to be administered through compassionate use to TK2-deficient mitochondrial DNA depletion syndrome patients in Spain and the United States in 2011. Later, patients were transferred to treatment with dT plus dC[270] based on the aforementioned preclinical findings. Clinical studies are ongoing, however a retrospective study found that dT plus dC (and dTMP plus dCMP) was highly effective, with remarkable increases in motor function and lifespan, and with tolerable side effects[97]. Collectively, these data indicate that dT can be effectively administered orally and reach bioactive doses in circulation, with acceptable safety profiles in patients including children. Based on these results as well as my findings demonstrating that dT supplementation increases telomere length in human cells, including TBD patient cells, an investigation of dT supplementation as an oral therapy for TBD patients may be of significant interest.

dT can be catabolized by TYMP to form thymine and the associated sugar. Inherited defects in *TYMP* lead to Mitochondrial neurogastrointestinal encephalomyopathy (MNGIE)[271], a disease characterized by gastrointestinal dysmotility and motor dysfunction. In MNGIE patients, the impaired degradation of dT by TYMP causes ~50 fold increases in circulating levels of dT, which can reach up to ~10 micromolar in the plasma[272]. Elevated dT causes cellular dTTP accumulation that, via allosteric action on RNR, leads to reduced dCTP levels. This reduction in dCTP levels is thought to drive inefficient mitochondrial DNA replication and subsequent mitochondrial DNA depletion[273]. Based on this disease mechanism, it is conceivable that supplemental dT could have deleterious effects on mitochondrial function. While oral dT appears to be beneficial for mitochondrial function in the setting of inherited TK2 deficiency, these patients may be somewhat

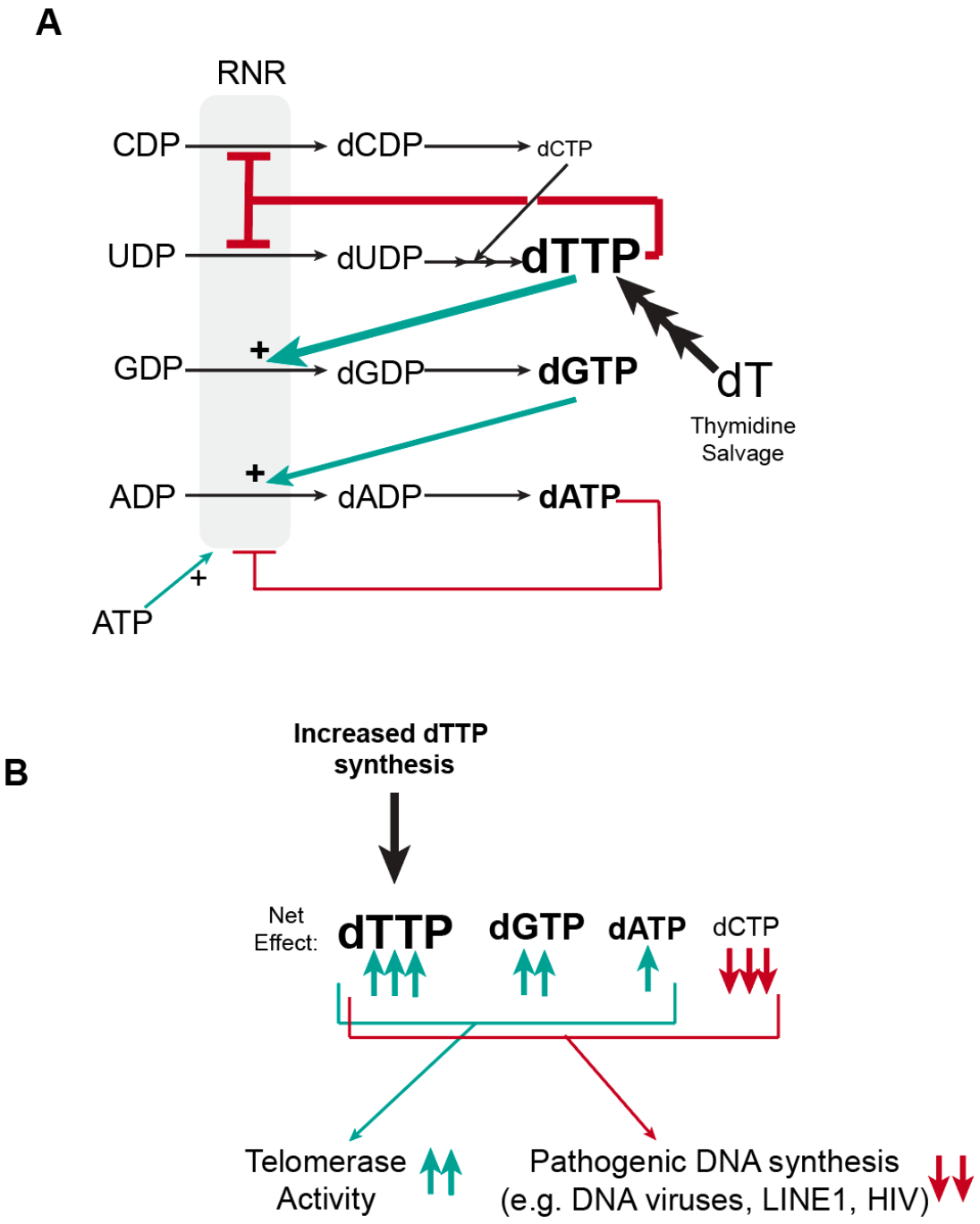
protected from a potential dT-mediated mitochondrial depletion due to the underlying dysregulation of their mitochondrial dNTP pools. Additionally, given these patients are treated with a combination of dT plus dC, dC salvage may also protect against mitochondrial DNA loss via dCTP pool depletion. The combination of dT and dC could therefore be considered in a trial for TBD patients. Additionally, the apparent negative effects of elevated dT levels on mitochondrial function seen in MNGIE patients may be mitigated in patients with functional TYMP, as would be expected in TBD patients. Going forward, given the association between deficiency in TYMP, elevated dT levels, and mitochondrial depletion, it could be valuable to monitor mitochondrial function in a trial using oral dT for TBD patients. Telomere length testing in patients being treated with dT plus dC for TK2 deficiency could provide information relevant to the design of a trial for dT in TBDs. While dT supplementation appears to be a promising approach, there are several drawbacks to using this nucleoside therapeutically, including its poor bioavailability and short half-life. Additionally, our data indicate that telomere lengthening from dT treatment requires that cells express both telomerase and TK1. The co-expression of telomerase and TK1 in TBD relevant cells such as hematopoietic stem cells will therefore be of interest for further study.

As discussed above, the upregulation of dNTP synthesis has been implicated in the pathogenesis of infections with DNA viruses, retroviruses, and endogenous retroelements. Unlike these pathogenic forms of DNA synthesis, telomerase does not require a full repertoire of dNTP substrates for its activity, as dCTP is not encoded in the telomerase RNA template. Thanks to the intricate allosteric regulation of RNR (**Figure 4-2a**)[78,82,216], thymidine metabolism is, in a sense, complementary to the substrate requirements of telomerase: dTTP accumulation drives dGTP synthesis which in turn drives dATP synthesis while depleting dCTP synthesis. Therefore, I

hypothesize that thymidine metabolism offers a means to increase telomerase activity independently from the activity of DNA viruses and pathogenic retroelements (**Figure 4-2b**). In illustration of this phenomena, I have shown that dT supplementation drives robust telomerase activation and telomere lengthening in human cells, whereas supplementation of dT to human cells has been shown to inhibit HIV proliferation[192] as well as proliferation of the LINE1 retroelement[274]. These divergent effects of dT treatment on telomerase activity and pathogenic DNA synthesis suggest that dT supplementation may offer wider or unique therapeutic window compared with approaches to upregulate all four canonical dNTPs, as would occur in the setting of SAMHD1 inhibition for example, as discussed below.

Figure 4-2. Unique activation of telomerase from thymidine supplementation driven by RNR allosteric regulation. A. Schematic of how thymidine (dT) supplementation influences dNTP levels via allosteric regulation of RNR. dT can be efficiently salvaged by cellular kinases to generate high dTTP levels. Allosteric binding of dTTP to RNR promotes reduction of GDP to form dGDP and while inhibiting the reduction of the pyrimidines CDP and UDP. Allosteric binding of dGTP promotes ADP reduction by RNR. **B.** Schematic of the net effect of dT supplementation on dNTP pools and the anticipated effects on telomerase and other DNA synthesizing enzymes. Telomerase synthesizes 5'-GGTTAG-3' repeats, thus is activated by dT supplementation, while other pathogenic DNA synthesizing elements are inhibited via dCTP depletion.

Figure 4-2. (Continued)



PNP inhibitors: I found that treatment with dG plus the PNP inhibitor ulodesine led to telomere lengthening in human cells including TBD patient fibroblast cells. PNP inhibitor treatment has been show to increase circulating dG levels as well as cellular dGTP levels in clinical studies, and therefore may increase telomerase activity and promote telomere lengthening as a single agent[221]. However, dGTP elevations from PNP inhibition are dependent on cellular DCK and SAMHD1 levels, and therefore may be cell type restricted[218]. While PNP inhibitors appear well tolerated[225], in some cell types PNP inhibition can lead to toxicity, potentially due to highly increased dGTP levels[275]. This phenomena has been proposed to explain the T-cell deficiency observed in patients with germline PNP deficiency[218].

SAMHD1 inhibition: I found that SAMHD1 inhibition led to rapid telomere lengthening in multiple cell lines including TBD patient derived iPSCs, a finding in line with a recent report from another group[205]. The development of small molecule SAMHD1 inhibitors is being actively pursued[276], which could offer a promising approach for systemic treatment for TBD patients. SAMHD1 has been ascribed roles in addition to limiting dNTP pools, including contributing to homologous recombination and resolving replication stress[176,177]. Selective inhibition of the dNTPase activity of SAMHD1 using a small molecule-based approach could therefore limit off target effects compared with protein depletion. As discussed above, the elevation of all four dNTPs following SAMHD1 inhibition may increase endogenous retroelement proliferation and trigger excess interferon signaling, as has been hypothesized to occur in SAMHD1 deficient AGS patients[92,258]. Reverse transcriptase inhibitors have shown promise in AGS patients, including patients with SAMHD1 mutations[260], and could therefore be considered in combination with SAMHD1 inhibition, provided they do not have inhibitory activity against the telomerase reverse transcriptase.

***Dm-dNK expression**:* I found that ectopic expression of Dm-dNK drove dramatic increases in telomere length in human cells including fibroblasts from TBD patients. Overexpression of Dm-dNK has been previously considered in the treatment of TK2-related mitochondrial depletion disorder, where in a TK2 deficient mouse model, germline Dm-dNK overexpression improved lifespan, increased dTTP pools, rescued mitochondrial depletion, and had no apparent effects on nuclear genome integrity[277,278]. Engineered expression of Dm-dNK could be considered in the setting of autologous hematopoietic cell transplant in TBD patients, and could perhaps be delivered simultaneously with genome editing enzymes aimed at correcting the TBD causing mutation in the patients' cells.

An evolutionary perspective on the relationship between telomeres, telomerase, and dNTP metabolism

Telomere length is tightly distributed in the population and is associated with diseases at either extreme[33,114,116,121,157]. I have shown that telomere length homeostasis is highly sensitive to changes in cellular dNTP metabolism: alterations leading to higher dNTP levels cause telomere lengthening, while impairment of dNTP synthesis causes telomere shortening. Elevated dNTP pools have been linked with numerous diseases including viral infections, autoinflammatory diseases, and cancer. I propose that competing selective pressures to restrict dNTP pools provides a potential mechanism by which population telomere length may deviate from its evolutionary optimum.

Host-virus conflicts have been shown to drive strong and rapid evolutionary selection both on virus genes and host genes[279,280]. One example of this phenomena involves the dNTPase SAMHD1. SAMHD1 was identified as a lentiviral restriction factor, and subsequently was

demonstrated to restrict the propagation of several DNA viruses and retroviruses by depleting dNTP pools available for genome replication[92,94]. Several primate lentiviruses encode the accessory proteins Vpx and Vpr which target SAMHD1 for proteasomal degradation, demonstrating the critical importance of SAMHD1 in restricting lentiviral infections. Examination of the evolution of lentiviruses and the species they infect has revealed an evolutionary arms race between host SAMHD1 and viral Vpx/Vpr, with strong positive selection on the SAMHD1 residues which bind to Vpx/Vpr[281–283]. In addition to restricting exogenous retroviruses, SAMHD1 has also been shown to limit the propagation of endogenous retroelements, including LINE1[284]. LINE1 has generated approximately one third of the human genome[285], has been shown to drive rapid evolution in hosts genes[279], and remains an active cause of human disease[285,286]. Inherited mutations in SAMHD1 can cause the Aicardi-Goutières syndrome (AGS), a severe inflammatory disorder[254]. In SAMHD1 mutant AGS patients, elevated dNTP pools have been proposed to enable increased activity of retroelements, leading to elevated levels of cytosolic polynucleotides and chronic interferon signaling[92,258]. In support of the notion that elevated retroelement activity plays a role in AGS pathogenesis, nucleoside reverse transcriptase inhibitors have shown promise in clinical trials for the treatment of AGS, including in SAMHD1 deficient patients[260]. SAMHD1 has also been implicated in the restriction of DNA viruses, and some of these viruses have been found to actively counteract SAMHD1, for example in the case of the EBV protein BGLF4 which has been shown to inactivate SAMHD1[253]. Furthermore, DNA viruses commonly carry dNTP synthesizing genes including thymidine kinases and ribonucleotide reductases[287,288]. Collectively, these data suggest that dNTP pools are under strong negative selective pressure to limit proliferation of DNA synthesizing viruses and endogenous retroelements.

Given my data demonstrating that telomerase activity is highly sensitive to changes in dNTP metabolism, including being negatively regulated by the dNTPase activity of SAMHD1, I propose that evolutionary pressures to restrict dNTP pools offer a possible mechanism by which telomere length in the population may deviate from its evolutionary optimum (**Figure 4-3**). By driving selection for individuals with low dNTP pools, DNA viruses or retroelements could simultaneously select for shorter telomere length in the population leading to higher rates of TBDs. Telomere synthesis is highest in the germline and during development. Therefore, viruses which cause congenital infections as well as endogenous retroelements may be particularly relevant for applying selective pressures on dNTP pools that could influence telomere length.

Figure 4-3

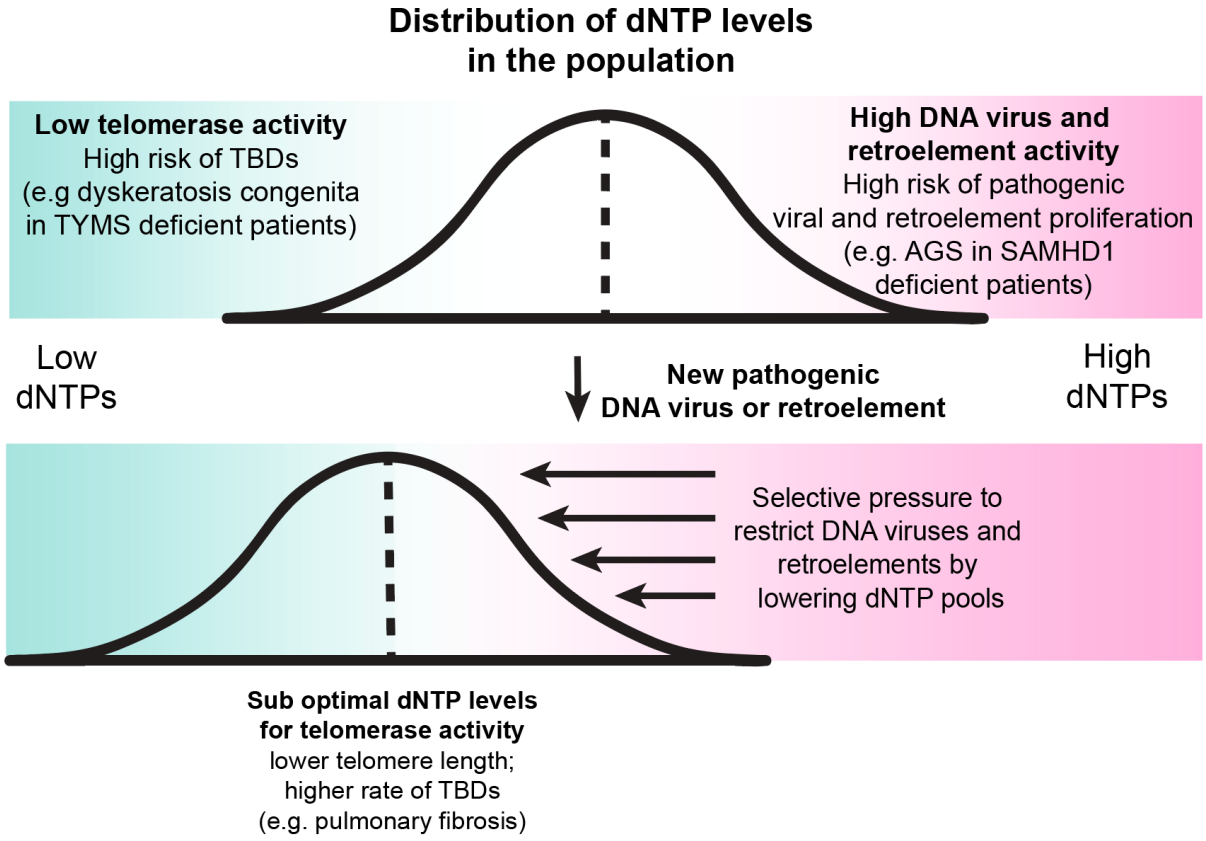


Figure 4-3. A model for how competing evolutionary pressures on dNTP pools could reduce telomere length in the population.

In addition to evolutionary pressures on dNTP pools driving changes in telomere homeostasis, the need to maintain telomerase activity could also influence dNTP pool homeostasis. I found that telomerase activity in human cells is highly sensitive to dNTP metabolism perturbations, and germline mutations in the rate limiting *de novo* thymidine synthesis gene TYMS have recently been associated with TBD dyskeratosis congenita[32]. Together, these findings suggest that the need to maintain telomere synthesis by telomerase may place a lower bound on tolerable dNTP pools. This lower bound may be enabling the continued proliferation of DNA viruses and pathogenic retroelements in the population.

Telomerase has been hypothesized to have emerged from a retroviral element[23], and is related to reverse transcriptases from group II introns[289,290]. The tension between promoting telomerase activity and restricting pathogenic retroelement proliferation may have been most intense early on in the specialization of telomerase, before this enzyme had the opportunity to significantly diverge from its pathogenic retroelement ancestors. One outstanding question about the origin of telomeres remains: why is the ancestral telomeric repeat TTAGGG[24]? The highly conserved allosteric regulation of RNR[82] may offer an answer to this question: elevated dTTP levels stimulate dGTP production, and dATP production while inhibiting dCTP production (**Figure 4-2a**). Therefore, the emergence of a telomerase encoding only T's, A's, and G's may have provided an evolutionary advantage by allowing cells to upregulate thymidine synthesis to increase telomerase activity while restricting other retroelements which need the full complement of dNTPs for their proliferation (**Figure 4-2b**). Future investigations into the co-evolution of dNTP metabolizing genes, human DNA viruses and pathogenic retroelements, and telomerase may reveal an ongoing evolutionary battle over dNTP pool homeostasis.

Concluding Statement

Human telomere length is tightly regulated and associated with severe diseases. In this thesis, I have identified dNTP metabolism as a critical and previously unappreciated pathway controlling human telomere length. I rigorously demonstrate that telomere length changes from dNTP manipulations are mediated by alterations in the specific activity of telomerase. I propose that dNTP substrate-level regulation of telomerase activity underlies this connection, offering mechanistic insight into the recent association of human genetic variation in dNTP metabolism genes with telomere length and telomere related disease. By uncovering dNTP metabolism as a critical pathway for telomere length control, I identified small molecule and genetic approaches to lengthen telomeres in human cells, including in cells from patients with TBDs, opening new paths forward towards identifying treatments for these lethal diseases. Given its unique substrate requirements and enzymatic mechanism, I propose telomerase is uniquely sensitive to changes in dNTP pools amongst the nuclear DNA synthesis machines, and hypothesize that the need to maintain telomerase activity may place a lower bound on tolerable dNTP levels. Nuclear dNTP pool homeostasis is under competing selective pressures including the need to restrict the proliferation of pathogenetic reverse transcriptases, and I propose that these pressures have likely impacted telomere length homeostasis throughout evolution. Harnessing the unique substrate requirements for 5'-GGTTAG'-3 repeat synthesis by telomerase may enable a window to augment telomerase activity while limiting the activity of pathogenic retroelements. The regulation of telomerase activity by nucleotide metabolism offers a new paradigm for telomere length control and could shed light on the origin and evolution of telomerase.

References

1. McClintock, B. *Cytological Observations of Deficiencies Involving Known Genes, Translocations and an Inversion in Zea Mays*. (University of Missouri, College of Agriculture, Agricultural Experiment Station, 1931).
2. Muller, H. J. The remaking of chromosomes.". in vols 13, 181–95, 198. (The Collecting Net, Woods Hole, 1938).
3. Kornberg, A. & Baker, T. A. *DNA Replication*. (University Science Books, 2005).
4. Brutlag, D., Schekman, R. & Kornberg, A. A Possible Role for RNA Polymerase in the Initiation of M13 DNA Synthesis. *Proceedings of the National Academy of Sciences* **68**, 2826–2829 (1971).
5. Wickner, W., Brutlag, D., Schekman, R. & Kornberg, A. RNA synthesis initiates in vitro conversion of M13 DNA to its replicative form. *Proc Natl Acad Sci U S A* **69**, 965–969 (1972).
6. Olovnikov, A. M. A theory of marginotomy: The incomplete copying of template margin in enzymic synthesis of polynucleotides and biological significance of the phenomenon. *Journal of Theoretical Biology* **41**, 181–190 (1973).
7. Watson, J. D. Origin of Concatemeric T7DNA. *Nature New Biology* **239**, 197–201 (1972).
8. Blackburn, E. H. & Gall, J. G. A tandemly repeated sequence at the termini of the extrachromosomal ribosomal RNA genes in Tetrahymena. *J Mol Biol* **120**, 33–53 (1978).
9. Blackburn, E. H. *et al.* DNA Termini in Ciliate Macronuclei. *Cold Spring Harb Symp Quant Biol* **47**, 1195–1207 (1983).
10. Shampay, J., Szostak, J. W. & Blackburn, E. H. DNA sequences of telomeres maintained in yeast. *Nature* **310**, 154–157 (1984).

11. Szostak, J. W. & Blackburn, E. H. Cloning yeast telomeres on linear plasmid vectors. *Cell* **29**, 245–255 (1982).
12. Greider, C. W. & Blackburn, E. H. Identification of a specific telomere terminal transferase activity in tetrahymena extracts. *Cell* **43**, 405–413 (1985).
13. Greider, C. W. & Blackburn, E. H. A telomeric sequence in the RNA of Tetrahymena telomerase required for telomere repeat synthesis. *Nature* **337**, 331–337 (1989).
14. Greider, C. W. & Blackburn, E. H. The telomere terminal transferase of Tetrahymena is a ribonucleoprotein enzyme with two kinds of primer specificity. *Cell* **51**, 887–898 (1987).
15. Moyzis, R. K. *et al.* A highly conserved repetitive DNA sequence, (TTAGGG)n, present at the telomeres of human chromosomes. *Proc Natl Acad Sci U S A* **85**, 6622–6626 (1988).
16. Feng, J. *et al.* The RNA component of human telomerase. *Science* **269**, 1236–1241 (1995).
17. Meyerson, M. *et al.* hEST2, the putative human telomerase catalytic subunit gene, is up-regulated in tumor cells and during immortalization. *Cell* **90**, 785–795 (1997).
18. Nakamura, T. M. *et al.* Telomerase catalytic subunit homologs from fission yeast and human. *Science* **277**, 955–959 (1997).
19. Lange, T. de. Shelterin: the protein complex that shapes and safeguards human telomeres. *Genes Dev.* **19**, 2100–2110 (2005).
20. de Lange, T. Shelterin-Mediated Telomere Protection. *Annual Review of Genetics* **52**, 223–247 (2018).
21. Hockemeyer, D. & Collins, K. Control of telomerase action at human telomeres. *Nat Struct Mol Biol* **22**, 848–852 (2015).
22. Cai, S. W. & Lange, T. de. CST–Polα/Primase: the second telomere maintenance machine. *Genes Dev.* (2023) doi:10.1101/gad.350479.123.

23. de Lange, T. A loopy view of telomere evolution. *Front Genet* **6**, 321 (2015).
24. Podlevsky, J. D. & Chen, J. J.-L. Evolutionary perspectives of telomerase RNA structure and function. *RNA Biol* **13**, 720–732 (2016).
25. Myler, L. R. *et al.* The evolution of metazoan shelterin. *Genes Dev* **35**, 1625–1641 (2021).
26. de Lange, T. How Telomeres Solve the End-Protection Problem. *Science* **326**, 948–952 (2009).
27. Harley, C. B., Futcher, A. B. & Greider, C. W. Telomeres shorten during ageing of human fibroblasts. *Nature* **345**, 458–460 (1990).
28. Telomere reduction in human colorectal carcinoma and with ageing | Nature. https://www.nature.com/articles/346866a0.
29. de Lange, T. *et al.* Structure and variability of human chromosome ends. *Mol Cell Biol* **10**, 518–527 (1990).
30. Huffman, K. E., Levene, S. D., Tesmer, V. M., Shay, J. W. & Wright, W. E. Telomere Shortening Is Proportional to the Size of the G-rich Telomeric 3′-Overhang*. *Journal of Biological Chemistry* **275**, 19719–19722 (2000).
31. Revy, P., Kannengiesser, C. & Bertuch, A. A. Genetics of human telomere biology disorders. *Nat Rev Genet* **24**, 86–108 (2023).
32. Tummala, H. *et al.* Germline thymidylate synthase deficiency impacts nucleotide metabolism and causes dyskeratosis congenita. *The American Journal of Human Genetics* **109**, 1472–1483 (2022).
33. Codd, V. *et al.* Polygenic basis and biomedical consequences of telomere length variation. *Nat Genet* **53**, 1425–1433 (2021).

34. Li, C. *et al.* Genome-wide Association Analysis in Humans Links Nucleotide Metabolism to Leukocyte Telomere Length. *The American Journal of Human Genetics* **106**, 389–404 (2020).

35. Ghanim, G. E. *et al.* Structure of human telomerase holoenzyme with bound telomeric DNA. *Nature* **593**, 449–453 (2021).

36. Kim, N. W. *et al.* Specific Association of Human Telomerase Activity with Immortal Cells and Cancer. *Science* **266**, 2011–2015 (1994).

37. Wright, W. E., Piatyszek, M. A., Rainey, W. E., Byrd, W. & Shay, J. W. Telomerase activity in human germline and embryonic tissues and cells. *Dev Genet* **18**, 173–179 (1996).

38. Chiu, C.-P. *et al.* Differential Expression of Telomerase Activity in Hematopoietic Progenitors from Adult Human Bone Marrow. *STEM CELLS* **14**, 239–248 (1996).

39. Bodnar, A. G. *et al.* Extension of Life-Span by Introduction of Telomerase into Normal Human Cells. *Science* **279**, 349–352 (1998).

40. Horn, S. *et al.* TERT Promoter Mutations in Familial and Sporadic Melanoma. *Science* **339**, 959–961 (2013).

41. Huang, F. W. *et al.* Highly recurrent TERT promoter mutations in human melanoma. *Science* **339**, 957–959 (2013).

42. Penev, A. *et al.* Alternative splicing is a developmental switch for hTERT expression. *Mol Cell* **81**, 2349-2360.e6 (2021).

43. Wong, J. M. Y. & Collins, K. Telomerase RNA level limits telomere maintenance in X-linked dyskeratosis congenita. *Genes Dev.* **20**, 2848–2858 (2006).

44. Moon, D. H. *et al.* Poly(A)-specific ribonuclease (PARN) mediates 3'-end maturation of the telomerase RNA component. *Nat Genet* **47**, 1482–1488 (2015).

45. Boyraz, B. *et al.* Posttranscriptional manipulation of TERC reverses molecular hallmarks of telomere disease. *J Clin Invest* **126**, 3377–3382 (2016).

46. Venteicher, A. S. *et al.* A human telomerase holoenzyme protein required for Cajal body localization and telomere synthesis. *Science* **323**, 644–648 (2009).

47. Schmidt, J. C. & Cech, T. R. Human telomerase: biogenesis, trafficking, recruitment, and activation. *Genes Dev* **29**, 1095–1105 (2015).

48. Cristofari, G. & Lingner, J. Telomere length homeostasis requires that telomerase levels are limiting. *EMBO J* **25**, 565–574 (2006).

49. Zhong, F. L. *et al.* TPP1 OB-fold domain controls telomere maintenance by recruiting telomerase to chromosome ends. *Cell* **150**, 481–494 (2012).

50. Nandakumar, J. *et al.* The TEL patch of telomere protein TPP1 mediates telomerase recruitment and processivity. *Nature* **492**, 285–289 (2012).

51. Abreu, E. *et al.* TIN2-tethered TPP1 recruits human telomerase to telomeres in vivo. *Mol Cell Biol* **30**, 2971–2982 (2010).

52. van Steensel, B. & de Lange, T. Control of telomere length by the human telomeric protein TRF1. *Nature* **385**, 740–743 (1997).

53. Kim, S., Kaminker, P. & Campisi, J. TIN2, a new regulator of telomere length in human cells. *Nat Genet* **23**, 405–412 (1999).

54. Loayza, D. & de Lange, T. POT1 as a terminal transducer of TRF1 telomere length control. *Nature* **423**, 1013–1018 (2003).

55. Ouellette, M. M. *et al.* Subsenescent telomere lengths in fibroblasts immortalized by limiting amounts of telomerase. *J Biol Chem* **275**, 10072–10076 (2000).

56. Zhu, L. *et al.* Telomere length regulation in mice is linked to a novel chromosome locus. *Proceedings of the National Academy of Sciences* **95**, 8648–8653 (1998).

57. Greider, C. W. Regulating telomere length from the inside out: the replication fork model. *Genes Dev* **30**, 1483–1491 (2016).

58. Chen, L.-Y., Redon, S. & Lingner, J. The human CST complex is a terminator of telomerase activity. *Nature* **488**, 540–544 (2012).

59. Feng, X. *et al.* CTC1-STN1 terminates telomerase while STN1-TEN1 enables C-strand synthesis during telomere replication in colon cancer cells. *Nat Commun* **9**, 2827 (2018).

60. Zaug, A. J. *et al.* CST does not evict elongating telomerase but prevents initiation by ssDNA binding. *Nucleic Acids Res* **49**, 11653–11665 (2021).

61. Cai, S. W., Takai, H., Walz, T. & Lange, T. de. POT1 recruits and regulates CST–Polα/Primase at human telomeres. 2023.05.08.539880 Preprint at https://doi.org/10.1101/2023.05.08.539880 (2023).

62. Wang, H. *et al.* CTC1 OB-B interaction with TPP1 terminates telomerase and prevents telomere overextension. *Nucleic Acids Res* **51**, 4914–4928 (2023).

63. Bagshaw, C. R., Hentschel, J. & Stone, M. D. The Processivity of Telomerase: Insights from Kinetic Simulations and Analyses. *Molecules* **26**, 7532 (2021).

64. Jansson, L. I. *et al.* Telomere DNA G-quadruplex folding within actively extending human telomerase. *Proceedings of the National Academy of Sciences* **116**, 9350–9359 (2019).

65. Latrick, C. M. & Cech, T. R. POT1–TPP1 enhances telomerase processivity by slowing primer dissociation and aiding translocation. *The EMBO Journal* **29**, 924–933 (2010).

66. Sekne, Z., Ghanim, G. E., van Roon, A.-M. M. & Nguyen, T. H. D. Structural basis of human telomerase recruitment by TPP1-POT1. *Science* **375**, 1173–1176 (2022).

67. Patrick, E. M., Slivka, J., Payne, B., Comstock, M. J. & Schmidt, J. C. Observation of processive telomerase catalysis using high-resolution optical tweezers. *Nat Chem Biol* **16**, 801–809 (2020).

68. Zhao, Y. *et al.* Telomere Extension Occurs at Most Chromosome Ends and Is Uncoupled from Fill-In in Human Cancer Cells. *Cell* **138**, 463–475 (2009).

69. Zhao, Y. *et al.* Processive and Distributive Extension of Human Telomeres by Telomerase under Homeostatic and Nonequilibrium Conditions. *Molecular Cell* **42**, 297–307 (2011).

70. Wu, R. A., Tam, J. & Collins, K. DNA-binding determinants and cellular thresholds for human telomerase repeat addition processivity. *The EMBO Journal* **36**, 1908–1927 (2017).

71. Chen, Y., Podlevsky, J. D., Logeswaran, D. & Chen, J. J.-L. A single nucleotide incorporation step limits human telomerase repeat addition activity. *EMBO J* **37**, e97953 (2018).

72. Morin, G. B. The human telomere terminal transferase enzyme is a ribonucleoprotein that synthesizes TTAGGG repeats. *Cell* **59**, 521–529 (1989).

73. Maine, I. P., Chen, S. F. & Windle, B. Effect of dGTP concentration on human and CHO telomerase. *Biochemistry* **38**, 15325–15332 (1999).

74. Sun, D., Lopez-Guajardo, C. C., Quada, J., Hurley, L. H. & Von Hoff, D. D. Regulation of Catalytic Activity and Processivity of Human Telomerase. *Biochemistry* **38**, 4037–4044 (1999).

75. Coggins, S. A., Mahboubi, B., Schinazi, R. F. & Kim, B. Mechanistic cross-talk between DNA/RNA polymerase enzyme kinetics and nucleotide substrate availability in cells: Implications for polymerase inhibitor discovery. *J Biol Chem* **295**, 13432–13443 (2020).

76. Traut, T. W. Physiological concentrations of purines and pyrimidines. *Mol Cell Biochem* **140**, 1–22 (1994).

77. Sanford, S. L., Welfer, G. A., Freudenthal, B. D. & Opresko, P. L. Mechanisms of telomerase inhibition by oxidized and therapeutic dNTPs. *Nat Commun* **11**, 5288 (2020).

78. Matsuda, S. & Kasahara, T. Simultaneous and absolute quantification of nucleoside triphosphates using liquid chromatography–triple quadrupole tandem mass spectrometry. *Genes Environ* **40**, 13 (2018).

79. Bohman, C. & Eriksson, S. Deoxycytidine kinase from human leukemic spleen: preparation and characteristics of homogeneous enzyme. *Biochemistry* **27**, 4258–4265 (1988).

80. Munch-Petersen, B., Cloos, L., Tyrsted, G. & Eriksson, S. Diverging substrate specificity of pure human thymidine kinases 1 and 2 against antiviral dideoxynucleosides. *Journal of Biological Chemistry* **266**, 9032–9038 (1991).

81. Knecht, W. *et al.* A few amino acid substitutions can convert deoxyribonucleoside kinase specificity from pyrimidines to purines. *The EMBO Journal* **21**, 1873–1880 (2002).

82. Nordlund, P. & Reichard, P. Ribonucleotide Reductases. *Annual Review of Biochemistry* **75**, 681–706 (2006).

83. 3.3-Å resolution cryo-EM structure of human ribonucleotide reductase with substrate and allosteric regulators bound | eLife. https://elifesciences.org/articles/31502.

84. Chabes, A. & Thelander, L. Controlled protein degradation regulates ribonucleotide reductase activity in proliferating mammalian cells during the normal cell cycle and in response to DNA damage and replication blocks. *J Biol Chem* **275**, 17747–17753 (2000).

85. Mathews, C. K. Deoxyribonucleotide metabolism, mutagenesis and cancer. *Nature Reviews Cancer* **15**, 528–539 (2015).

86. Carreras, C. W. & Santi, D. V. The Catalytic Mechanism and Structure of Thymidylate Synthase. *Annual Review of Biochemistry* **64**, 721–762 (1995).

87. Martínez-Arribas, B. *et al.* DCTPP1 prevents a mutator phenotype through the modulation of dCTP, dTTP and dUTP pools. *Cell. Mol. Life Sci.* **77**, 1645–1660 (2020).

88. Maley, G. F. & Maley, F. Feedback Control of Purified Deoxycytidylate Deaminase. *Science* **141**, 1278–1279 (1963).

89. El-Hattab, A. W. & Scaglia, F. Mitochondrial DNA Depletion Syndromes: Review and Updates of Genetic Basis, Manifestations, and Therapeutic Options. *Neurotherapeutics* **10**, 186–198 (2013).

90. Eriksson, S., Munch-Petersen, B., Johansson, K. & Eklund, H. Structure and function of cellular deoxyribonucleoside kinases. *Cell Mol Life Sci* **59**, 1327–1346 (2002).

91. Bianchi, V. *et al.* Cell cycle-dependent metabolism of pyrimidine deoxynucleoside triphosphates in CEM cells. *J Biol Chem* **272**, 16118–16124 (1997).

92. Goldstone, D. C. *et al.* HIV-1 restriction factor SAMHD1 is a deoxynucleoside triphosphate triphosphohydrolase. *Nature* **480**, 379–382 (2011).

93. Franzolin, E. *et al.* The deoxynucleotide triphosphohydrolase SAMHD1 is a major regulator of DNA precursor pools in mammalian cells. *PNAS* **110**, 14272–14277 (2013).

94. Lahouassa, H. *et al.* SAMHD1 restricts HIV-1 by reducing the intracellular pool of deoxynucleotide triphosphates. *Nat Immunol* **13**, 223–228 (2012).

95. Dos Santos, R. S. *et al.* dUTPase (DUT) Is Mutated in a Novel Monogenic Syndrome With Diabetes and Bone Marrow Failure. *Diabetes* **66**, 1086–1096 (2017).

96. Jordheim, L. P., Durantel, D., Zoulim, F. & Dumontet, C. Advances in the development of nucleoside and nucleotide analogues for cancer and viral diseases. *Nat Rev Drug Discov* **12**, 447–464 (2013).

97. Domínguez-González, C. *et al.* Deoxynucleoside Therapy for Thymidine Kinase 2–Deficient Myopathy. *Ann Neurol* **86**, 293–303 (2019).

98. Adams, A. K. & Holm, C. Specific DNA replication mutations affect telomere length in Saccharomyces cerevisiae. *Mol Cell Biol* **16**, 4614–4620 (1996).

99. Toussaint, M., Dionne, I. & Wellinger, R. J. Limited TTP supply affects telomere length regulation in a telomerase-independent fashion. *Nucleic Acids Res* **33**, 704–713 (2005).

100. Gupta, A. *et al.* Telomere length homeostasis responds to changes in intracellular dNTP pools. *Genetics* **193**, 1095–1105 (2013).

101. Bosoy, D. & Lue, N. F. Yeast telomerase is capable of limited repeat addition processivity. *Nucleic Acids Research* **32**, 93–101 (2004).

102. Cihlar, T. & Ray, A. S. Nucleoside and nucleotide HIV reverse transcriptase inhibitors: 25 years after zidovudine. *Antiviral Research* **85**, 39–58 (2010).

103. Baldwin, E. T. *et al.* Structures, functions, and adaptations of the human LINE-1 ORF2 protein. *Nature* 1–3 (2023) doi:10.1038/s41586-023-06947-z.

104. Murakami, J., Nagai, N., Shigemasa, K. & Ohama, K. Inhibition of telomerase activity and cell proliferation by a reverse transcriptase inhibitor in gynaecological cancer cell lines. *Eur J Cancer* **35**, 1027–1034 (1999).

105. Hukezalie, K. R., Thumati, N. R., Côté, H. C. F. & Wong, J. M. Y. In vitro and ex vivo inhibition of human telomerase by anti-HIV nucleoside reverse transcriptase inhibitors (NRTIs) but not by non-NRTIs. *PLoS One* **7**, e47505 (2012).

106. Mender, I., Gryaznov, S., Dikmen, Z. G., Wright, W. E. & Shay, J. W. Induction of Telomere Dysfunction Mediated By the Telomerase Substrate Precursor 6-Thio-2'-Deoxyguanosine. *Cancer Discov* **5**, 82–95 (2015).

107. Fouquerel, E. *et al.* Oxidative guanine base damage regulates human telomerase activity. *Nat Struct Mol Biol* **23**, 1092–1100 (2016).

108. Schaich, M. A. *et al.* Mechanisms of nucleotide selection by telomerase. *eLife* **9**, e55438 (2020).

109. Demanelis, K. *et al.* Determinants of telomere length across human tissues. *Science* **369**, eaaz6876 (2020).

110. Alder, J. K. *et al.* Diagnostic utility of telomere length testing in a hospital-based setting. *Proc Natl Acad Sci U S A* **115**, E2358–E2365 (2018).

111. Aubert, G., Baerlocher, G. M., Vulto, I., Poon, S. S. & Lansdorp, P. M. Collapse of telomere homeostasis in hematopoietic cells caused by heterozygous mutations in telomerase genes. *PLoS Genet* **8**, e1002696 (2012).

112. Broer, L. *et al.* Meta-analysis of telomere length in 19 713 subjects reveals high heritability, stronger maternal inheritance and a paternal age effect. *European journal of human genetics* **21**, 1163–1168 (2013).

113. Taub, M. A. *et al.* Genetic determinants of telomere length from 109,122 ancestrally diverse whole-genome sequences in TOPMed. *Cell Genomics* **2**, 100084 (2022).

114. The Telomeres Mendelian Randomization Collaboration *et al.* Association Between Telomere Length and Risk of Cancer and Non-Neoplastic Diseases: A Mendelian Randomization Study. *JAMA Oncol* **3**, 636 (2017).

115. Henry, M.-L., Osborne, J. & Else, T. POT1 Tumor Predisposition. in *GeneReviews®* (eds. Adam, M. P. et al.) (University of Washington, Seattle, Seattle (WA), 1993).

116. Schmutz, I. *et al.* TINF2 is a haploinsufficient tumor suppressor that limits telomere length. *eLife* **9**, e61235 (2020).

117. Aoude, L. G. *et al.* Nonsense Mutations in the Shelterin Complex Genes ACD and TERF2IP in Familial Melanoma. *J Natl Cancer Inst* **107**, dju408 (2014).

118. Denchi, E. L. & de Lange, T. Protection of telomeres through independent control of ATM and ATR by TRF2 and POT1. *Nature* **448**, 1068–1071 (2007).

119. Ramsay, A. J. *et al.* POT1 mutations cause telomere dysfunction in chronic lymphocytic leukemia. *Nat Genet* **45**, 526–530 (2013).

120. Kim, W. *et al.* Cancer-associated POT1 mutations lead to telomere elongation without induction of a DNA damage response. *The EMBO Journal* **40**, e107346 (2021).

121. DeBoy, E. A. *et al.* Familial Clonal Hematopoiesis in a Long Telomere Syndrome. *New England Journal of Medicine* **388**, 2422–2433 (2023).

122. Barthel, F. P. *et al.* Systematic analysis of telomere length and somatic alterations in 31 cancer types. *Nat Genet* **49**, 349–357 (2017).

123. Chiba, K. *et al.* Cancer-associated TERT promoter mutations abrogate telomerase silencing. *eLife* **4**, e07918 (2015).

124. Heiss, N. S. *et al.* X-linked dyskeratosis congenita is caused by mutations in a highly conserved gene with putative nucleolar functions. *Nat Genet* **19**, 32–38 (1998).

125. Mitchell, J. R., Cheng, J. & Collins, K. A box H/ACA small nucleolar RNA-like domain at the human telomerase RNA 3’ end. *Mol Cell Biol* **19**, 567–576 (1999).

126. Mitchell, J. R., Wood, E. & Collins, K. A telomerase component is defective in the human disease dyskeratosis congenita. *Nature* **402**, 551–555 (1999).

127. Vulliamy, T. *et al.* The RNA component of telomerase is mutated in autosomal dominant dyskeratosis congenita. *Nature* **413**, 432–435 (2001).

128. Tsakiri, K. D. *et al.* Adult-onset pulmonary fibrosis caused by mutations in telomerase. *Proceedings of the National Academy of Sciences* **104**, 7552–7557 (2007).

129. Armanios, M. Y. *et al.* Telomerase Mutations in Families with Idiopathic Pulmonary Fibrosis. *New England Journal of Medicine* **356**, 1317–1326 (2007).

130. Yamaguchi, H. *et al.* Mutations in TERT, the gene for telomerase reverse transcriptase, in aplastic anemia. *N Engl J Med* **352**, 1413–1424 (2005).

131. Glousker, G., Touzot, F., Revy, P., Tzfati, Y. & Savage, S. A. Unraveling the Pathogenesis of Hoyeraal-Hreidarsson Syndrome, a Complex Telomere Biology Disorder. *Br J Haematol* **170**, 457–471 (2015).

132. Savage, S. A. *et al.* TINF2, a component of the shelterin telomere protection complex, is mutated in dyskeratosis congenita. *Am J Hum Genet* **82**, 501–509 (2008).

133. Anderson, B. H. *et al.* Mutations in CTC1, encoding conserved telomere maintenance component 1, cause Coats plus. *Nat Genet* **44**, 338–342 (2012).

134. Polvi, A. *et al.* Mutations in CTC1, encoding the CTS telomere maintenance complex component 1, cause cerebroretinal microangiopathy with calcifications and cysts. *Am J Hum Genet* **90**, 540–549 (2012).

135. Armanios, M. Telomerase and idiopathic pulmonary fibrosis. *Mutation Research/Fundamental and Molecular Mechanisms of Mutagenesis* **730**, 52–58 (2012).

136. Walne, A. J., Vulliamy, T., Beswick, R., Kirwan, M. & Dokal, I. TINF2 mutations result in very short telomeres: analysis of a large cohort of patients with dyskeratosis congenita and related bone marrow failure syndromes. *Blood* **112**, 3594–3600 (2008).

137. Kermasson, L. *et al.* Inherited human Apollo deficiency causes severe bone marrow failure and developmental defects. *Blood* **139**, 2427–2440 (2022).

138. Takai, H. *et al.* A POT1 mutation implicates defective telomere end fill-in and telomere truncations in Coats plus. *Genes Dev.* **30**, 812–826 (2016).

139. Savage, S. A. & Niewisch, M. R. Dyskeratosis Congenita and Related Telomere Biology Disorders. in *GeneReviews®* (eds. Adam, M. P. et al.) (University of Washington, Seattle, Seattle (WA), 1993).

140. Lehmann, L. E., Williams, D. A., London, W. B. & Agarwal, S. Full Donor Myeloid Engraftment with Minimal Toxicity in Dyskeratosis Congenita Patients Undergoing Allogeneic Bone Marrow Transplantation without Radiation or Alkylating Agents. *Blood* **124**, 2941–2941 (2014).

141. Agarwal, S. Evaluation and Management of Hematopoietic Failure in Dyskeratosis Congenita. *Hematol Oncol Clin North Am* **32**, 669–685 (2018).

142. Danazol Treatment for Telomere Diseases | NEJM. https://www.nejm.org/doi/full/10.1056/nejmoa1515319.

143. Khincha, P. P. *et al.* Similar telomere attrition rates in androgen-treated and untreated patients with dyskeratosis congenita. *Blood Advances* **2**, 1243–1249 (2018).

144. Borie, R. *et al.* Severe hematologic complications after lung transplantation in patients with telomerase complex mutations. *The Journal of Heart and Lung Transplantation* **34**, 538–546 (2015).

145. Silhan, L. L. *et al.* Lung transplantation in telomerase mutation carriers with pulmonary fibrosis. *European Respiratory Journal* **44**, 178–187 (2014).

146. Duckworth, A. *et al.* Telomere length and risk of idiopathic pulmonary fibrosis and chronic obstructive pulmonary disease: a mendelian randomisation study. *Lancet Respir Med* **9**, 285–294 (2021).

147. Alter, B. P. *et al.* Telomere length is associated with disease severity and declines with age in dyskeratosis congenita. *Haematologica* **97**, 353–359 (2012).

148. Vulliamy, T. *et al.* Disease anticipation is associated with progressive telomere shortening in families with dyskeratosis congenita due to mutations in TERC. *Nat Genet* **36**, 447–449 (2004).

149. van der Vis, J. J. *et al.* Pulmonary fibrosis in non-mutation carriers of families with short telomere syndrome gene mutations. *Respirology* **26**, 1160–1170 (2021).

150. Epigenetic inheritance of telomere length obscures identification of causative PARN locus - PMC. https://www.ncbi.nlm.nih.gov/pmc/articles/PMC4875813/.

151. Vulliamy, T. J., Knight, S. W., Dokal, I. & Mason, P. J. Skewed X-inactivation in carriers of X-linked dyskeratosis congenita. *Blood* **90**, 2213–2216 (1997).

152. Jaiswal, S. *et al.* Age-Related Clonal Hematopoiesis Associated with Adverse Outcomes. *New England Journal of Medicine* **371**, 2488–2498 (2014).

153. Genovese, G. *et al.* Clonal Hematopoiesis and Blood-Cancer Risk Inferred from Blood DNA Sequence. *New England Journal of Medicine* **371**, 2477–2487 (2014).

154. Schratz, K. E. *et al.* Somatic reversion impacts myelodysplastic syndromes and acute myeloid leukemia evolution in the short telomere disorders. *Journal of Clinical Investigation* **131**, e147598 (2021).

155. Fagagna, F. d'Adda di *et al.* A DNA damage checkpoint response in telomere-initiated senescence. *Nature* **426**, 194–198 (2003).

156. Takai, H., Smogorzewska, A. & Lange, T. de. DNA Damage Foci at Dysfunctional Telomeres. *Current Biology* **13**, 1549–1556 (2003).

157. Armanios, M. & Blackburn, E. H. The telomere syndromes. *Nature Reviews Genetics* **13**, 693–704 (2012).

158. Niewisch, M. R. & Savage, S. A. An update on the biology and management of dyskeratosis congenita and related telomere biology disorders. *Expert Review of Hematology* **12**, 1037–1052 (2019).

159. Buj, R. & Aird, K. M. Deoxyribonucleotide Triphosphate Metabolism in Cancer and Metabolic Disease. *Front Endocrinol (Lausanne)* **9**, 177 (2018).

160. Meuth, M., L'Heureux-Huard, N. & Trudel, M. Characterization of a mutator gene in Chinese hamster ovary cells. *Proc Natl Acad Sci U S A* **76**, 6505–6509 (1979).

161. Weinberg, G., Ullman, B. & Martin, D. W. Mutator phenotypes in mammalian cell mutants with distinct biochemical defects and abnormal deoxyribonucleoside triphosphate pools. *Proc Natl Acad Sci U S A* **78**, 2447–2451 (1981).

162. Hwang, H., Opresko, P. & Myong, S. Single-molecule real-time detection of telomerase extension activity. *Sci Rep* **4**, 6391 (2014).

163. Hardy, C. D., Schultz, C. S. & Collins, K. Requirements for the dGTP-dependent Repeat Addition Processivity of Recombinant Tetrahymena Telomerase*. *Journal of Biological Chemistry* **276**, 4863–4871 (2001).

164. Hammond, P. W. & Cech, T. R. dGTP-dependent processivity and possible template switching of euplotes telomerase. *Nucleic Acids Res* **25**, 3698–3704 (1997).

165. Doench, J. G. *et al.* Optimized sgRNA design to maximize activity and minimize off-target effects of CRISPR-Cas9. *Nat Biotechnol* **34**, 184–191 (2016).

166. Baerlocher, G. M., Vulto, I., de Jong, G. & Lansdorp, P. M. Flow cytometry and FISH to measure the average length of telomeres (flow FISH). *Nature Protocols* **1**, 2365–2376 (2006).

167. Li, W. *et al.* MAGeCK enables robust identification of essential genes from genome-scale CRISPR/Cas9 knockout screens. *Genome Biology* **15**, 554 (2014).

168. Lee, T. H. *et al.* Essential role of Pin1 in the regulation of TRF1 stability and telomere maintenance. *Nat Cell Biol* **11**, 97–105 (2009).

169. O'Connor, M. S., Safari, A., Liu, D., Qin, J. & Songyang, Z. The Human Rap1 Protein Complex and Modulation of Telomere Length *. *Journal of Biological Chemistry* **279**, 28585–28591 (2004).

170. Wang, B. *et al.* Integrative analysis of pooled CRISPR genetic screens using MAGeCKFlute. *Nat Protoc* **14**, 756–780 (2019).

171. Reichard, P. Interactions Between Deoxyribonucleotide and Dna Synthesis. *Annual Review of Biochemistry* **57**, 349–374 (1988).

172. Powell, R. D., Holland, P. J., Hollis, T. & Perrino, F. W. Aicardi-Goutieres syndrome gene and HIV-1 restriction factor SAMHD1 is a dGTP-regulated deoxynucleotide triphosphohydrolase. *J Biol Chem* **286**, 43596–43600 (2011).

173. Jamburuthugoda, V. K., Chugh, P. & Kim, B. Modification of Human Immunodeficiency Virus Type 1 Reverse Transcriptase to Target Cells with Elevated Cellular dNTP Concentrations *. *Journal of Biological Chemistry* **281**, 13388–13395 (2006).

174. Yuan, M., Breitkopf, S. B., Yang, X. & Asara, J. M. A positive/negative ion-switching, targeted mass spectrometry-based metabolomics platform for bodily fluids, cells, and fresh and fixed tissue. *Nat Protoc* **7**, 872–881 (2012).

175. Majerska, J., Feretzaki, M., Glousker, G. & Lingner, J. Transformation-induced stress at telomeres is counteracted through changes in the telomeric proteome including SAMHD1. *Life Science Alliance* **1**, (2018).

176. Daddacha, W. *et al.* SAMHD1 Promotes DNA End Resection to Facilitate DNA Repair by Homologous Recombination. *Cell Rep* **20**, 1921–1935 (2017).

177. Coquel, F. *et al.* SAMHD1 acts at stalled replication forks to prevent interferon induction. *Nature* **557**, 57–61 (2018).

178. Beloglazova, N. *et al.* Nuclease Activity of the Human SAMHD1 Protein Implicated in the Aicardi-Goutières Syndrome and HIV-1 Restriction*. *Journal of Biological Chemistry* **288**, 8101–8110 (2013).

179. Morris, E. R. *et al.* Crystal structures of SAMHD1 inhibitor complexes reveal the mechanism of water-mediated dNTP hydrolysis. *Nat Commun* **11**, 3165 (2020).

180. Xeros, N. Deoxyriboside control and synchronization of mitosis. *Nature* **194**, 682–683 (1962).

181. Bootsma, D., Budke, L. & Vos, O. Studies on synchronous division of tissue culture cells initiated by excess thymidine. *Experimental Cell Research* **33**, 301–309 (1964).

182. Lee, S. S., Bohrson, C., Pike, A. M., Wheelan, S. J. & Greider, C. W. ATM kinase is required for telomere elongation in mouse and human cells. *Cell Rep* **13**, 1623–1632 (2015).

183. Tong, A. S. *et al.* ATM and ATR Signaling Regulate the Recruitment of Human Telomerase to Telomeres. *Cell Reports* **13**, 1633–1646 (2015).

184. Sfeir, A. *et al.* Mammalian Telomeres Resemble Fragile Sites and Require TRF1 for Efficient Replication. *Cell* **138**, 90–103 (2009).

185. Yamaguchi, M., Hendrickson, E. A. & DePamphilis, M. L. DNA primase-DNA polymerase alpha from simian cells: sequence specificity of initiation sites on simian virus 40 DNA. *Molecular and Cellular Biology* **5**, 1170–1183 (1985).

186. Roth, Y.-F. Eucaryotic primase. *European Journal of Biochemistry* **165**, 473–481 (1987).

187. Cesare, A. J. & Griffith, J. D. Telomeric DNA in ALT Cells Is Characterized by Free Telomeric Circles and Heterogeneous t-Loops. *Molecular and Cellular Biology* **24**, 9948–9957 (2004).

188. Desmarais, J. A., Unger, C., Damjanov, I., Meuth, M. & Andrews, P. Apoptosis and failure of checkpoint kinase 1 activation in human induced pluripotent stem cells under replication stress. *Stem Cell Res Ther* **7**, 17 (2016).

189. Tummala, H., Walne, A. & Dokal, I. The biology and management of dyskeratosis congenita and related disorders of telomeres. *Expert Rev Hematol* **15**, 685–696 (2022).

190. Maicher, A. *et al.* Rnr1, but not Rnr3, facilitates the sustained telomerase-dependent elongation of telomeres. *PLoS Genet* **13**, e1007082 (2017).

191. Broen, J. C. A. & van Laar, J. M. Mycophenolate mofetil, azathioprine and tacrolimus: mechanisms in rheumatology. *Nat Rev Rheumatol* **16**, 167–178 (2020).

192. Meyerhans, A. *et al.* Restriction and enhancement of human immunodeficiency virus type 1 replication by modulation of intracellular deoxynucleoside triphosphate pools. *J Virol* **68**, 535–540 (1994).

193. Agarwal, S. *et al.* Telomere elongation in induced pluripotent stem cells from dyskeratosis congenita patients. *Nature* **464**, 292–296 (2010).

194. Paulsen, B. S. *et al.* Ectopic expression of RAD52 and dn53BP1 improves homology-directed repair during CRISPR–Cas9 genome editing. *Nat Biomed Eng* **1**, 878–888 (2017).

195. Warlich, E. *et al.* Lentiviral Vector Design and Imaging Approaches to Visualize the Early Stages of Cellular Reprogramming. *Mol Ther* **19**, 782–789 (2011).

196. Sanson, K. R. *et al.* Optimized libraries for CRISPR-Cas9 genetic screens with multiple modalities. *Nature Communications* **9**, 5416 (2018).

197. Nagpal, N. *et al.* Small-Molecule PAPD5 Inhibitors Restore Telomerase Activity in Patient Stem Cells. *Cell Stem Cell* **26**, 896-909.e8 (2020).

198. Lai, T.-P., Wright, W. E. & Shay, J. W. Generation of digoxigenin-incorporated probes to enhance DNA detection sensitivity. *Biotechniques* **60**, 306–309 (2016).

199. Lyčka, M. *et al.* WALTER: an easy way to online evaluate telomere lengths from terminal restriction fragment analysis. *BMC Bioinformatics* **22**, 145 (2021).

200. Herbert, B.-S., Hochreiter, A. E., Wright, W. E. & Shay, J. W. Nonradioactive detection of telomerase activity using the telomeric repeat amplification protocol. *Nat Protoc* **1**, 1583–1590 (2006).

201. Mannherz, W. TRAP Nanopore Analysis. Zenodo https://doi.org/10.5281/zenodo.7607615 (2023).

202. Wagih, O. ggseqlogo: a versatile R package for drawing sequence logos. *Bioinformatics* **33**, 3645–3647 (2017).

203. Kimura, M. & Aviv, A. Measurement of telomere DNA content by dot blot analysis. *Nucleic Acids Res* **39**, e84 (2011).

204. Greider, C. W. & Blackburn, E. H. Identification of a specific telomere terminal transferase activity in Tetrahymena extracts. *Cell* **43**, 405–413 (1985).

205. D'Aronco, G. *et al.* SAMHD1 restricts the deoxyguanosine triphosphate pool contributing to telomere stability in telomerase-positive cells. *FASEB J* **37**, e22883 (2023).

206. Mannherz, W. & Agarwal, S. Thymidine nucleotide metabolism controls human telomere length. *Nat Genet* **55**, 568–580 (2023).

207. Damm, K. *et al.* A highly selective telomerase inhibitor limiting human cancer cell proliferation. *EMBO J* **20**, 6958–6968 (2001).

208. Snetselaar, R. *et al.* Short telomere length in IPF lung associates with fibrotic lesions and predicts survival. *PLoS One* **12**, e0189467 (2017).

209. Xin, Z.-T. *et al.* Functional characterization of natural telomerase mutations found in patients with hematologic disorders. *Blood* **109**, 524–532 (2007).

210. Boyraz, B., Bellomo, C. M., Fleming, M. D., Cutler, C. S. & Agarwal, S. A novel TERC CR4/CR5 domain mutation causes telomere disease via decreased TERT binding. *Blood* **128**, 2089–2092 (2016).

211. Lewandowicz, A., Tyler, P. C., Evans, G. B., Furneaux, R. H. & Schramm, V. L. Achieving the Ultimate Physiological Goal in Transition State Analogue Inhibitors for Purine Nucleoside Phosphorylase. *Journal of Biological Chemistry* **278**, 31465–31468 (2003).

212. Kicska, G. A. *et al.* Immucillin H, a powerful transition-state analog inhibitor of purine nucleoside phosphorylase, selectively inhibits human T lymphocytes. *Proc Natl Acad Sci U S A* **98**, 4593–4598 (2001).

213. Osada, Y. *et al.* Hypouricemic effect of the novel xanthine oxidase inhibitor, TEI-6720, in rodents. *European Journal of Pharmacology* **241**, 183–188 (1993).

214. Diehl, F. F. *et al.* Nucleotide imbalance decouples cell growth from cell proliferation. *Nat Cell Biol* **24**, 1252–1264 (2022).

215. Batiuk, T. D., Schnizlein-Bick, C., Plotkin, Z. & Dagher, P. C. Guanine nucleosides and Jurkat cell death: roles of ATP depletion and accumulation of deoxyribonucleotides. *Am J Physiol Cell Physiol* **281**, C1776-1784 (2001).

216. Bjursell, G. & Reichard, P. Effects of Thymidine on Deoxyribonucleoside Triphosphate Pools and Deoxyribonucleic Acid Synthesis in Chinese Hamster Ovary Cells. *Journal of Biological Chemistry* **248**, 3904–3909 (1973).

217. Sarup, J. C. & Fridland, A. Identification of purine deoxyribonucleoside kinases from human leukemia cells: substrate activation by purine and pyrimidine deoxyribonucleosides. *Biochemistry* **26**, 590–597 (1987).

218. Abt, E. R. *et al.* Purine nucleoside phosphorylase enables dual metabolic checkpoints that prevent T cell immunodeficiency and TLR7-associated autoimmunity. *J Clin Invest* **132**, (2022).

219. Poddar, S. *et al.* Development and preclinical pharmacology of a novel dCK inhibitor, DI-87. *Biochem Pharmacol* **172**, 113742 (2020).

220. Munch-Petersen, B., Piskur, J. & Søndergaard, L. Four Deoxynucleoside Kinase Activities from Drosophila melanogaster Are Contained within a Single Monomeric Enzyme, a New Multifunctional Deoxynucleoside Kinase *. *Journal of Biological Chemistry* **273**, 3926–3931 (1998).

221. A proof-of-principle pharmacokinetic, pharmacodynamic, and clinical study with purine nucleoside phosphorylase inhibitor immucillin-H (BCX-1777, forodesine). *Blood* **106**, 4253–4260 (2005).

222. Gustafson, E. A., Schinazi, R. F. & Fingeroth, J. D. Human Herpesvirus 8 Open Reading Frame 21 Is a Thymidine and Thymidylate Kinase of Narrow Substrate Specificity That Efficiently Phosphorylates Zidovudine but Not Ganciclovir. *J Virol* **74**, 684–692 (2000).

223. Bellon, M. & Nicot, C. Regulation of Telomerase and Telomeres: Human Tumor Viruses Take Control. *JNCI: Journal of the National Cancer Institute* **100**, 98–108 (2008).

224. Gandhi, V. *et al.* A proof-of-principle pharmacokinetic, pharmacodynamic, and clinical study with purine nucleoside phosphorylase inhibitor immucillin-H (BCX-1777, forodesine). *Blood* **106**, 4253–4260 (2005).

225. Al-Kali, A., Gandhi, V., Ayoubi, M., Keating, M. & Ravandi, F. Forodesine: review of preclinical and clinical data. *Future Oncology* **6**, 1211–1217 (2010).

226. Roake, C. M. & Artandi, S. E. Regulation of human telomerase in homeostasis and disease. *Nat Rev Mol Cell Biol* **21**, 384–397 (2020).

227. Westin, E. R. *et al.* Telomere restoration and extension of proliferative lifespan in dyskeratosis congenita fibroblasts. *Aging Cell* **6**, 383–394 (2007).

228. Fu, D. & Collins, K. Distinct Biogenesis Pathways for Human Telomerase RNA and H/ACA Small Nucleolar RNAs. *Molecular Cell* **11**, 1361–1372 (2003).

229. Venteicher, A. S., Meng, Z., Mason, P. J., Veenstra, T. D. & Artandi, S. E. Identification of ATPases pontin and reptin as telomerase components essential for holoenzyme assembly. *Cell* **132**, 945–957 (2008).

230. Reilly, C. R. *et al.* The clinical and functional effects of TERT variants in myelodysplastic syndrome. *Blood* **138**, 898–911 (2021).

231. Shalem, O. *et al.* Genome-Scale CRISPR-Cas9 Knockout Screening in Human Cells. *Science* **343**, 84–87 (2014).

232. Bertoli, A., Franco, M., Balzarini, J., Johansson, M. & Karlsson, A. Altered deoxyribonucleotide pools in T-lymphoblastoid cells expressing the multisubstrate nucleoside kinase of Drosophila melanogaster. *The FEBS Journal* **272**, 3918–3928 (2005).

233. Jády, B. E., Richard, P., Bertrand, E. & Kiss, T. Cell cycle-dependent recruitment of telomerase RNA and Cajal bodies to human telomeres. *Mol Biol Cell* **17**, 944–954 (2006).

234. Tomlinson, R. L., Ziegler, T. D., Supakorndej, T., Terns, R. M. & Terns, M. P. Cell cycle-regulated trafficking of human telomerase to telomeres. *Mol Biol Cell* **17**, 955–965 (2006).

235. Flynn, R. L. & Zou, L. ATR: a master conductor of cellular responses to DNA replication stress. *Trends in Biochemical Sciences* **36**, 133–140 (2011).

236. Pan, X. *et al.* FANCM, BRCA1, and BLM cooperatively resolve the replication stress at the ALT telomeres. *PNAS* **114**, E5940–E5949 (2017).

237. Rivera, T., Haggblom, C., Cosconati, S. & Karlseder, J. A balance between elongation and trimming regulates telomere stability in stem cells. *Nat Struct Mol Biol* **24**, 30–39 (2017).

238. Zhang, T. *et al.* Looping-out mechanism for resolution of replicative stress at telomeres. *EMBO reports* **18**, 1412–1428 (2017).

239. Baranovskiy, A. G. *et al.* Structural basis for inhibition of DNA replication by aphidicolin. *Nucleic Acids Research* **42**, 14013–14021 (2014).

240. Darzynkiewicz, Z., Halicka, H. D. & Zhao, H. Cell synchronization by inhibitors of DNA replication induces replication stress and DNA damage response: analysis by flow cytometry. *Methods Mol Biol* **761**, 85–96 (2011).

241. Pedrali-Noy, G. *et al.* Synchronization of HeLa cell cultures by inhibition of DNA polymerase a with aphidicolin. *Nucleic Acids Research* **8**, 377–387 (1980).

242. Buisson, R., Boisvert, J. L., Benes, C. H. & Zou, L. Distinct but Concerted Roles of ATR, DNA-PK, and Chk1 in Countering Replication Stress during S Phase. *Mol Cell* **59**, 1011–1024 (2015).

243. Le, T. M. *et al.* ATR inhibition facilitates targeting of leukemia dependence on convergent nucleotide biosynthetic pathways. *Nature Communications* **8**, 241 (2017).

244. Abt, E. R. *et al.* Reprogramming of nucleotide metabolism by interferon confers dependence on the replication stress response pathway in pancreatic cancer cells. *Cell Reports* **38**, 110236 (2022).

245. Alterations of DNA and Chromatin Structures at Telomeres and Genetic Instability in Mouse Cells Defective in DNA Polymerase α - PMC. https://www.ncbi.nlm.nih.gov/pmc/articles/PMC1316980/.

246. Bellelli, R. & Boulton, S. J. Spotlight on the Replisome: Aetiology of DNA Replication-Associated Genetic Diseases. *Trends in Genetics* **37**, 317–336 (2021).

247. Greenberg, A. & Simon, I. S Phase Duration Is Determined by Local Rate and Global Organization of Replication. *Biology* **11**, 718 (2022).

248. Clifford, R. *et al.* SAMHD1 is mutated recurrently in chronic lymphocytic leukemia and is involved in response to DNA damage. *Blood* **123**, 1021–1031 (2014).

249. Gramberg, T. *et al.* Restriction of diverse retroviruses by SAMHD1. *Retrovirology* **10**, 26 (2013).

250. Coggins, S. A., Mahboubi, B., Schinazi, R. F. & Kim, B. SAMHD1 Functions and Human Diseases. *Viruses* **12**, 382 (2020).

251. Deutschmann, J. & Gramberg, T. SAMHD1 … and Viral Ways around It. *Viruses* **13**, 395 (2021).

252. Laguette, N. *et al.* SAMHD1 is the dendritic- and myeloid-cell-specific HIV-1 restriction factor counteracted by Vpx. *Nature* **474**, 654–657 (2011).

253. Zhang, K., Lv, D.-W. & Li, R. Conserved Herpesvirus Protein Kinases Target SAMHD1 to Facilitate Virus Replication. *Cell Rep* **28**, 449-459.e5 (2019).

254. Rice, G. I. *et al.* Mutations involved in Aicardi-Goutières syndrome implicate SAMHD1 as regulator of the innate immune response. *Nat Genet* **41**, 829–832 (2009).

255. Bellon, M. & Nicot, C. Telomere Dynamics in Immune Senescence and Exhaustion Triggered by Chronic Viral Infection. *Viruses* **9**, 289 (2017).

256. O'Bryan, J. M., Potts, J. A., Bonkovsky, H. L., Mathew, A. & Rothman, A. L. Extended Interferon-Alpha Therapy Accelerates Telomere Length Loss in Human Peripheral Blood T Lymphocytes. *PLoS One* **6**, e20922 (2011).

257. Xu, D. *et al.* Interferon alpha down-regulates telomerase reverse transcriptase and telomerase activity in human malignant and nonmalignant hematopoietic cells. *Blood* **96**, 4313–4318 (2000).

258. Crow, Y. J. & Stetson, D. B. The type I interferonopathies: 10 years on. *Nat Rev Immunol* **22**, 471–483 (2022).

259. Hu, S. *et al.* SAMHD1 Inhibits LINE-1 Retrotransposition by Promoting Stress Granule Formation. *PLOS Genetics* **11**, e1005367 (2015).

260. Rice, G. I. *et al.* Reverse-Transcriptase Inhibitors in the Aicardi–Goutières Syndrome. *New England Journal of Medicine* **379**, 2275–2277 (2018).

261. Crow, Y. J. & Manel, N. Aicardi–Goutières syndrome and the type I interferonopathies. *Nat Rev Immunol* **15**, 429–440 (2015).

262. Vértessy, B. G. & Tóth, J. Keeping Uracil Out of DNA: Physiological Role, Structure and Catalytic Mechanism of dUTPases. *Acc. Chem. Res.* **42**, 97–106 (2009).

263. Ng, B. G. *et al.* Biallelic mutations in CAD, impair de novo pyrimidine biosynthesis and decrease glycosylation precursors. *Hum Mol Genet* **24**, 3050–3057 (2015).

264. Martin, D. S. *et al.* An overview of thymidine. *Cancer* **45**, 1117–1128 (1980).

265. Saada, A. *et al.* Mutant mitochondrial thymidine kinase in mitochondrial DNA depletion myopathy. *Nat Genet* **29**, 342–344 (2001).

266. Akman, H. O. *et al.* Thymidine kinase 2 (H126N) knockin mice show the essential role of balanced deoxynucleotide pools for mitochondrial DNA maintenance. *Hum Mol Genet* **17**, 2433–2440 (2008).

267. Deoxypyrimidine monophosphate bypass therapy for thymidine kinase 2 deficiency. *EMBO Molecular Medicine* **6**, 1016–1027 (2014).

268. Lopez-Gomez, C. *et al.* Deoxycytidine and deoxythymidine treatment for thymidine kinase 2 deficiency. *Ann Neurol* **81**, 641–652 (2017).

269. Blázquez-Bermejo, C. *et al.* Age-related metabolic changes limit efficacy of deoxynucleoside-based therapy in thymidine kinase 2-deficient mice. *EBioMedicine* **46**, 342–355 (2019).

270. Hirano, M. *et al.* Regulatory environment for novel therapeutic development in mitochondrial diseases. *J Inherit Metab Dis* **44**, 292–300 (2021).

271. Nishino, I., Spinazzola, A. & Hirano, M. Thymidine Phosphorylase Gene Mutations in MNGIE, a Human Mitochondrial Disorder. *Science* **283**, 689–692 (1999).

272. Spinazzola, A. *et al.* Altered Thymidine Metabolism Due to Defects of Thymidine Phosphorylase *. *Journal of Biological Chemistry* **277**, 4128–4133 (2002).

273. González-Vioque, E., Torres-Torronteras, J., Andreu, A. L. & Martí, R. Limited dCTP availability accounts for mitochondrial DNA depletion in mitochondrial neurogastrointestinal encephalomyopathy (MNGIE). *PLoS Genet* **7**, e1002035 (2011).

274. Mita, P. *et al.* LINE-1 protein localization and functional dynamics during the cell cycle. *eLife* **7**, e30058.

275. Davenne, T. *et al.* SAMHD1 Limits the Efficacy of Forodesine in Leukemia by Protecting Cells against the Cytotoxicity of dGTP. *Cell Reports* **31**, 107640 (2020).

276. Zhang, S. M. *et al.* Identification and evaluation of small-molecule inhibitors against the dNTPase SAMHD1 via a comprehensive screening funnel. 2023.01.17.524275 Preprint at https://doi.org/10.1101/2023.01.17.524275 (2023).

277. Krishnan, S. *et al.* Long Term Expression of Drosophila melanogaster Nucleoside Kinase in Thymidine Kinase 2-deficient Mice with No Lethal Effects Caused by Nucleotide Pool Imbalances. *J Biol Chem* **289**, 32835–32844 (2014).

278. Krishnan, S. *et al.* Transgene Expression of Drosophila melanogaster Nucleoside Kinase Reverses Mitochondrial Thymidine Kinase 2 Deficiency♦. *J Biol Chem* **288**, 5072–5079 (2013).

279. Jacobs, F. M. *et al.* An evolutionary arms race between KRAB zinc finger genes 91/93 and SVA/L1 retrotransposons. *Nature* **516**, 242–245 (2014).

280. Daugherty, M. D. & Malik, H. S. Rules of engagement: molecular insights from host-virus arms races. *Annu Rev Genet* **46**, 677–700 (2012).

281. Laguette, N. *et al.* Evolutionary and Functional Analyses of the Interaction between the Myeloid Restriction Factor SAMHD1 and the Lentiviral Vpx Protein. *Cell Host Microbe* **11**, 205–217 (2012).

282. Monit, C. *et al.* Positive selection in dNTPase SAMHD1 throughout mammalian evolution. *Proceedings of the National Academy of Sciences* **116**, 18647–18654 (2019).

283. Lim, E. S. *et al.* The ability of primate lentiviruses to degrade the monocyte restriction factor SAMHD1 preceded the birth of the viral accessory protein Vpx. *Cell Host Microbe* **11**, 194–204 (2012).

284. SAMHD1 Inhibits LINE-1 Retrotransposition by Promoting Stress Granule Formation | PLOS Genetics. https://journals.plos.org/plosgenetics/article?id=10.1371/journal.pgen.1005367.

285. Kazazian, H. H. & Moran, J. V. Mobile DNA in Health and Disease. *New England Journal of Medicine* **377**, 361–370 (2017).

286. Burns, K. H. Repetitive DNA in disease. *Science* **376**, 353–354 (2022).

287. Gentry, G. A. Viral thymidine kinases and their relatives. *Pharmacol Ther* **54**, 319–355 (1992).

288. Hollenbaugh, J. A. *et al.* Host Factor SAMHD1 Restricts DNA Viruses in Non-Dividing Myeloid Cells. *PLoS Pathog* **9**, e1003481 (2013).

289. Nakamura, T. M. & Cech, T. R. Reversing Time: Origin of Telomerase. *Cell* **92**, 587–590 (1998).

290. Dlakić, M. & Mushegian, A. Prp8, the pivotal protein of the spliceosomal catalytic center, evolved from a retroelement-encoded reverse transcriptase. *RNA* **17**, 799–808 (2011).

Appendix

Supplementary Figures

Figure S1. Telomere length CRISPR/Cas9 screening using flow-FISH. a-c. Histogram of GFP fluorescence from (**a**) K562 cells; (**b**) K562 cells transduced with the pXPR-011 vector which expresses EGFP and a gRNA targeting EGFP; (**c**) K562 cells expressing Cas9 and transduced with the pXPR-011 vector, 13 days post transduction. Presence of GFP-negative cells in (**c**) indicates functional Cas9 nuclease activity. **d-g**. Representative gating strategy for flow-FISH telomere length screening. Data from nucleotide metabolism library infected K562 cells, replicate 1. Cells are gated to enrich for single cells (**e**,**f**), and gated on low DAPI fluorescence to enrich for cells with 2N genome copy number and aid in identifying gRNAs which promote telomere elongation independent from changes in total DNA content (**g**) followed by gating on high and low TelC-Alexa 647 probe fluorescence populations. Gates adjusted to maintain approximately 5% of cells throughout the duration of the sort. **h,i**. gRNA enrichment in high (**h**) and low (**i**) telomere fluorescence populations compared to unsorted populations from K562 cells expressing Cas9 which were cultured for 49 days followed by flow-FISH sorting of the 5% of cells with the highest and lowest telomere population in two replicates performed on consecutive days. Enrichment score calculated using the MAGeCK RRA software. Known telomere length regulating genes indicated with orange dots, other genes indicated are involved in nucleotide metabolism. j. KEGG pathway enrichment analysis performed on the genes with gRNAs enriched in the sorted short telomere population (**i**), analysis performed using the MAGeCKFlute software package (see Methods). Plot includes top enriched KEGG terms, plotting -log10 adjusted *P* value, which includes q-value estimation for false discovery rate control, dot size indicates number of genes identified in that pathway out of the short telomere enriched genes.

Figure S1. (Continued)

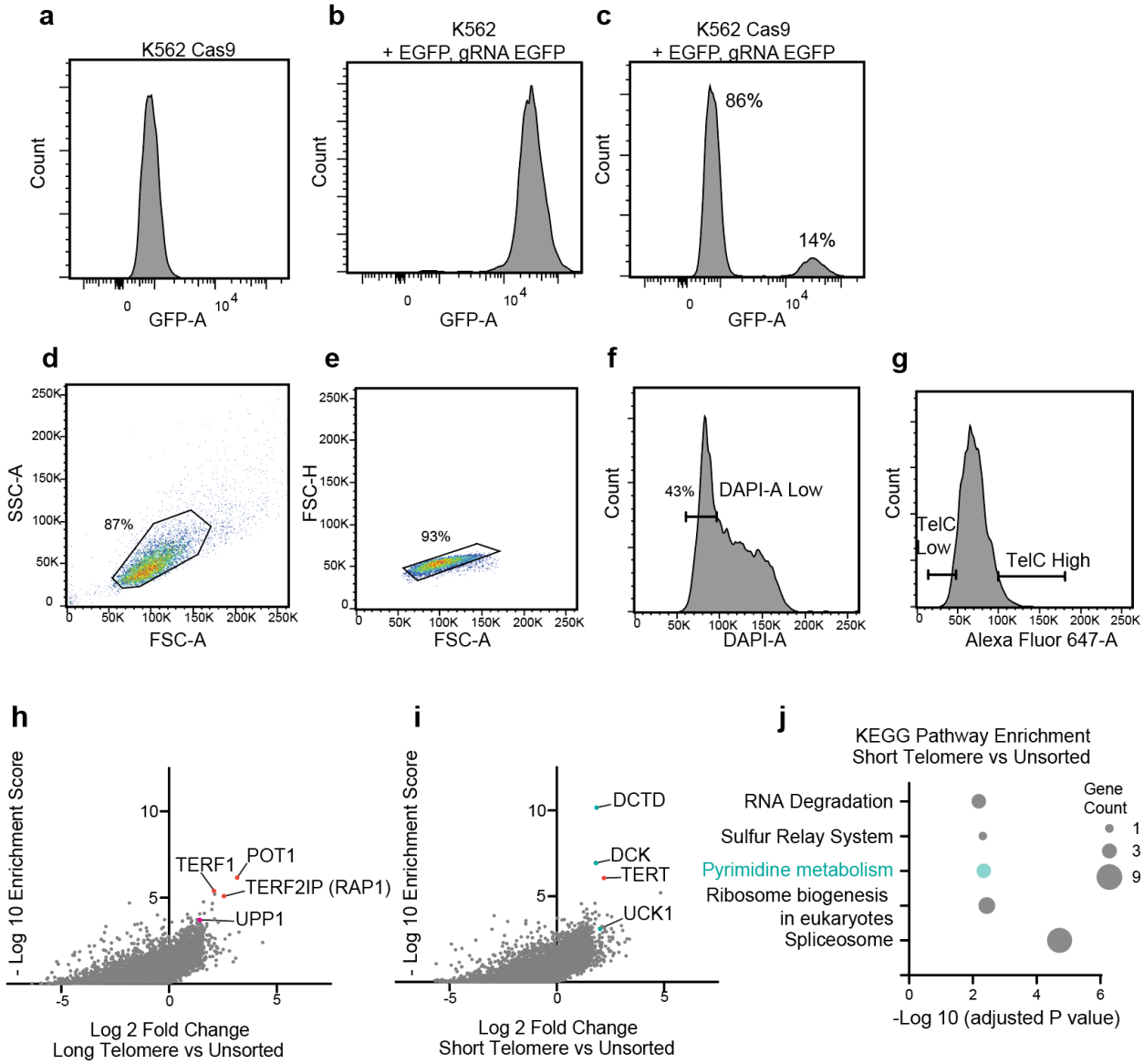


Figure S2. Characterization of *TERC*-null 293T cells. a. Schematic of *TERC* genotypes in *TERC*-null 293T cells generated by genome-editing, including a deletion of the essential box H domain on one allele, and an 821 bp *TERC* locus deletion which encompasses 74 bp from the 3' end of *TERC* on the other allele. **b**. Ethidium bromide stained agarose gel of PCR of 293T or 293T *TERC*-null genomic DNA using primers flanking the deletions indicated in **a**. **c**. Sanger sequencing of gel-purified PCR products from the (1) higher molecular weight bands in **b**, indicating that the non-deleted allele lacks the box H domain, and (2) the Δ821 bp deleted band from **b**, with trace file showing the deletion junction in a genomic context. **d**. RT-qPCR of *TERC* expression relative to *GAPDH* in wildtype 293T and *TERC*-null 293T cells, performed in technical triplicate, *P* value calculated by unpaired *t* test. Data are shown are means and error bars indicate standard deviation. **e**. Telomerase activity measured via the TRAP assay, performed on 5-fold serial dilutions of lysates. HI indicates heat inactivated lysate. IC indicates the internal control product. **f**. TRF of wildtype and *TERC*-null 293T cells. Days of culture were recorded beginning approximately two months after gene editing. Telomere length gradually declines with passage until cells universally senesce. **g**. Quantification of **f**, line fit using simple linear regression. Data presented in this Figure are the results of single experiments unless otherwise indicated.

Figure S2. (Continued)

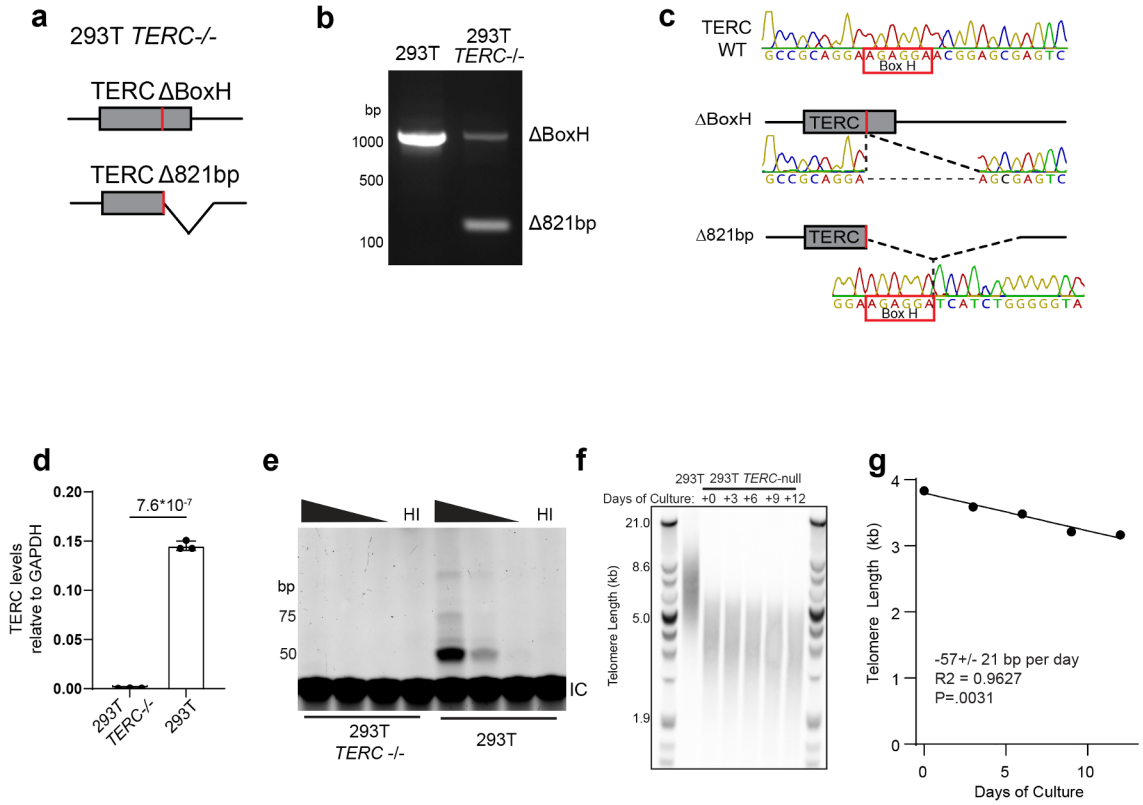


Figure S3. dT nucleotide metabolism perturbations and their effects on telomere length and polar metabolite homeostasis. **a**. TRF of 293T cells treated with the indicated dose of dT for 10 days. The 0μM dT lane is the same image as the rightmost lane in **Fig. 2-2f**. Manufacturer 2 = Santa Cruz Biotechnology; manufacturer 3 = MP Biomedicals. **b,c**. Genomic DNA from 293T or K562 cells manipulated with the indicated sgRNA(s) followed by dT treatment was PCR amplified using primers specific to the *TK1* (**a**) or *TK2* (**b**) genomic loci. Amplicons were separated by agarose gel electrophoresis, demonstrating the three pooled gRNAs targeting either *TK1* or *TK2* generated on-target genomic deletions. First lane is a molecular weight marker. PCR products were Sanger sequenced and editing efficiency was quantified using the Synthego ICE algorithm (shown as "Knockout Score"). The model fit of the ICE quantification is also displayed. Genomic DNA used in this figure was the same as the DNA used to generate **Fig. 2-3b-e**. **d**. Quantification of **Fig. 2-3b,d**, *n*=3 biological replicates for each cell line, *P* values calculated using paired two sided t test. **e**. Polar metabolite profiling by liquid chromatography mass spectrometry of 293T cells treated with or without 100μM dT for 24 hours, performed in biological triplicate, *P* value calculated by unpaired two-sided student's *t* test of average signal intensity in treatment vs control samples, nucleotide and nucleoside species detected in all samples displayed. Note: dGTP not detected. **f**. TRF of 293T cells treated with the indicated compound for 10 days. dU= deoxyuridine. **g**. Detection of CRISPR/Cas9 editing of TYMS locus using TYMS specific primers, performed as in **b-c**. Genomic DNA used was the same as the DNA used to generate data in figures **Fig. 2-3 g-j**. Data in **d** and **e** are shown as means, and error bars indicate standard deviation.

Figure S3. (Continued)

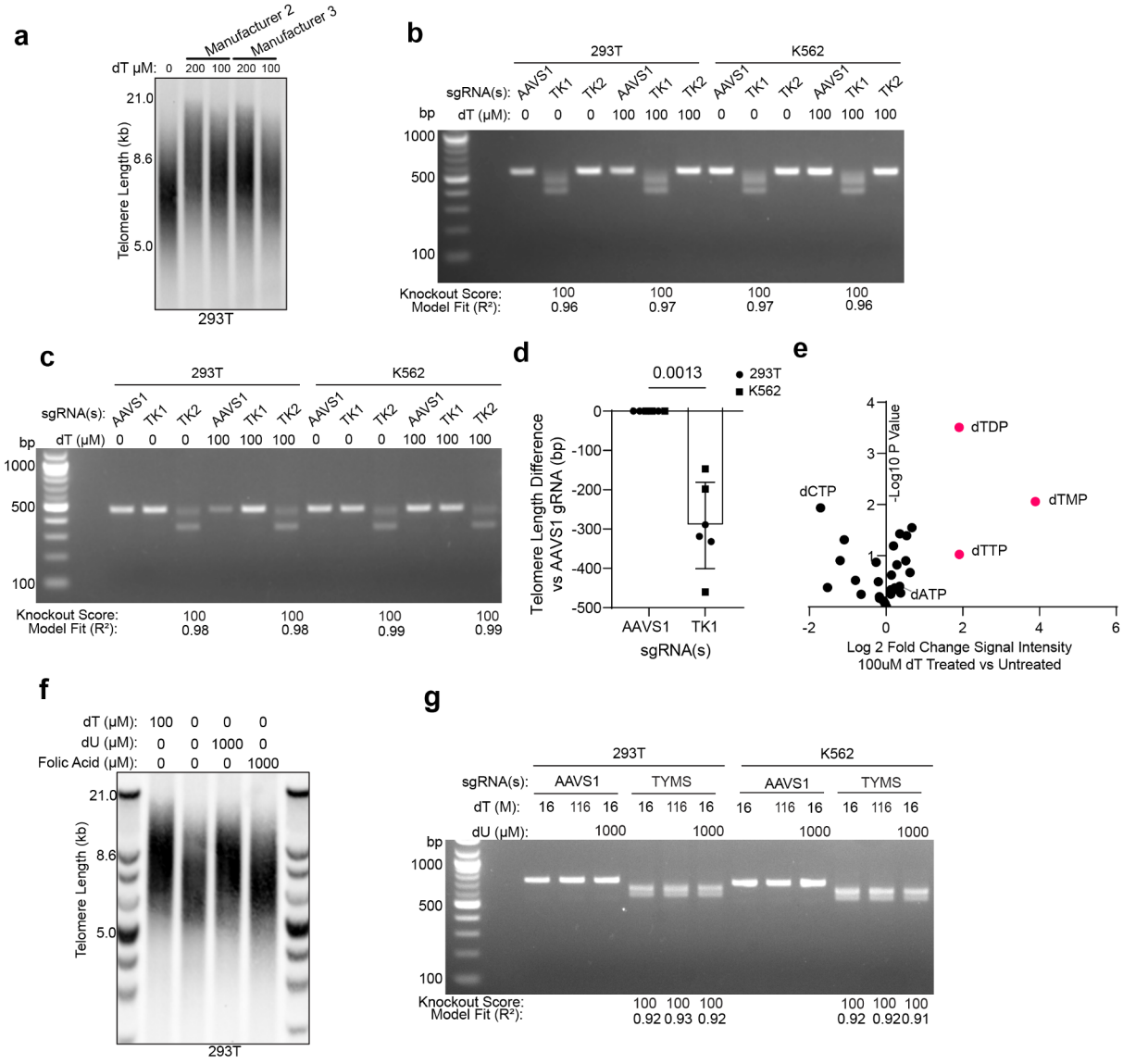


Figure S4. Manipulation of SAMHD1 levels by CRISPR/Cas9, shRNA, and lentiviral expression. a. Immunoblot of 293T and K562 cells electroporated with Cas9 and the indicated gRNA(s) using primary antibodies against SAMHD1 or β-Actin, corresponding to cell lines evaluated in **Figure 2-4b**. **b**. Immunoblot of K562 cells transduced with vectors expressing the indicated shRNA, corresponding to cell lines evaluated in **Figure 2-4c**. **c**. qRT-PCR of *SAMHD1* expression compared to β-Actin, performed in technical triplicate. Means of the replicates are shown. **d**. Immunoblot of 293T cells transduced with vectors expressing the indicated shRNA. **e**. TRF of indicated cell lines transduced with the indicated shRNA and cultured for 15 days, and quantification of the TRF using the WALTER webtool. The boxplot displays the 75th, 50th and 25th percentile molecular weight of the telomere signal distribution in the TRF blot. **f**. Immunoblot of 293T cells transduced with vectors to overexpress either EGFP or the indicated SAMHD1 variant and treated with the indicated dose of dT, corresponding to cell lines evaluated in **Figure 2-4i-j**. Data presented in this Figure are the results of single experiments unless otherwise stated.

Figure S4. (Continued)

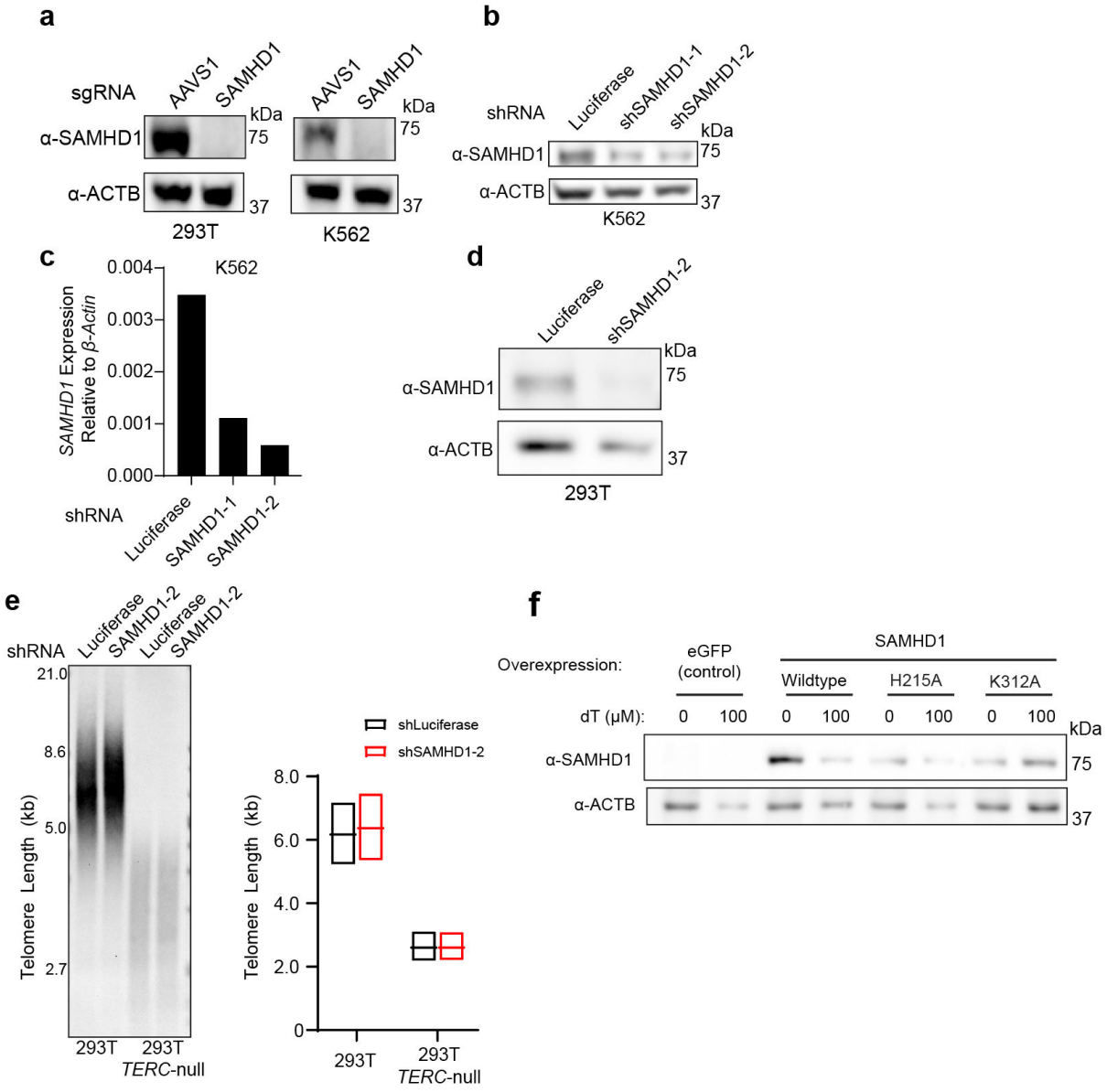


Figure S5.

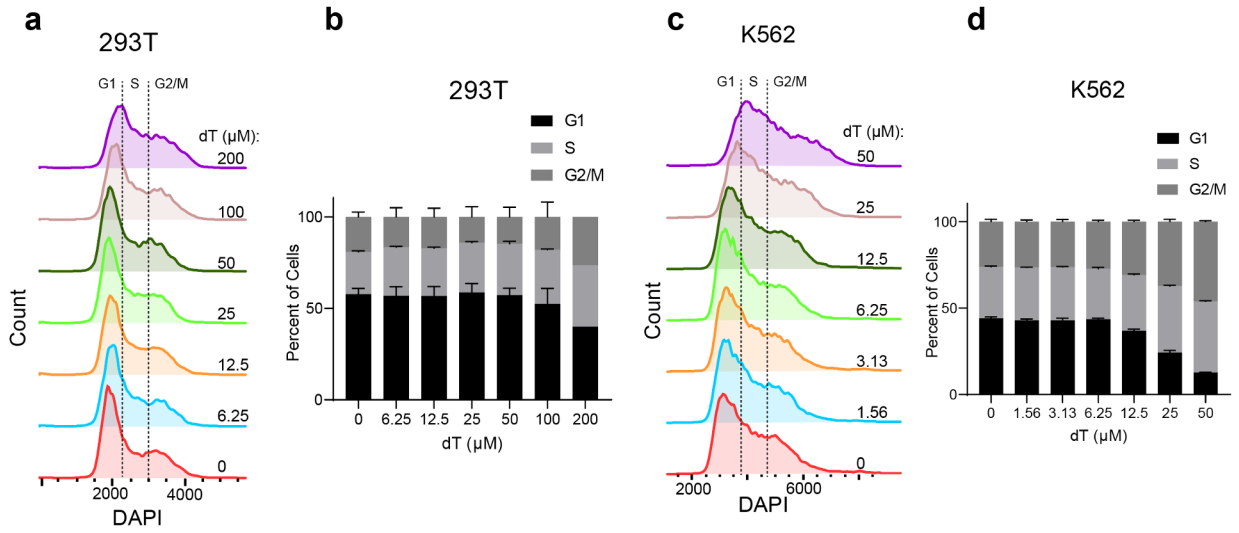


Figure S5. Cell cycle assessment of cells treated with dT a-d. DAPI staining of 293T (**a**,**b**) and K562 (**c**,**d**) cells treated with the indicated of dose of dT for 7 or 8 days respectively, measured by flow-cytometry, plotted as histograms of DAPI intensity, displaying representative samples from each treatment arm (**a,c**), and the percentage of cells in different stages of the cell cycle (**b,d**) gated based on the lines drawn on the histogram, gates determined based on untreated samples, *n*=2 biological replicates for 293T cells treated with 200μM dT and *n*=3 biological replicates for all other conditions, data presented are means, error bars indicate standard deviation.

Figure S6. Evaluation of telomere length and cell cycle progression changes from treatment with dT, aphidicolin, 5FU, or hydroxyurea. a. TRF Southern blot of 293T cells treated with the indicated doses of aphidicolin and hydroxyurea for 10 days. **b**. TRF Southern blot of 293T *TERC*-null cells transfected with TERT in addition to the indicated vector, cultured for 18 hours, then treated with the indicated dose of dT for 30 hours. **c**. TRF Southern blot of 293T *TERC*-null cells transfected with TERT in addition to the indicated vector, cultured for 18 hours, then treated with the indicated dose of dT for two days. **d**. TRF Southern blot of 293T TERC-null cells transfected with the indicated expression vectors, cultured for 18 hours, then treated with the indicated dose of dT for five days. **e-h**. Cell cycle analysis by DAPI staining and flow cytometry of 293T TERC null cells transfected with TERC and TERT expression vectors, cultured for 18 hours, then treated

Figure S6. (Continued)

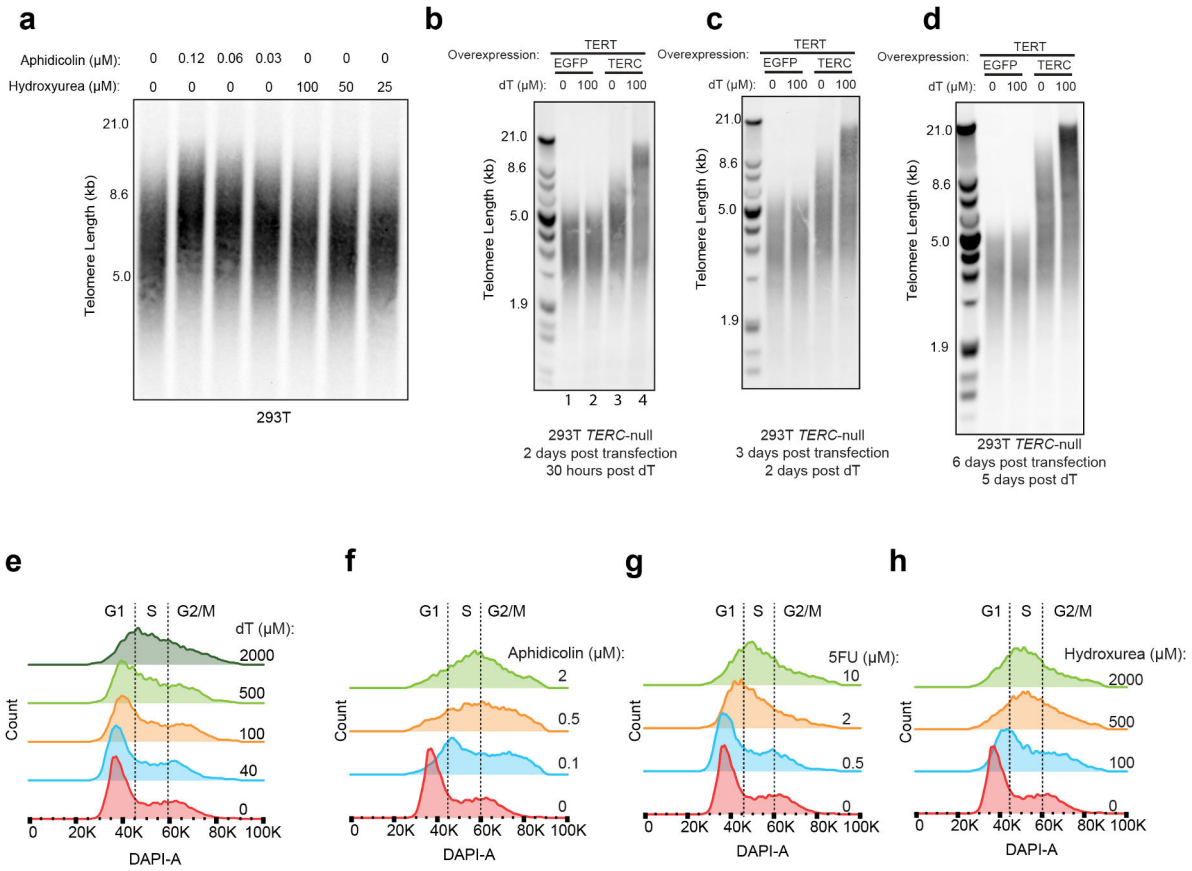


Figure S7. T-Free Telomerase is sensitive to dT nucleotide manipulations a. Representative modified TRAP assay performed on super- telomerase extracts using the indicated dose of dTTP and physiologic levels of dATP, dCTP and dGTP (See Methods). **b**. Quantification of **a**, *n*=2 biological replicates. **c**. GGAAAG TRAP assay performed on lysates from 293T *TERC*-null cells overexpressing T-free super-telomerase demonstrates linearity between cell input amount and telomerase signal. Fivefold serial dilutions performed. HI, heat inactivated. **d**. Quantification of lanes 1-3 from **c**. **e**. Representative modified GGAAAG TRAP assay performed on super telomerase extracts generated using the indicated TERC vector. Assay performed with the indicated dose of dTTP and physiologic levels of dATP, dCTP and dGTP (see Methods), HI, heat inactivated. **f**. Quantification of **e**, using two-sided unpaired student's *t* test, *n*=3 biological replicates. **g**. Representative modified GGAAAG TRAP assay performed on T-free super-telomerase extracts supplemented with the indicated dose of dTTP and physiologic levels of dATP and dGTP. **h**. Quantification of **g** as in **f**, *n*=3 biological replicates. **i**. Diagram of GGAAAG TRAP product sequencing and analysis strategy. Note * indicates T's encoded by the partially complementary reverse primer, preventing analysis of base composition in that portion of the read. **j**. Quantification of base pair composition of representative GGAAAG TRAP products from **g** with 0μM or 25μM dTTP, by nanopore sequencing (see Methods). Bits of information calculated using Shannon entropy, and plotted using ggseqlogo. **k**. Quantification of base pair composition of GGAAAG TRAP products from **g** using nanopore sequencing (see Methods). *P* value calculated using two-sided student's *t* test. *n*=3 biological replicates. **l**. Quantification of **Fig. 2-7d**, plotting the signal in the indicated telomerase product repeat relative to the signal of the corresponding repeat in the lane without dTTP added, normalized for loading (see Methods).

Figure S7. (Continued)

m. TRF Southern blot of 293T *TERC*-null cells transfected with TERT in addition to the indicated vector, cultured for 18 hours, then treated with the indicated dose of dT for 30 hours, probed with a GGTTAG complementary probe. Lanes 1-4 are the same blot shown in **Figure S6b**. **n**. Blot from **m** was stripped and re-probed with a probe complementary to the GGAAAG repeat. **o**. Slot blot of DNA from 293T *TERC*-null cells overexpressing EGFP and TERT, showing linear relationship between DNA input and signal, rows are technical triplicates. **p**. Quantification of **o**. **q**. Slot blot of DNA from 293T *TERC*-null cells overexpressing T-free super telomerase, rows are technical triplicates. **r**. Quantification of **q**. **s**. Slot blot of DNA from 293T-TERC null cells transfected with TERT and TERC, cultured for 18 hours, then treated with dT as indicated for 30 hours. Denatured DNA for each sample was split and loaded onto parallel blots which were probed for the indicated target. Performed in technical triplicate. **t**. Quantification of **s**, *P* values calculated with one way ANOVA using Dunnett's multiple comparisons test for each probe. For **b**,**d**,**f**,**h**,**k**,**p**,**r**, and **t**, the mean of the data is presented and error bars indicate s.d., ns = $P>0.05$.

Figure S7. (Continued)

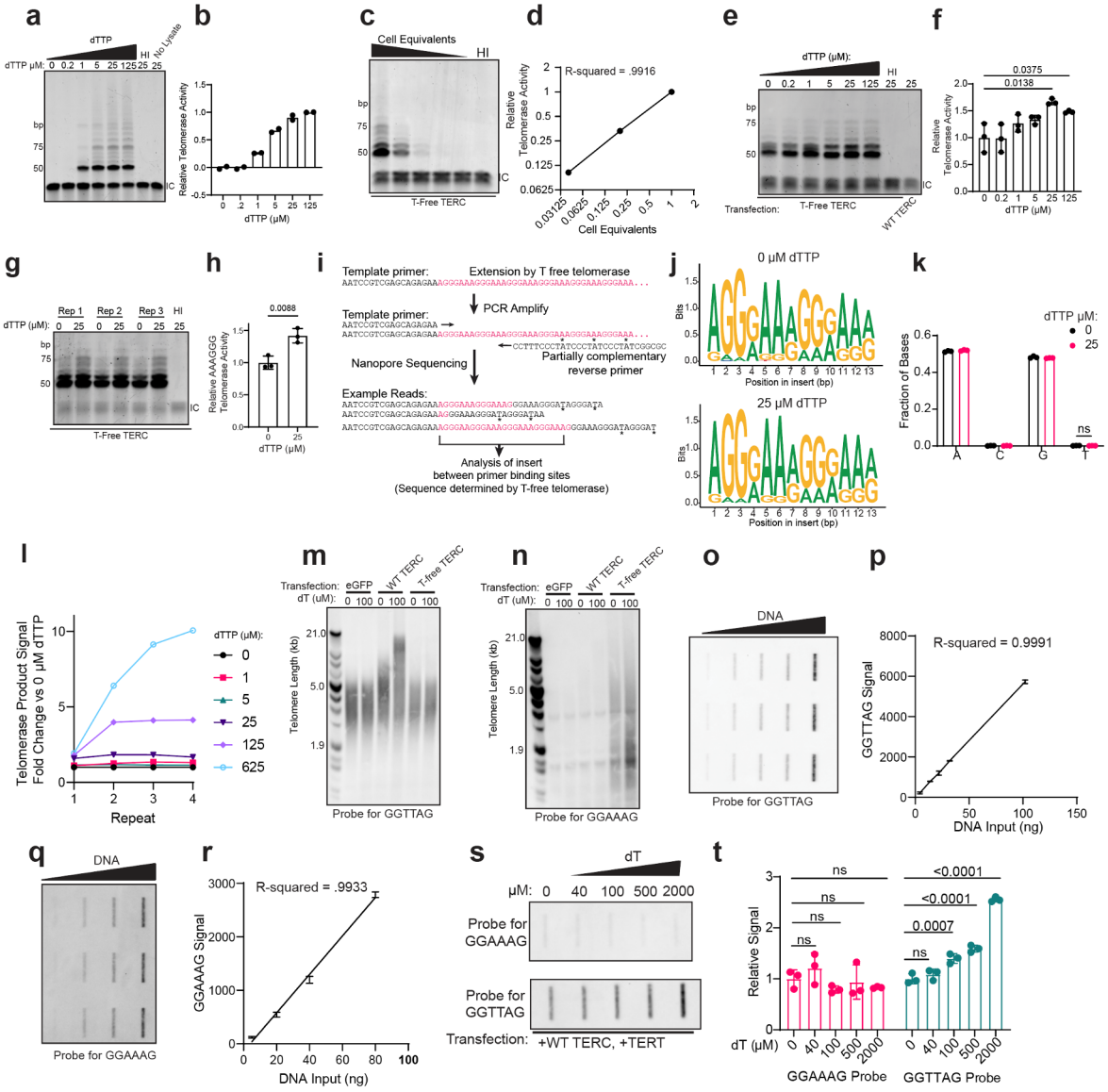


Figure S8. T-free telomerase products accumulate extrachromosomally. a. TRF Southern blot of 293T *TERC*-null cells transfected with vectors encoding TERT and T-free TERC, cultured for 18 hours, then treated with the indicated dose of dT for 30 hours, and probed with a GGAAAG complementary probe. DNA was treated with RsaI/HinfI, ExoI, and Mung Bean Nuclease (MBN) as indicated and gel purified to enrich for high molecular weight DNA fragments as indicated. **b.** Right from a displayed with higher exposure. **c.** Image of ethidium bromide signal of corresponding agarose gel from **a**.

Figure S8. (Continued)

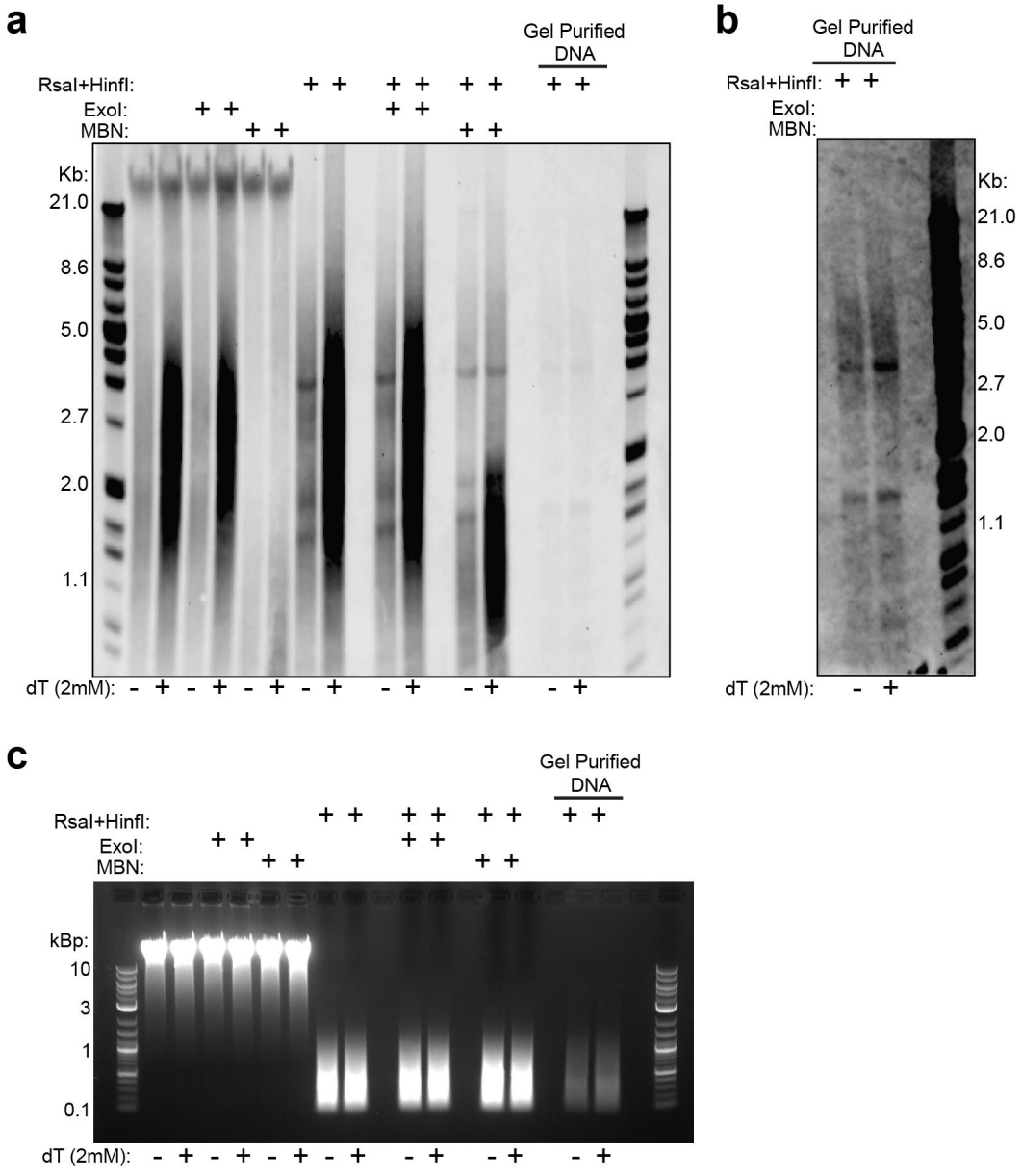


Figure S9. Effects of dT on iPSC cell cycle progression and replication stress signaling. **a**. Cell cycle analysis of wildtype iPSCs cultured in the indicated of dose of dT for 24 hours, measured by DAPI staining and flow cytometry, displayed as histograms of DAPI intensity, *n*=2 biological replicates, the mean of the replicates is presented. **b**. Representative histograms of DAPI signal for cells in **a**. Gates defined based on untreated cells. **c**. Immunoblot of cells treated as in **a**, all images of the same membrane blotted with the indicated primary antibodies. UV treated cells used as a positive control. Blot shows the results from a single experiment.

Figure S9. (Continued)

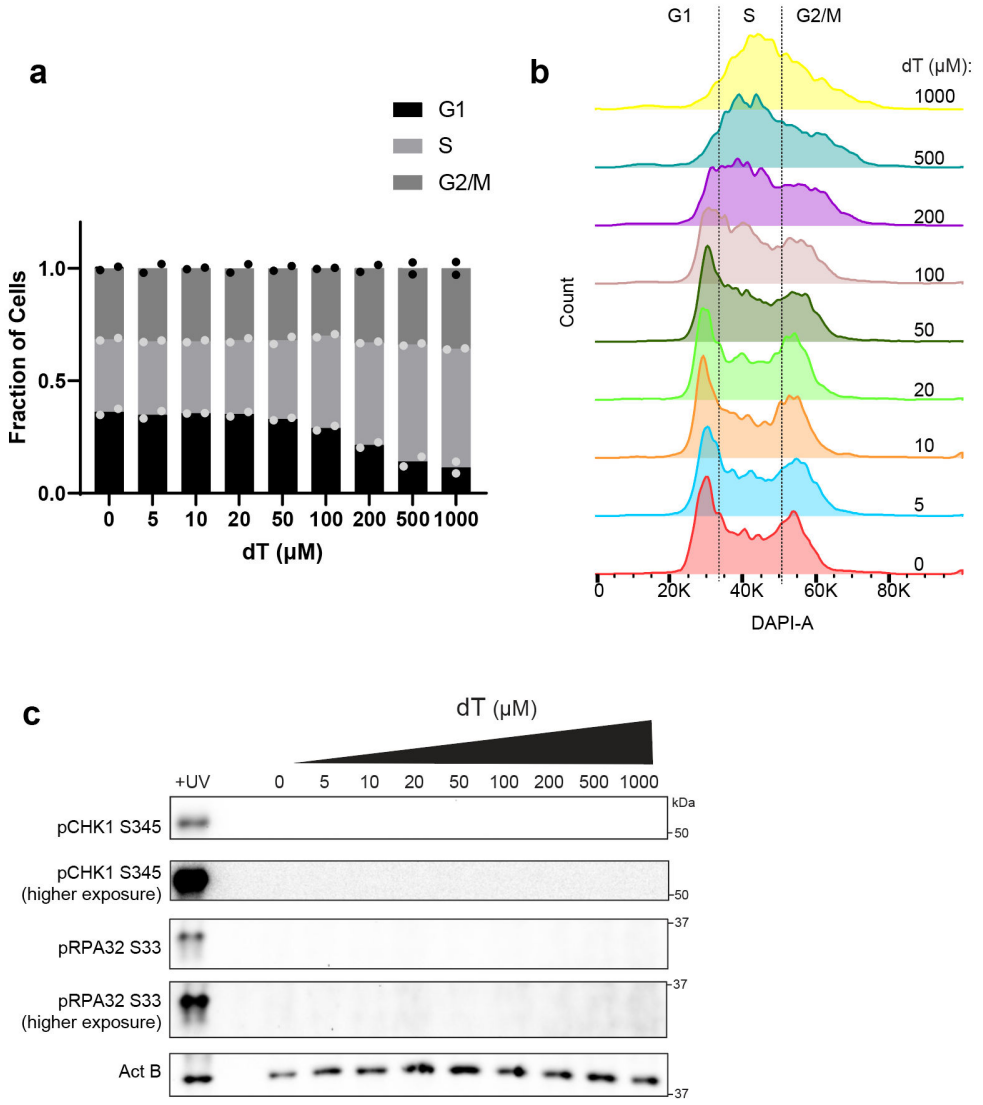


Figure S10.

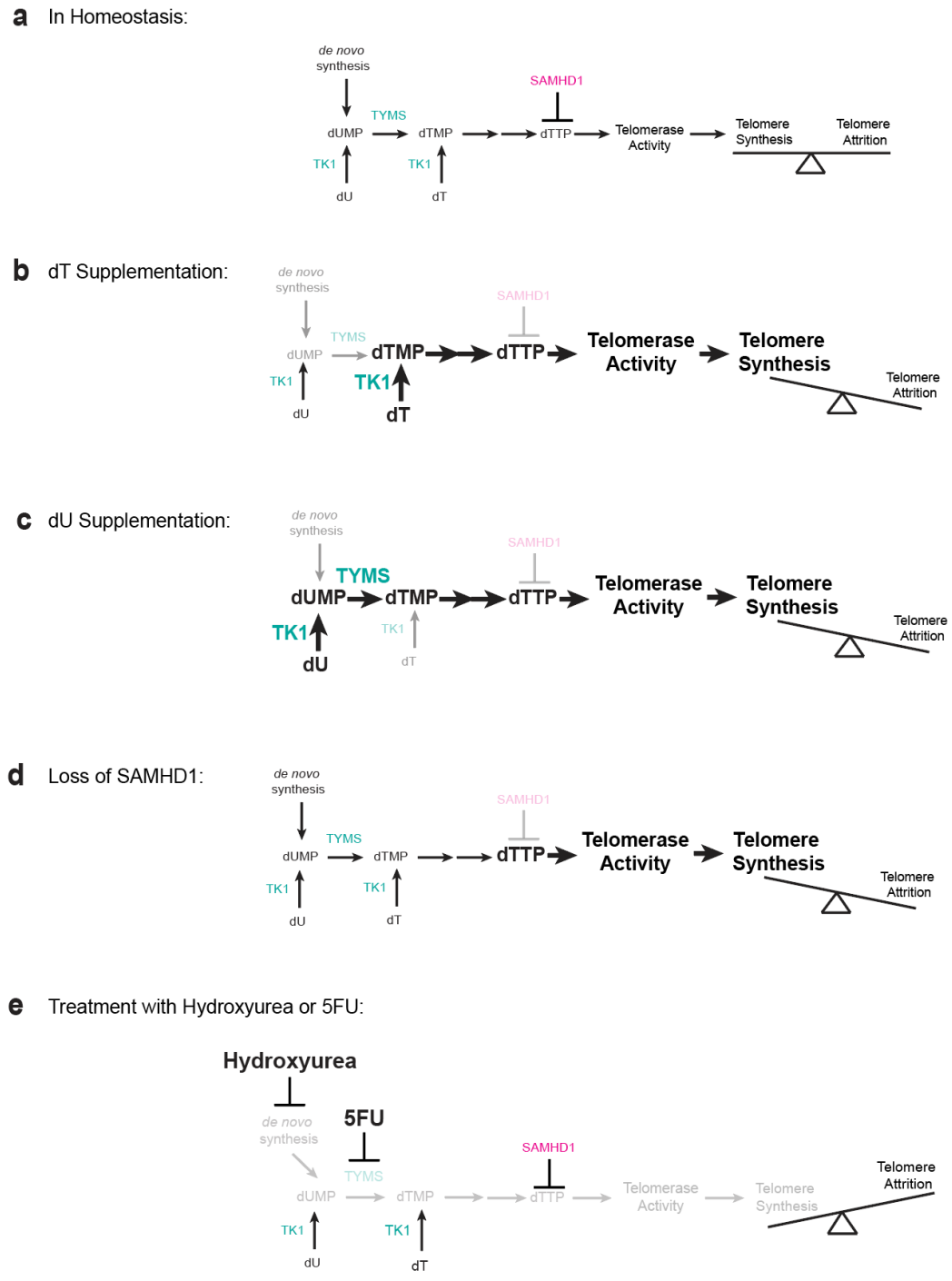


Figure S10. Relationship between dT nucleotide metabolism and telomere synthesis.

Figure S11. TRACE assay is sensitive to genetic and small molecule perturbations to telomerase homeostasis. (A) TRF from (1B) was stripped and re-probed for the C-strand strand, showing TRACE can assay for double stranded telomere synthesis. (B) TRF from TRACE assay performed as follows: *TERC*-/- 293T cells were transfected with the indicated expression vectors, split and harvested at the indicated timepoints after transfection. (C) TRF from TRACE assay performed as follows: *TERC*-/- 293T cells were transfected with the indicated expression vectors, split 18 hrs after transfected and cultured in the indicated doses of BIBR1532 for 30 hours prior to harvesting. A representative blot from two independent experiments is shown. (D) Quantification of (C). (E) TRF from TRACE assay where *TERC*-/- 293T cells were transfected with expression vectors harboring the indicated point mutations followed by culture for 90 hours. A representative blot from two independent experiments is shown. (F) Quantification of (E). Statistical significance was determined using paired two-sided t-test. (G) TRF from TRACE assay performed as in (E). A representative blot from two independent experiments is shown. (H) Quantification of (G) as in (F). (I-K) TRF from TRACE assay where cells were transfected as in (B), then split 18 hours after transfection and cultured in the indicated compounds for 30 hours prior to harvesting. The data in (D), (F), and (H) are presented as means and error bars indicate range.

Figure S11. (Continued)

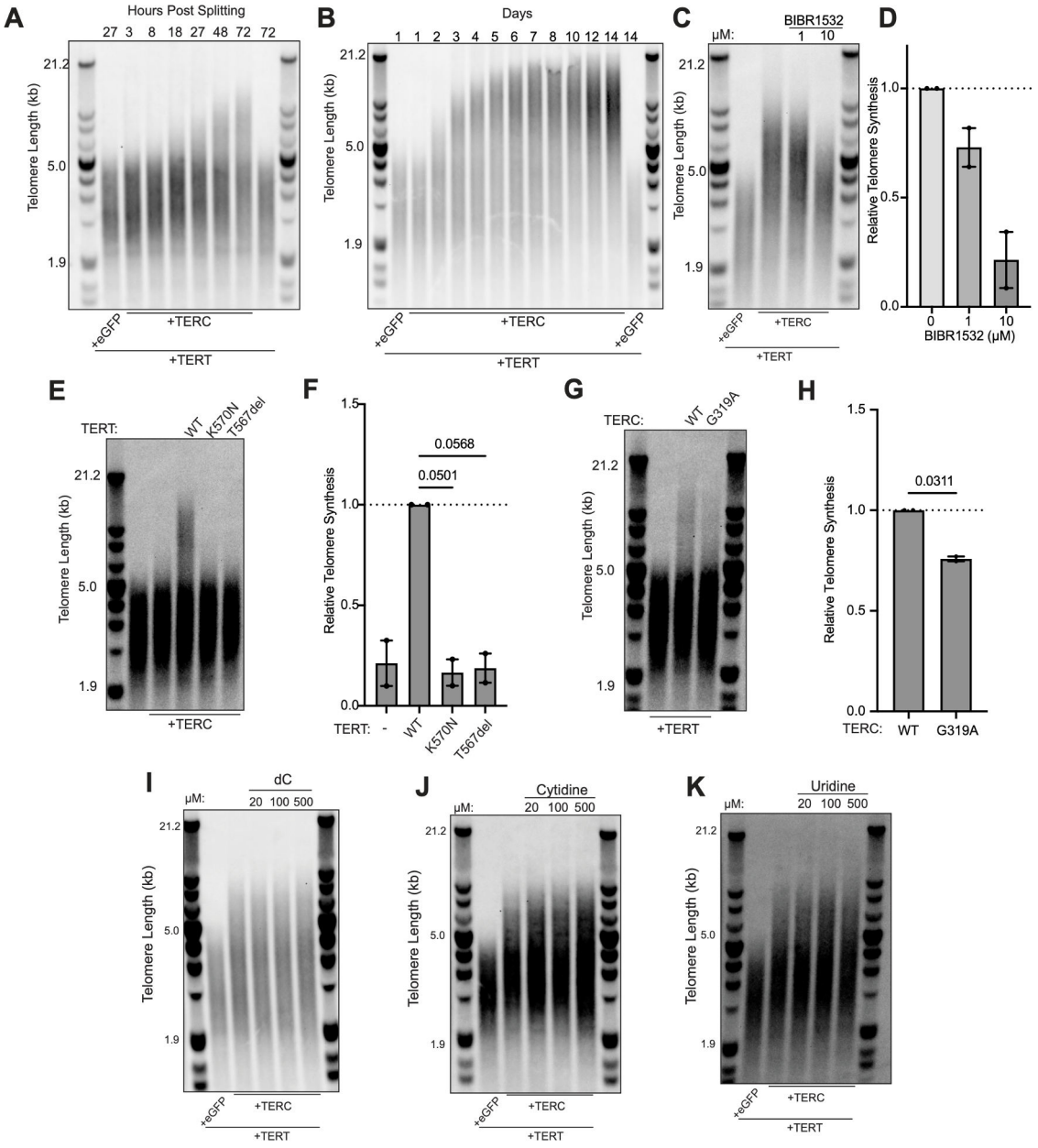


Figure S12. Telomerase inhibition from guanine supplementation. (A) TRF Southern blot of TRACE assay from *TERC*-/- 293T cells transfected with the indicated expression vectors, cultured for 18 hours, then split and cultured in the indicated compounds for 30 hours. Doses used: forodesine, 1μM; dG, 100μM; guanosine, 500μM; guanine, 500μM. (B-D) TRF Southern blot of TRACE assay performed as in (A). (E) Quantification of TRF Southern blot from Fig. 2j. Biological replicates per cell line: 293T, n=5; K562, n=3; Fibroblasts + hTERT, n=3. P values calculated using paired two-sided t-test. Data are plotted as means and error bars indicate s.d. (F and G) Genomic DNA from *TERC* -/- 293T cells manipulated with the indicated sgRNA(s) was PCR amplified with primers specific to the *HPRT1*, *APRT* or *GDA* loci as indicated, showing the pools of three sgRNAs targeting either *HPRT1*, *APRT*, or *GDA* generated targeted genomic deletions. (H and I) TRF Southern blot from TRACE assay. Performed on *TERC*-/- 293T targeted with the indicated sgRNA(s). Assay performed as in (A) with cells split into media containing the indicated doses of guanine. A representative set of blots is shown from two biological replicates. (J) Proposed model illustrating how salvaged guanine ribonucleotides could inhibit RNR and reduce telomerase activity in a manner which can be rescued by dT.

Figure S12. (Continued)

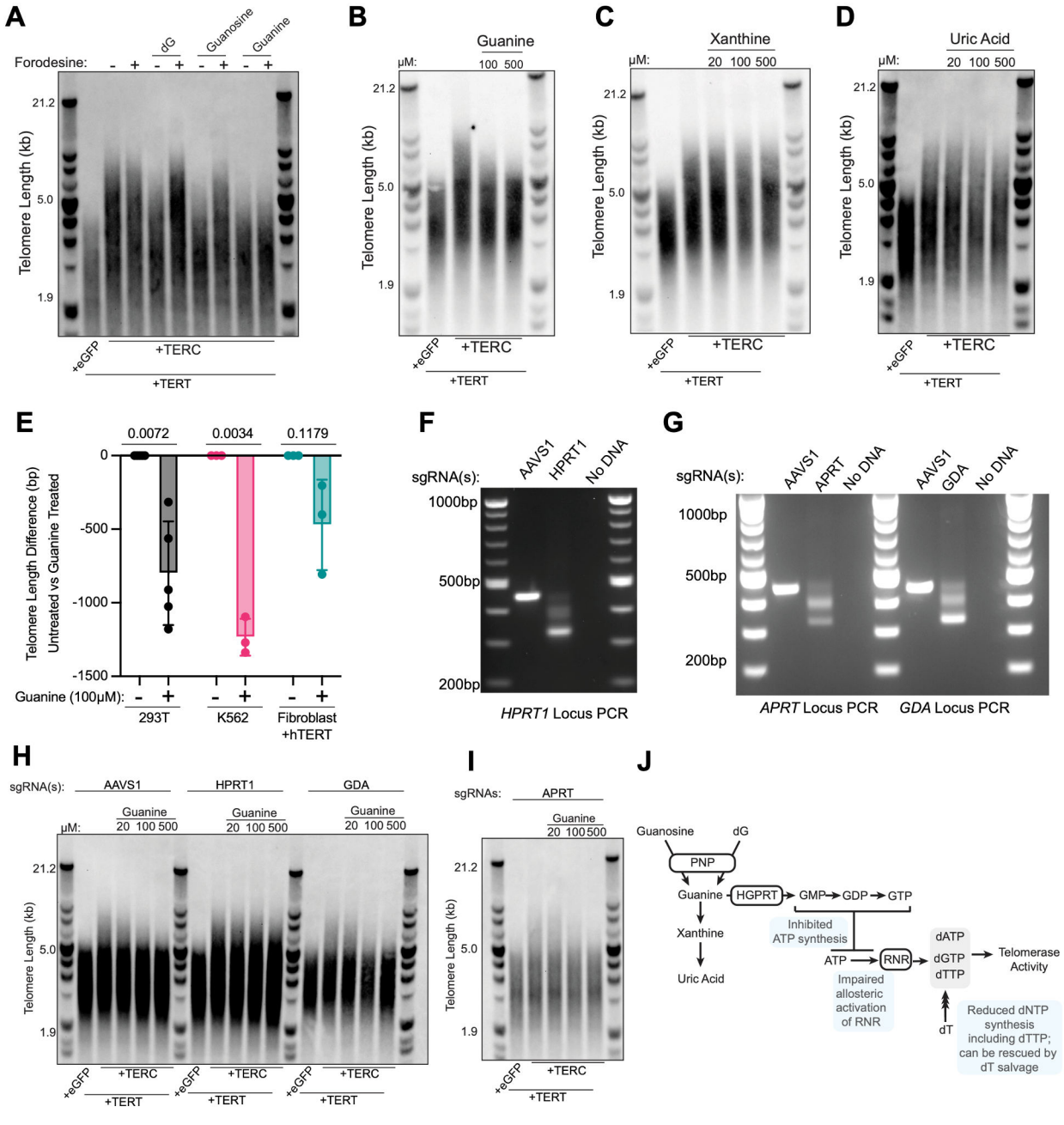
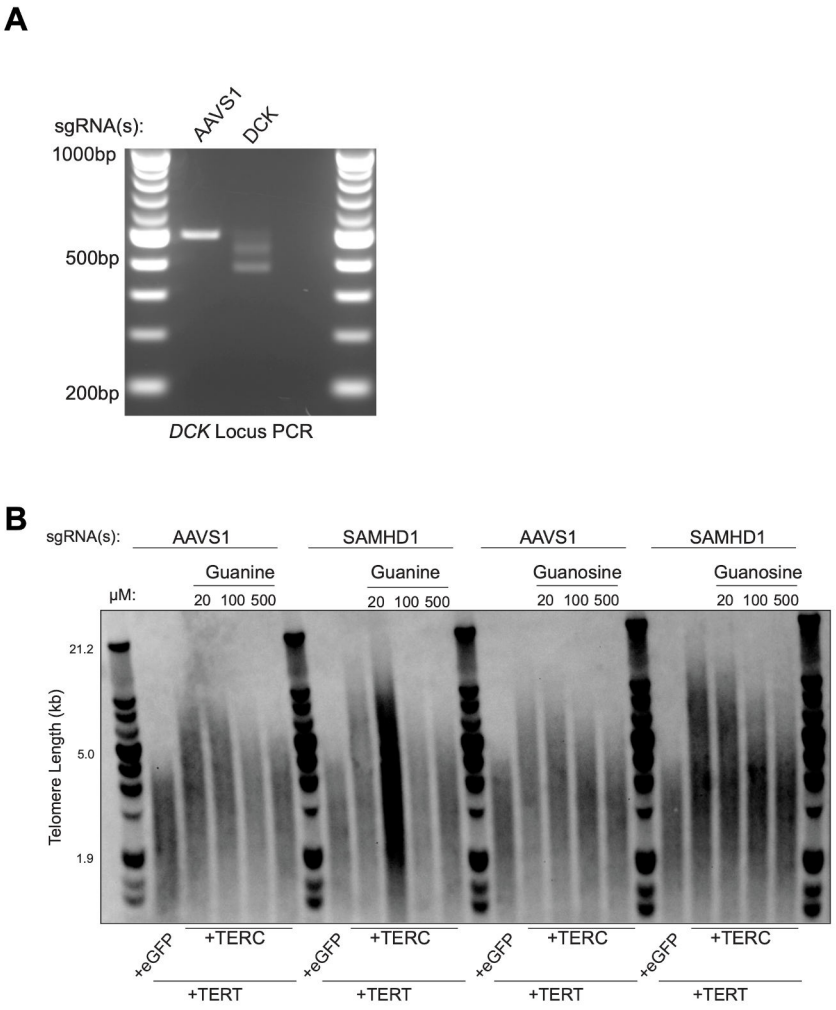


Figure S13. DCK and SAMHD1 contribute to telomerase regulation in response to manipulation of guanine nucleotide metabolism. (A) Genomic DNA from TERC -/- 293T cells manipulated with the indicated sgRNA(s) was PCR amplified with primers specific to the DCK locus, showing the three pooled sgRNAs targeting DCK generated on-target genomic deletions. (B) TRF Southern blot from TRACE assay of TERC-/- 293T cells targeted with the indicated sgRNA(s) which were transfected with the indicated expression vectors, cultured for 18 hours, then split and cultured in the indicated doses of guanine or guanosine for 30 hours. Note DNA was overloaded in the lane which had the SAMHD1 sgRNAs targeted cells treated with 20 μM guanine, which accounts for the abnormally high signal intensity.

Figure S13. (Continued)



This page has been intentionally left blank.

This page has been intentionally left blank.